Essays on Maritime Transport and International Trade

by

Philip Economides

A dissertation accepted and approved in partial
fulfillment of the requirements for the degree of Doctor of
Philosophy in Economics

Dissertation Committee:

Woan Foong Wong	Co–Chair
Bruce Blonigen	Co–Chair
Anca Cristea	Core Member
Nicole Ngo	Institutional Representative

University of Oregon
Spring 2024

DISSERTATION ABSTRACT

Philip Economides
Doctor of Philosophy in Economics
Department of Economics

Title: Essays on Maritime Transportation and International Trade

This dissertation considers topics which dovetail studies of maritime trade and transportation. Using theoretical models, empirical identification and structural analysis, I provide novel evidence on three key facts; (i) the repositioning of empty container units is a key logistical practice in maritime shipping that enables the sustained service of global trade imbalances, (ii) advancements in container shipping technology through increased vessel capacity between 1977-2023 have introduced negative spillovers on cargo handling times at port, and (iii) the newly introduced estimated time of arrival (ETA) based port queuing system has contributed to decarbonization in the maritime shipping sector.

In the first substantive chapter, I develop a model of containerized trade and transportation which embeds the logistical practice of container repositioning by transport operators. This involves bringing equipment to where it is most needed for further transport service, and may necessitate the transportation of empty containers when servicing commerce between countries with particularly large trade imbalances. I contrast the comparative statics of this model with novel container traffic data, collected individually from the key US ports. These reduced-form analyses demonstrate that the balanced exchange of container units can only be revealed upon accounting for empty units. Motivated by the recent passing of the Ocean Shipping Reform Act of 2022, I use a structural approach to examine the implications of restricting empty container outflows from the US in order to stimulate US exports. The results of this exercise suggest the policy backfires for the broader public. Although exports are stimulated by policymaker action, transport operators respond to this form of unconventional policy intervention by adjusting freight rates bilaterally. The resulting increase in freight rates for shipping routes destined for the US contributes to an overall reduction in trade activity and a pronounced decline in vessel capacity allocated towards the US containerized shipping market.

In the second substantive chapter, Woan Foong Wong, Simon Fuchs and I explore how technological innovation and port conditions contribute to variation in individual containership dwell time events across the US. Our data documents vessel size, container capacity, and port concentration from January 1977 to December 2023. We observe a four-fold increase in US port visits, peaking in 2010, followed by a downward trend until 2023. This pattern coincides with an accelerated rate of entry among the largest categories of containership classes. We suggest that transport operators are increasingly relying on improved vessel technology to meet growing demand for trade, rather than by supplying more vessels. Despite volume growing over time, average dwell times across US ports have remained centered around 2.4 days. Our empirical results suggest that this status quo is maintained by offsetting mechanisms; (i) larger vessels representing greater unloading efficiencies, and (ii) increased port traffic volumes introduce stronger negative spillover effects on visiting vessels.

In the third substantive chapter, I examine how logistical practices by port authorities can influence vessel emissions. I use the case study of San Pedro Bay, California, which introduced a new vessel queuing system. Under the former system, vessels would be required to enter within 25 nautical miles of the ports of Los Angeles and Long Beach before being eligible to be admitted to the vessel queue. Additionally, those awaiting service could anchor near the port area or drift nearby. After observing a swelling of anchorage zone and drift areas use, authorities introduced a queuing system in which each vessel's calculated time of arrival determined their queue position and mandated no idling within a 150 nautical mile area of the ports. I find evidence which suggests that the policy slowed down inbound vessels, reduced idling time prior to port admittance, but increased the extent to which vessels would reposition while waiting. Accounting for all three factors, I find that the policy contributed to a 30.2% decline in containership emissions relative to control ports along the US West Coast.

The dissertation includes previously unpublished co-authored research.

CURRICULUM VITAE

NAME OF AUTHOR: Philip Economides

GRADUATE AND UNDERGRADUATE SCHOOLS ATTENDED:

University of Oregon, Eugene, OR
University College Dublin, Dublin, Ireland
Trinity College Dublin, Dublin Ireland

DEGREES AWARDED:

Doctor of Philosophy, Economics, 2024, University of Oregon
Masters of Science, Economics, 2020, University of Oregon
Masters of Science, Applied Economics, 2017, University College Dublin
Bachelors of Arts, Economics, 2014, Trinity College Dublin

AREAS OF SPECIAL INTEREST:

International Economics, Transport Economics, Applied Microeconomics

PUBLICATIONS:

Economides, P., and G. Nikolaishvili (2023) "Measuring Economic Activity in the Presence of Superstar MNEs", Economics Letters, Vol. 226, 111077

Economides, P., K. McQuinn, and C. O'Toole (2021) "Household Savings Constraints, Uncertainty, and Macroprudential Policy", Scottish Journal of Political Economy, Vol. 68(2), pp. 238-260

GRANTS, AWARDS, AND HONORS:

PhD Scholars Fund, RES 2024 Conference (Queen's University Belfast), 2024
Best Graduate Student Paper Award, West Coast Trade Workshop (UC Berkeley), 2024
Gerlof Homan Scholarship in International Economics, University of Oregon, 2023
Dissertation & Thesis Award, Division of Graduate Studies, University of Oregon, 2023
WEAI Graduate Workshop 2023, University of Oregon Nominee, 2022
Kleinsorge Summer Fellowship, University of Oregon, 2021
Edward G. Daniel Scholarship, University of Oregon, 2020
Graduate Teaching Fellowship, University of Oregon, 2019 – 2024

ACKNOWLEDGEMENTS

I wish to express my gratitude for the support, guidance and patience I have received from Woan Foong Wong, Bruce Blonigen, Anca Cristea and Nicole Ngo. I am grateful for the generous times and many fruitful discussions my peers have afforded me too. A special thanks to Mark Colas, Gio Nikolaishvili, Tami Ren, Emmett Saulnier, and Brock Wilson for their dedicated input. I am very thankful to the participants at the University of Oregon International Trade group. Furthermore, versions of Chapter II were presented at the 2023 WEAI Graduate Workshop, the 2023 Midwest International Trade Conference, the 2024 West Coast Trade Workshop, the 2024 RES Conference and the Atlanta FED. I thank the audience members and, in particular, Jefferey Bergstrand, Carsten Eckel, Benjamin Faber, Simon Fuchs, David Hummels, Nayul Kim, Pearl Li, James Markusen, Adam Pfander, Andrés Rodríguez-Clare, Thomas Sampson, and Larry White for their many helpful comments. Any remaining errors are my own.

The financial support I received through the Gerlof Homan Graduate Scholarship in International Economics and Dissertation & Thesis Award, which funded data requirements for Chapters II and IV, respectively, are also gratefully acknowledged.

To my wife, Alina, and our parents, Carol, Irina, and Vitaly, for their unwavering support.

Contents

List of Figures

List of Tables

Chapter 1

Introduction

In the past four years, transport services around the world have been tested to their limits. The increased volatility in the demand for final goods imports, partly attributed to bouts of precautionary accumulations of inventory and repeated cases of COVID-19 shutdowns, has led to the emergence of widespread log-jams across international transport networks. The resulting disruptions in these supply chains have exposed a number of key vulnerabilities across transport networks, particularly with respect to maritime transport, which services over 80% of traded goods volumes.[1] My dissertation seeks to provide insight into critical policy questions related to a reliance on available transport equipment, potential limitations in port infrastructure and concerns surrounding the resulting pollution of vessel congestion. This dissertation contains previously published and unpublished co-authored material. Chapter 3 is joint work with Woan Foong Wong and Simon Fuchs.

Chapter 2 considers a setting in which roundtrip transport services, operated by containerships, routinely travel back and forth between origin–destination pairs. Due to potential imbalances in shipping volumes and a persistent need for available transport equipment on the larger-volume leg of a given round trip, vessel operators must include empty containers on the low-volume leg. Using a novel data set of bilateral container flows, which separately reports empty and loaded container traffic across key US ports, I document a system of balanced container flows between the US its trade partners. I develop a partial equilibrium model of round trip trade & container redistribution to assess a counterfactual of restrictions to empty container outflows, in favor of making more equipment available for US exporters.

I find this unconventional form of protectionism lowers vessel capacity on a given roundtrip by almost 20%, which contributes to higher import prices (+1.75%) and a reduction in the overall value and volume of trade between the US and the rest of the world (-8.5%). My findings suggest that interference with the manner in which container equipment is freely redistributed may backfire, depending on which party of interest is focused upon. From the policymaker perspective, exports have been successfully grown. However, I show evidence that policymaker concerns may need to be extended to effects on the opposite return-leg of trade, which reveals an overall decline in US access to containerized goods, lower available transport capacity and associated inflation.

Chapter 3 shows that vessels of relatively larger size have developed economies of scale in container handling at the port-level, although negative externalties of increased vessel mass have contributed to negative spillovers for the existing fleet. Despite containership mass growing 5-fold between January 1977 and December 2023, port visit times have remained largely stable at 2.4 days in duration due to these offsetting factors. We

[1]UNCTAD (2021) Review of Maritime Transport 2021, Challenges faced by seafarers in view of the COVID-19 crisis. https://unctad.org/publication/review-maritime-transport-2021

document the evolution of containership technology and its adoption among the major ports of the US.

We find monotonic efficiency gains across containership categories, with some of the largest vessels servicing the merchant fleet in the US offering a 47.8–55.7% reduction in dwell times per container. Given the recent trends in weaker market competition in containerized shipping and skewedness in the extent to which large operators can build new ships relative to smaller operators, this mechanism may be propagating a faster rate of market concentration. We conclude with remarks on how to approach the next stage of this paper, in which we develop a micro-model of containership queuing theory and explore means by which to estimate exogenous model primitives for the purpose of evaluating counterfactuals related to port infrastructure and vessel technology.

In Chapter 4, I use the case study of the new containership queuing system in San Pedro Bay, California, to assess how an estimated time of arrival based queue position influences vessel emissions both locally and globally. To recover fuel consumption and emissions of individual vessels, I first combine the use of MarineTraffic records port of origins and departure timestamps of vessels inbound for the US West Coast with highly granular vessel position data for US waters. I then use prevailing approaches in the maritime engineering and transportation strands of literature to impute fuel and emission levels. This allows me to identify individual vessels repeatedly over time and control for strategic responses to the policy, such as lane switching, market exits and market entry.

I find that the policy featured offsetting effects on the voyage and queuing stages of transit for individual vessels. Using a difference-in-difference approach for this quasi-experimental setting, I find that the policy reduced associated vessel CO_2 levels by 30.2% relative to control ports along the US West Coast. While the policy did somewhat slowdown vessel travel speeds, the biggest boon in emission reductions was achieved through reduced idling in the port vicinity. Now that containership operators had certain queue positions upon departure from a prior port, rather than receiving that information within 20 nautical miles of arrival, they could minimize their associated idle time and better purpose the use of their transport equipment. Use of this logistical practice across ports may be of interest to policymakers and port authorities seeking to decarbonize ports, particularly for facilities subject to extensive queuing experiences.

Chapter 2

Unconventional Protectionism in Containerized Shipping

Unconventional Protectionism in Containerized Shipping

Philip Economides*

April 15th, 2023

Abstract

The containerized shipping market operates similarly to a bus system, where vessels maintain round trip transport services between origin-destination pairs. Intermediary transport operators must commit to sufficient shipping capacity, while accounting for bilateral shipping imbalances. To ensure necessary transport equipment availability, vessel owners reposition empty container units on the low-volume leg of a round trip, from net importer origins to net exporter destinations. I provide evidence of bilateral US container traffic being consistently balanced – only when accounting for empty container repositioning. Motivated by the Ocean Shipping Reform Act of 2022, I explore the effects of a US restriction to empty container outflows in favor of stimulating US exports. This form of policy intervention – although helpful in meeting policymaker goals of stimulating exports – backfires for the broader public through elevated import prices, lower transport capacity, and reduced trade activity.

JEL classification: F14, F18, F64, Q52, R49
Keywords: trade costs, transport costs, transportation, trade policy, container shipping

*Department of Economics, University of Oregon.
I am indebted to Woan Foong Wong, Bruce Blonigen, Anca Cristea, and Nicole Ngo for their advice and guidance. I would like to thank Mark Colas, Mike Kuhn, Benjamin Hansen, Kathleen Mullen, David Evans, and seminar participants at the University of Oregon for suggestions and comments. I am also thankful to the conference organizers at the WEAI and my cohort advisor, Prof. Lawrence J. White, for the opportunity to present this work at the 2023 WEAI graduate workshop. All remaining errors of this draft are my own.

2.1 Introduction

Approximately 70% of international trade values travels via maritime transport, two-thirds of which is attributed to containerized shipping (Notteboom et al., 2022). These services specialize in providing round trip transport, where ports are routinely visited back-and-forth between specific origin-destination combinations. Containers are repositioned within these continuous loops of transport services, creating a persistent circulation of transport equipment. In cases of imbalanced demand and asymmetric shipping volumes, repositioning includes empty containers. This phenomenon introduces the *empty container repositioning problem* for transport operators – a need to relocate empty containers on the low-volume leg of a given round trip, from net importer countries back to net exporter countries (Song, 2021). The repositioning of empty containers is estimated to represent 20% of total ocean container movements and 15% of fleet management costs (Drewry, 2006; Rodrigue, 2020). This implies that variation in repositioning influences vessel-owning intermediaries' costs, which leads to changes in allocated vessel capacity, freight rate pricing and trade outcomes on round trip routes. Although container repositioning has been well-documented in the maritime logistics literature (Crainic et al., 1993; Lee and Song, 2017; Song, 2007), little is known of how frictions in container availability affect trade outcomes. The recent passing of the Ocean Shipping Reform Act, henceforth OSRA22, embodies an example of a restriction to container repositioning. Under this bill, the Federal Maritime Commission (FMC) has been tasked with *limiting* the extent to which transport operators can refuse allocating portions of vessel capacity to US containerized exports in favor of transporting additional empty container units.

In this paper, I examine container repositioning under round trip trade and quantitatively evaluate how policy restrictions to empty container outflows, such as OSRA22, may influence US trade outcomes. My main findings suggest that empty container repositioning is key in sustaining prevailing trade imbalances and existing transport capacity levels. When empty repositioning is restricted in favor of stimulating domestic exports, shipping supply declines, which in turn leads to added inflationary pressure and an overall reduction in bilateral trade activity.

I first build a quantitative model of round trip trade based on Armington (1969), which is capable of featuring both balanced and imbalanced exchanges of goods, and includes a richer specification of endogenous trade costs. A representative exporter faces both the domestic cost of producing a good and the freight rate

issued by a transport operator. The transport operator maintains bilateral round trip services between two countries. Price setting for these services accounts for differences in demand between regions and partly reflects the cost of repositioning empty containers on the low-volume leg of a given round trip. Should the cost of handling empty container units rise, a transport operator lowers their exposure to trade volume asymmetries through bilateral freight rate adjustments and reduced shipping capacity. From the perspective of a net importer country, such as the US, the model predicts that when the import-export ratio rises, resulting empty container traffic as a proportion of total outbound container units must rise too.

Using novel port-level loaded & empty container traffic data[1], I empirically examine the validity of these comparative statics and establish three key facts; (i) the scale of the empty container repositioning problem grows as asymmetries in shipping volumes intensify, (ii) balanced exchanges of national bilateral flows of total container flows are evident only when accounting for empty container repositioning across these US ports, and (iii) the relative size of a port is predictive of the role each location plays – large ports such as Los Angeles & New York generate persistent net inflows of containers while mid-tier US ports are sources of net outflows. Findings (ii) and (iii) suggest that the US maintains an interdependent container repositioning system between US ports and the hinterland, indicating a reliance on the accessibility of inter-modal transport. Only upon a national aggregation across US ports does the model's constraint of a balanced container flow network appear evident.

In preparing a quantitative analysis of OSRA22, I combine my measures of container traffic with US census data on monthly port-level bilateral containerized trade flows (by product type, value, and weight) and auxiliary country-level data. This allows me to calibrate and estimate model primitives of the baseline scenario of my model through a two-stage estimation strategy.

The first stage estimates bilateral loaded container flows between US ports and the main trading partners of the US. This is achieved by exploiting variation in metric tonne weights of 2-digit Harmonized System (HS2) goods shipped on these same trade routes across each year-month of the sample. Suppose that for a given shipping lane, there is a marginal increase in the metric tonnes of a product's weight. Given that each container maintains a weight capacity, a greater amount of a given good suggests an increased number of containers allocated for transport. Furthermore, the rate at which each product's weight increases total

[1]This balanced panel represents over 80% of US container throughput for 2012–2021.

container count usage varies due to the volume constraint each container represents. For example, a metric ton of sheet metal likely takes up far less volume in a container unit compared to a metric ton of furniture. By estimating each product's "loading factor" – the rate at which weight contributes to loaded container flows – I recover origin-destination loaded container flows between US ports and key US trade partners. I provide evidence of a striking fit between country-specific estimated loaded container flows and UNCTAD data of East Asian–North American and European–North American bilateral loaded container traffic.

The second stage uses a Generalized Method of Moments (GMM) approach to recover four model primitives for each shipping route – the underlying pair of preference parameters each country's consumer base maintains for their trade partner's manufactured goods, as well as per-unit costs of handling empty and loaded container units. The remaining primitives are calibrated using a combination of public data sourced from the International Labor Organization, OECD, and World Bank. Estimated primitives align well with what is known of shipping. For example, depending on the lane, my estimate of empty container handling costs varies between 14.9% and 21.3% of total fleet management costs, which is rather close to the 15% share reported in Rodrigue (2020). Furthermore, implied freight rates are consistently higher on the higher-volume lanes of a given round trip, as established in Hummels et al. (2009).

To capture the intent of OSRA22's unconventional trade policy, I consider the effects of an empty container outflow (ECO) quota, which effectively reallocates vessel space towards US exporters. I specifically consider a moderate regime, where the policymaker seeks to return to a status-quo represented by the 40% long-run average of empty container outflows as a percentage of total container outflows originating from the US. I find that restricting the return of empty transport equipment meets the sole objective for higher exports for the US policymaker, but conflicts with the broader interests of the public once accounting for the full roundtrip effect. Constraining repositioning contributes to an 18.6% decline in round trip shipping capacity, a 17.7% decline in US containerized imports and an 8.5% reduction in the total value of US containerized trade. Additionally, imported inflation grows by just under 2 percentage points.

To the best of my knowledge, this paper is the first to provide empirical evidence of the affect of empty container repositioning in round trip transport services on trade outcomes. Additionally, the micro-founded model of this paper enables the assessment of a relatively modern and unique trade policy concern, represented by

OSRA22. The results of this paper contribute to several strands of the literature.

First, this paper adds to the international trade literature on endogenous trade costs. Transport costs represent an increasingly prominent factor in determining overall trade costs. For example, Hummels (2007) finds that for every $1 exporters paid in tariff duties to send goods to the US, $9 was paid in transportation costs. Although earlier studies used ad-hoc transport costs,[2] more recent theoretical frameworks use a variety of endogenous approaches (Irarrazabal et al., 2015; Hayakawa et al., 2020; Bonadio, 2022). Atkin and Donaldson (2015), Brancaccio et al. (2020) and Ignatenko (2023) use differences in market power across intermediary transport service operators for variation in transport costs. Allen and Arkolakis (2022) and Wong and Fuchs (2022) highlight how the quality of infrastructure and traffic congestion across regions can also explain variation in transport costs. Using bilateral container traffic data at the port level, I document how the cost of servicing imbalanced trade routes through empty container repositioning affects round trip trade flows.

Secondly, this paper is closely related to studies focused on particular facets of maritime transport. These technological and logistical innovations play important roles in influencing key economics outcomes. Bernhofen et al. (2016) suggests container technology introductions between 1962-1990, on average, contributed to a 85% higher trade ten years later. Brooks et al. (2021) highlights how container technology led to substantial population and employment growth in US counties near containerized ports. Following the 2016 Panama Canal expansion, Heiland et al. (2022) estimates an average increase in trade of 9-10% across affected shipping lanes. Ganapati et al. (2021) provides evidence of logistical hubs known as *entrepôts* fostering advancements in vessel technology and size, which lowered transport costs. Carreras-Valle (2022) shows that technological innovations reduced internationally-sourced input costs.[3] Through the novel container traffic data available to me, I demonstrate a joint dependency on the logistical practice of empty container repositioning on both legs of round trip services between the US and the rest of the world. I find that limitations on this practice may undermine the aforementioned benefits of containerization. Furthermore, routes that maintain particularly high asymmetries in trade volume, such as shipping lanes

[2]Transport costs are often treated as an exogenous model primitive, commonly referred as an iceberg cost, which represented a fixed percentage of value-attrition while a good is in transit (Samuelson, 1952).

[3]These cost saving measures also coincided with greater precautionary inventory management and higher delivery time volatility.

between the US and China or Japan, are far more exposed to the malaise effects from intervention in empty repositioning.

Third, this paper adds to the literature examining the motivation and effects of resurgent trade protectionism. Such decisions are largely a reflection of the state of policymakers' underlying constituent bases, which are subject to adverse developments in social identification patterns (Grossman and Helpman, 2021; Bombardini et al., 2023). While resurgent protectionism often leads to welfare losses (Sampson, 2017; Fajgelbaum et al., 2020; Bown, 2021; Fajgelbaum and Khandelwal, 2022), infant industries may find themselves on more favourable growth trajectories (Juhász, 2018). While there is a well-documented understanding of how demand-side interventions influence trade outcomes (e.g., tariffs and quotas), OSRA22 relates to supply-side elements of trade by constraining the use and availability of transport equipment. This study represents the first and only paper to consider this unconventional form of protectionism. I find that although exports are stimulated by these restrictions, overall trade activity declines – suggesting that the policy is protectionist in nature. My results also suggest that this new tool is precise in targeting net exporters, particularly those with a greater reliance on empty containers from the US.

Lastly, this paper relates to the theoretical literature of round trip transport services. Given that the volumes of transported goods between two locations are often imbalanced, shipping capacity on the lower volume 'backhaul' route is underutilized. As Demirel et al. (2010) demonstrates, the 'backhaul' freight rate drops to zero under perfect competition and perfect information. Both Demirel et al. (2010) and Wong (2022) remedy this deviation from observed freight rates by either (i) enforcing balanced trade flows across round trips, or (ii) introducing imperfect information and a matching process into the model. Ishikawa and Tarui (2018) solves for positive bilateral freight rates by introducing imperfect competition. I approach this challenge by instead using physical equipment as inputs in a joint profit function of round trip transport services. To ensure the continued service of the high-volume leg of an imbalanced round trip, a transport operator redistributes empties. Under imbalanced trade, the marginal revenue of shipping an additional loaded container on the high-volume route is equal to the cost of handling that loaded unit plus the cost of returning one empty container. In contrast, transporting one additional loaded unit on the low-volume leg of a round trip occupies an existing empty, resulting in a freight rate equal to the loaded handling cost less the cost of returning an empty unit. Under specific assump-

tions, bilateral freight rates are both positive and the low-volume route maintains a relatively lower freight rate, as predicted in Hummels et al. (2009). This pricing scheme under asymmetric volumes relates closely to peak load pricing strategies featured in round trip passenger flights and the dynamic pricing on highway toll lanes (Williamson, 1966; Cooks and Li, 2023).

The remainder of the paper proceeds as follows. I detail how container redistribution operates and outline the factors which contribute to empty container redistribution. Section 3 outlines a partial equilibrium model of containerized trade. Section 4 provides a brief description of the novel data that I have collected, and Section 5 presents stylized facts of containerized trade. In Section 6, I calibrate and estimate the exogenous parameters of the empty container model and consider the counterfactual effects of government intervention aimed at limiting the outflow of empty container units from the US. Section 7 concludes.

2.2 Background

Since the emergence of container technology, this form of transport equipment has grown to become a worldwide norm. As Levinson (2016) explains, container unit standardization was the key development that led to the modern day scale of intermodal transportation. This challenge, starting in the late 1950s, represented ten years of negotiations in which time the industry determined that the standard containers would be 20-ft & 40-ft in length. Additionally, corner fittings used to lift individual units and interlock units together were also agreed upon. These efforts resulted in a flexible, harmonized system in which transport equipment could be freely redistributed back and forth within a given round trip. The subsequent global adoption of container technology across ports has yielded a complex network of supply chains which operates at lower costs but represents greater risks through increased uncertainty surrounding delivery times (Carreras-Valle, 2022).

Although container shipping and the repositioning of empty containers have been a long-held practice in international trade, it is important to understand why economic agents coordinate in this manner. For a transport operator, bilateral transport service demand within a given round trip can differ. This would contribute towards net exporters shipping more loaded container units out to a given destination than those that make their way back from the net importer. To accommodate required container inventory across ports, container repositioning

features empty units on the backhaul (lower volume) leg of a given round trip. In essence, this behaviour reflects an inventory management problem in which a cost–minimizing assignment of container capacity and flows must be determined.[4]

Lee and Song (2017) describes two considerations that transport operators face under imbalanced round trip trade; (i) a quantity decision, in which the firm decides how many empty containers to store at each port, and when and how many to move between ports, and (ii) a cost estimation of empty repositioning, which contributes to how freight rate prices are determined. Regarding the quantity decision, Song and Dong (2015) refers to two key considerations. Upon adopting a network flow model, origin-destination based matrices specify the quantity of empty containers to be moved from one node to another. The goal of this decision is to satisfy flow balancing, where container flows between two nodes should be equal. The second item addresses uncertainties by adopting inventory control models to produce decision-making rules which dynamically determine the amount of empty repositions in and out of a node. I incorporate the associated contribution of empty container repositioning costs to freight rates and enforce a balanced container flow constraint between nodes such that combinations of loaded and empty container units can be accounted for on the backhaul (lower volume) leg of a given round trip. However, given that I use a static model, I do not feature decision-making rules and uncertainty for individual firms.

The transport logistics literature therefore recognizes the scale of the empty container repositioning problem to be a product of underlying asymmetries in import demand volumes between service nodes and uncertainty surrounding vessel delivery times, inter-reliances on other modes of transport and demand volatility. For the purposes of this paper, I focus on the long-term determinants of variation in empty container repositioning through imbalanced trade. The greater the asymmetry in loaded container flows within a given round trip, the larger the volume of empty container repositioning. Furthermore, the empty container repositioning problem should be considered a longstanding and necessary feature of containerized trade rather than a specific byproduct of recent episodes of port congestion and delays.

[4]As Lee and Song (2017) highlights, empty container repositioning functions similarly to conventional manufacturing logistics in which firms strategically relocate their inventory in order to meet consumer demand. In the case of containerized round trip shipping, exporters consume transport services from transport operators and container units are redistributed in order to be readily available for further shipping service demand. When volumes of service demand differ on these continuous loops of transportation, firms strategically relocate empty container units to sustain the service of their larger export volume destination.

2.3 Model

In this section, I specify the empty container repositioning problem in an augmented Armington model based on Hummels et al. (2009) and Wong (2022). I include three representative agents: consumers, producers and transport operators. Endogenous transport costs are a function of per-unit loaded and empty container handling costs. I first outline key assumptions and then solve the model. Lastly, I establish a set of comparative statics that explain variation in empty repositioning.

2.3.1 Assumptions

I consider an international economy of round trip containerized trade that features J heterogeneous countries, where each country produces a unique variety of a tradeable good. The term $\overset{\leftrightarrow}{ij}$ denotes a round trip route that services trade between countries i and j. Consumers in country j are endowed with one unit of labor that is supplied elastically, exhibit a love of variety across consumable goods and are geographically immobile. A representative consumer at location j is assumed to maximize a quasi-linear utility function:

$$\max_{\{l_{j0},\ldots,l_{ij}\}} U_j = l_{j0} + \sum_{i=1}^{M} a_{ij} l_{ij}^{(\epsilon-1)/\epsilon}, \quad \epsilon > 1, \tag{2.1}$$

where l_{j0} represents the quantity of the numeraire good consumed in country j and l_{ij} represents the quantity of a tradeable variety sourced from country i.[5] Heterogeneous countries maintain route-specific preference parameters, a_{ij}, for each tradeable variety. A single unit of a good is associated with one unit of transport equipment utilized. Therefore, l_{ij} is equivalent to the number of loaded containers shipped from i to j. The price elasticity of demand, ϵ, is common across varieties and routes.

Producers are perfectly competitive and produce variety j using inputs of labor. I assume that the price of transported goods from i to j increases through the following components; (i) the domestic wage rate, w_i; (ii) the specific tariff rate of the given ij leg of the round trip, τ_{ij}; and (iii) the per-container freight rate, T_{ij}.[6]

[5] The numeraire good is traded at no cost and maintains a unit price of 1.

[6] Holmes and Singer (2018) highlights an indivisibility of transport costs due to per-container freight rates not varying based on variation in the usage of containers' cubic volume capacity.

$$p_{ij} = w_i \tau_{ij} + T_{ij} \tag{2.2}$$

Intermediary transport operators are perfectly competitive and service a given bilateral trade route, $\overset{\leftrightarrow}{ij}$. The profit maximization problem for the transport operator servicing route $\overset{\leftrightarrow}{ij}$ is a joint-profit function that considers the optimal bundle of container inputs. This is a variation of the joint-profit function featured in Behrens and Picard (2011), in which I add a balanced container flow constraint.

$$\begin{aligned} \max_{\{l_{ij}, l_{ji}, e_{ij}, e_{ji}\}} \pi^{\leftrightarrow}_{\overset{\leftrightarrow}{ij}} = & T_{ij} l_{ij} + T_{ji} l_{ji} - c^{\leftrightarrow}_{\overset{\leftrightarrow}{ij}} (l_{ij} + l_{ji}) - r^{\leftrightarrow}_{\overset{\leftrightarrow}{ij}} (e_{ij} + e_{ji}) \\ \text{s.t. } & l_{ij} + e_{ij} = l_{ji} + e_{ji} \end{aligned} \tag{2.3}$$

Revenue generated from servicing route $\overset{\leftrightarrow}{ij}$ is the sum of each leg's respective freight rate times the loaded container quantity. Costs are determined by loaded and empty states of container inputs used to provide services. The costs of per-unit loaded and empty container handling is represented, respectively, by the set $\{c^{\leftrightarrow}_{\overset{\leftrightarrow}{ij}}, r^{\leftrightarrow}_{\overset{\leftrightarrow}{ij}}\}$.[7] Due to equidistant travel across routes ij and ji and the minimal attention that incoming empty containers $\{e_{ij}, e_{ji}\}$ require to be repurposed, I assume that handling costs are invariant to voyage direction and empties are cheaper to handle.[8] Bilateral flows of container units, irrespective of their state, are balanced as a result of transport operators needing to sustain container inputs on both sides of a given round trip. This constraint is affirmed in the first stylized fact in Section 3 (Figure 2.1).

In the next subsection, I depict the profit maximization problem under *weakly* imbalanced trade. In the case of balanced trade, Eq. (2.3) is subject to a constraint of equivalent bilateral flows of loaded container units and the empty container redistribution problem is nonexistent. The resulting system of equations are solved for in Appendix II and mirror the balanced container case featured in Wong (2022).

[7] Following Notteboom et al. (2022), I attribute container handling costs to the transport operator. This study highlights that operators spend, on average, 15% of fleet management costs on empty repositioning.

[8] Appendix I considers homogeneous input prices. Similarly to a footloose capital model of Behrens and Picard (2011), this specification yields zero freight rates on low volume legs of round trip trade. Given that I do not observe zero empty container flows, nor zero freight rates across observed data, I conclude that there must be differences input prices across containers which vary by their state.

2.3.2 Weakly Imbalanced Trade

Suppose country j is a weak net importer of route $\overset{\leftrightarrow}{ij}$, where $l_{ij} \geq l_{ji}$. This leads to a prevailing empty redistribution problem, and the profit function is subject to a balanced container flow constraint, $l_{ij} = l_{ji} + e_{ji}$, where maximum service capacity is pinned down by $\max\{l_{ij}, l_{ji}\}$. This is consistent with other imbalanced trade models under a round trip setting (Ishikawa and Tarui, 2018). To ensure positive bilateral freight rates under imbalanced trade, I assume that the per-unit shipment cost of empties is cheaper than loaded handling on every route: $c_{\overset{\leftrightarrow}{ij}} > r_{\overset{\leftrightarrow}{ij}} \; \forall \; \overset{\leftrightarrow}{ij}$.

The profit maximization problem is expressed as

$$\max_{\{l_{ij}, l_{ji}, e_{ji}\}} \pi_{\overset{\leftrightarrow}{ij}} = T_{ij} l_{ij} + T_{ji} l_{ji} - c_{\overset{\leftrightarrow}{ij}}(l_{ij} + l_{ji}) - r_{\overset{\leftrightarrow}{ij}}(0 + e_{ji}) \qquad (2.4)$$

$$\text{s.t. } e_{ji} = l_{ij} - l_{ji}$$

Upon substituting the balanced container flow constraint into the profit maximization problem, freight rates for both legs of a given round trip $\overset{\leftrightarrow}{ij}$ are determined. Due to the price-taking nature of this perfectly competitive transport operator, these prices are underpinned by the marginal costs of container redistribution.

$$T^*_{ij} = c_{\overset{\leftrightarrow}{ij}} + r_{\overset{\leftrightarrow}{ij}} \; , \; T^*_{ji} = c_{\overset{\leftrightarrow}{ij}} - r_{\overset{\leftrightarrow}{ij}} \qquad (2.5)$$

These first order conditions intuitively state that the marginal benefit of an additional loaded container on the larger volume leg, from net exporter i to net importer j, is equal to the the direct per unit shipping cost, $c_{\overset{\leftrightarrow}{ij}}$, and the cost of an additional empty container on the return trip, $r_{\overset{\leftrightarrow}{ij}}$. An additional loaded container transported from j to i represents one less empty on route $\overset{\leftrightarrow}{ij}$, which implies the added cost of $c_{\overset{\leftrightarrow}{ij}}$ being partially compensated for by a cost reduction of $r_{\overset{\leftrightarrow}{ij}}$. Expressions for these bilateral freight rates can be substituted into Eq. (2.2).

$$p^*_{ij} = w_i \tau_{ij} + c_{\overset{\leftrightarrow}{ij}} + r_{\overset{\leftrightarrow}{ij}}, \qquad p^*_{ji} = w_j \tau_{ji} + c_{\overset{\leftrightarrow}{ij}} - r_{\overset{\leftrightarrow}{ij}} \qquad (2.6)$$

To solve for $\{l^*_{ij}, l^*_{ji}\}$, I insert Eq. (2.6) into the demand function for imported varieties.

$$l_{ij}^{*} = \left(\frac{\epsilon}{\epsilon-1}\frac{1}{a_{ij}}\right)^{-\epsilon}\left(w_i\tau_{ij} + c_{\overset{\leftrightarrow}{ij}} + r_{\overset{\leftrightarrow}{ij}}\right)^{-\epsilon}$$
$$l_{ji}^{*} = \left(\frac{\epsilon}{\epsilon-1}\frac{1}{a_{ji}}\right)^{-\epsilon}\left(w_j\tau_{ji} + c_{\overset{\leftrightarrow}{ij}} - r_{\overset{\leftrightarrow}{ij}}\right)^{-\epsilon}$$

The net difference in flows determines the empty container flow quantity and direction of flow. In this case $l_{ij}^{*} = \max\{l_{ij}, l_{ji}\} geq l_{ji}^{*}$, which implies that empties will travel on the lower volume backhaul route ji.

$$e_{ji}^{*} = \left(\frac{\epsilon}{\epsilon-1}\right)^{-\epsilon}\left(\frac{1}{a_{ij}}^{-\epsilon}\left(w_i\tau_{ij} + c_{\overset{\leftrightarrow}{ij}} + r_{\overset{\leftrightarrow}{ij}}\right)^{-\epsilon} - \frac{1}{a_{ji}}^{-\epsilon}\left(w_j\tau_{ji} + c_{\overset{\leftrightarrow}{ij}} - r_{\overset{\leftrightarrow}{ij}}\right)^{-\epsilon}\right) \tag{2.7}$$

The resulting equilibrium trade quantities, $\{l_{ij}, l_{ji}\}$, and values, $\{X_{ij}, X_{ji}\}$, on route $\overset{\leftrightarrow}{ij}$ are decreasing in the marginal cost of loaded container transport, local wages, and import tariffs imposed by the destination country.

$$X_{ij}^{*} = \left(\frac{\epsilon}{\epsilon-1}\frac{1}{a_{ij}}\right)^{-\epsilon}\left(w_i\tau_{ij} + c_{\overset{\leftrightarrow}{ij}} + r_{\overset{\leftrightarrow}{ij}}\right)^{1-\epsilon}$$
$$X_{ji}^{*} = \left(\frac{\epsilon}{\epsilon-1}\frac{1}{a_{ji}}\right)^{-\epsilon}\left(w_j\tau_{ji} + c_{\overset{\leftrightarrow}{ij}} - r_{\overset{\leftrightarrow}{ij}}\right)^{1-\epsilon} \tag{2.8}$$

However, variation in empty container handling costs, $r_{\overset{\leftrightarrow}{ij}}$, will have counteracting effects on outcome variables for a given round trip, highlighting a round trip effect in the model. For example, suppose the cost of empty outflows from country j rises. Not only does this stimulate j's exports, as existing cargo space on leg ji is reallocated from empty repositioning to exports, but in addition, transport capacity of route route $\overset{\leftrightarrow}{ij}$, relfected by l_{ij}^{*}, declines. Transport services on route $\overset{\leftrightarrow}{ij}$ decline due to the associated cost of maintaining imbalanced container flows.

2.3.3 Comparative Statics

Consider first a set of demand shocks to consumer preferences $\{a_{ij}, a_{ji}\}$ and import tariff adjustments $\{\tau_{ij}, \tau_{ji}\}$. In each case, a marginal change implies the following adjustments to the trade outcomes for route $\overset{\leftrightarrow}{ij}$. Recall for the trade value expression that we assume $\epsilon > 1$.

$$\frac{\partial T^*_{ij}}{\partial \tau_{ij}} = 0 \quad , \quad \frac{\partial T^*_{ji}}{\partial \tau_{ij}} = 0 \quad , \qquad \frac{\partial p^*_{ij}}{\partial \tau_{ij}} = w_i > 0 \quad , \quad \frac{\partial p^*_{ji}}{\partial \tau_{ij}} = 0$$
$$\frac{\partial l^*_{ij}}{\partial \tau_{ij}} = -\epsilon w_i \left(\frac{\epsilon}{\epsilon - 1}\frac{1}{a_{ij}}\right)^{-\epsilon} \left(w_i \tau_{ij} + c^{\leftrightarrow}_{ij} + r^{\leftrightarrow}_{ij}\right)^{-(\epsilon+1)} < 0 \quad , \quad \frac{\partial l^*_{ji}}{\partial \tau_{ij}} = 0$$
$$\frac{\partial X^*_{ij}}{\partial \tau_{ij}} = (1-\epsilon) w_i \left(\frac{\epsilon}{\epsilon - 1}\frac{1}{a_{ij}}\right)^{-\epsilon} \left(w_i \tau_{ij} + c^{\leftrightarrow}_{ij} + r^{\leftrightarrow}_{ij}\right)^{-\epsilon} < 0 \quad , \quad \frac{\partial X^*_{ji}}{\partial \tau_{ij}} = 0$$
$$\frac{\partial e^*_{ji}}{\partial \tau_{ij}} = -\epsilon w_i \left(\frac{\epsilon}{\epsilon - 1}\frac{1}{a_{ij}}\right)^{-\epsilon} \left(w_i \tau_{ij} + c^{\leftrightarrow}_{ij} + r^{\leftrightarrow}_{ij}\right)^{-(\epsilon+1)} < 0$$

A preference shock in country j for goods from country i would be represented by a_{ij} increasing. The resulting adjustments to outcome variables in this model are as follows.

$$\frac{\partial T^*_{ij}}{\partial a_{ij}} = 0 \quad , \quad \frac{\partial T^*_{ji}}{\partial a_{ij}} = 0 \quad , \qquad \frac{\partial p^*_{ij}}{\partial a_{ij}} = 0 \quad , \quad \frac{\partial p^*_{ji}}{\partial a_{ij}} = 0$$
$$\frac{\partial l^*_{ij}}{\partial a_{ij}} = \epsilon \frac{\epsilon - 1}{\epsilon} \left(\frac{\epsilon - 1}{\epsilon} a_{ij}\right)^{\epsilon-1} \left(w_i \tau_{ij} + c^{\leftrightarrow}_{ij} + r^{\leftrightarrow}_{ij}\right)^{-\epsilon} > 0 \quad , \quad \frac{\partial l^*_{ji}}{\partial a_{ij}} = 0$$
$$\frac{\partial X^*_{ij}}{\partial a_{ij}} = \epsilon \frac{\epsilon - 1}{\epsilon} \left(\frac{\epsilon - 1}{\epsilon} a_{ij}\right)^{\epsilon-1} \left(w_i \tau_{ij} + c^{\leftrightarrow}_{ij} + r^{\leftrightarrow}_{ij}\right)^{1-\epsilon} > 0 \quad , \quad \frac{\partial X^*_{ji}}{\partial a_{ij}} = 0$$
$$\frac{\partial e^*_{ji}}{\partial a_{ij}} = \epsilon \frac{\epsilon - 1}{\epsilon} \left(\frac{\epsilon - 1}{\epsilon} a_{ij}\right)^{\epsilon-1} \left(w_i \tau_{ij} + c^{\leftrightarrow}_{ij} + r^{\leftrightarrow}_{ij}\right)^{-\epsilon} > 0$$

Since these are perfectly competitive firms providing transport services, quantity supplied and freight rates are unresponsive to demand-side adjustments. However, when underlying costs of these services adjust, the corresponding freight rates charged will be adjusted uniformly. Endogenous transport costs are simply a linear function of underlying costs of shipping the required container inputs. Suppose the underlying cost of repositioning empty containers increases. This will make the existing trade balance less viable to manage. In response, firms must exhibit a widening of the freight rate 'gap' between ij and ji, where the net exporter countries sees freight rates of outgoing goods increase and net importer countries see freight rates of outgoing goods decline. This results in the trade balance narrowing and the 'backhaul' problem shrinking in scale.

$$\frac{\partial T^*_{ij}}{\partial r^{\leftrightarrow}_{ij}} = \frac{\partial p^*_{ij}}{\partial r^{\leftrightarrow}_{ij}} \quad > 0 \quad , \quad \frac{\partial T^*_{ji}}{\partial r^{\leftrightarrow}_{ij}} = \frac{\partial p^*_{ji}}{\partial r^{\leftrightarrow}_{ij}} \quad < 0$$

$$\frac{\partial l^*_{ij}}{\partial r^{\leftrightarrow}_{ij}} = -\epsilon \left(\frac{\epsilon}{\epsilon - 1} \frac{1}{a_{ij}} \right)^{-\epsilon} \left(w_i \tau_{ij} + c^{\leftrightarrow}_{ij} + r^{\leftrightarrow}_{ij} \right)^{-\epsilon - 1} \quad < 0 \quad ,$$

$$\frac{\partial l^*_{ji}}{\partial r^{\leftrightarrow}_{ij}} = \epsilon \left(\frac{\epsilon}{\epsilon - 1} \frac{1}{a_{ji}} \right)^{-\epsilon} \left(w_j \tau_{ji} + c^{\leftrightarrow}_{ij} - r^{\leftrightarrow}_{ij} \right)^{-\epsilon - 1} \quad > 0 \quad ,$$

$$\frac{\partial X^*_{ij}}{\partial r^{\leftrightarrow}_{ij}} = (1 - \epsilon) \left(\frac{\epsilon}{\epsilon - 1} \frac{1}{a_{ij}} \right)^{-\epsilon} \left(w_i \tau_{ij} + c^{\leftrightarrow}_{ij} + r^{\leftrightarrow}_{ij} \right)^{-\epsilon} < 0 \quad ,$$

$$\frac{\partial X^*_{ji}}{\partial r^{\leftrightarrow}_{ij}} = (\epsilon - 1) \left(\frac{\epsilon}{\epsilon - 1} \frac{1}{a_{ji}} \right)^{-\epsilon} \left(w_j \tau_{ji} + c^{\leftrightarrow}_{ij} - r^{\leftrightarrow}_{ij} \right)^{-\epsilon} \quad > 0,$$

$$\frac{\partial e^*_{ji}}{\partial r^{\leftrightarrow}_{ij}} = -\epsilon \left(\frac{\epsilon}{\epsilon - 1} \frac{1}{a_{ij}} \right)^{-\epsilon} \left(w_i \tau_{ij} + c^{\leftrightarrow}_{ij} + r^{\leftrightarrow}_{ij} \right)^{-\epsilon - 1} - \epsilon \left(\frac{\epsilon}{\epsilon - 1} \frac{1}{a_{ji}} \right)^{-\epsilon} \left(w_j \tau_{ji} + c^{\leftrightarrow}_{ij} - r^{\leftrightarrow}_{ij} \right)^{-\epsilon - 1} < 0$$

Proposition 1. Under the assumption of competitive transport firms and imbalanced trade,

(i) When transport costs are endogenous and constrained under balanced container flows, an increase in the tariff rate of imports from i to a net importer country j, τ_{ij}, reduces the scale of the backhaul problem destined for the partner net exporter country i: $\frac{\partial e^*_{ji}}{\partial \tau_{ij}} < 0$

(ii) When transport costs are endogenous and constrained under balanced container flows, an increase in j's preferences for variety i, a_{ij}, increases the scale of the backhaul problem destined for the partner net exporter country i: $\frac{\partial e^*_{ji}}{\partial a_{ij}} > 0$

(iii) When transport costs are endogenous and constrained under balanced container flows, an increase in the per unit cost of empty container inputs, $r^{\leftrightarrow}_{ij}$, reduces the scale of the backhaul problem, given that freight rates resultingly rise on the full route ij and lessen on the return route ji: $\frac{\partial T^*_{ij}}{\partial r^{\leftrightarrow}_{ij}} > 0, \frac{\partial T^*_{ji}}{\partial r^{\leftrightarrow}_{ji}} < 0, \frac{\partial e^*_{ji}}{\partial r^{\leftrightarrow}_{ij}} < 0$

The relationship between the scale of the empty container redistribution problem and the skewness of the existing trade balance can be examined in a proportional manner. These expressions simplify otherwise non-linear relationships between outcome variables to a reduced linear relationship that can be taken directly to the surrounding data, should one be equipped with bilateral container traffic flows, as well as containerized trade values. I represent the scale of the empty container redistribution problem with E_{ji}, which indicates the share of empties as a percentage of total container outflows from a net importer country j to net exporter i.

$$E^*_{ji} = \frac{e^*_{ji}}{l^*_{ji} + e^*_{ji}} = 1 - \left(\frac{a_{ji}}{a_{ij}}\right)^{\epsilon} \left(\frac{w_i\tau_{ij} + c^{\leftrightarrow}_{ij} + r^{\leftrightarrow}_{ij}}{w_j\tau_{ji} + c^{\leftrightarrow}_{ij} - r^{\leftrightarrow}_{ij}}\right)^{\epsilon} \tag{2.9}$$

Proposition 2. Under the assumption of competitive transport firms and imbalanced trade,

(i) When transport costs are endogenous and constrained under balanced container flows, an increase in the tariff rate of imports from i to a net importer country j, τ_{ij}, reduces the scale of the backhaul problem destined for the partner net exporter country i: $\frac{\partial E^*_{ji}}{\partial \tau_{ij}} < 0$

(ii) When transport costs are endogenous and constrained under balanced container flows, an increase in j's preferences for variety i, a_{ij}, increases the scale of the backhaul problem destined for the partner net exporter country i: $\frac{\partial E^*_{ji}}{\partial a_{ij}} > 0$

(iii) When transport costs are endogenous and constrained under balanced container flows, an increase in the per unit cost of empty container inputs, $r^{\leftrightarrow}_{ij}$, reduces the scale of the backhaul problem, given that freight rates rise on the full route ij and lessen on the return route ji: $\frac{\partial T^*_{ij}}{\partial r^{\leftrightarrow}_{ij}} > 0$, $\frac{\partial T^*_{ji}}{\partial r^{\leftrightarrow}_{ji}} > 0$, $\frac{\partial E^*_{ji}}{\partial r^{\leftrightarrow}_{ij}} < 0$

Examining the skewness of the trade balance using an import-export ratio from j's perspective: $\frac{X_{ji}}{X_{ij}}$

$$\frac{X^*_{ij}}{X^*_{ji}} = \left(\frac{a_{ji}}{a_{ij}}\right)^{-\epsilon} \left(\frac{w_i\tau_{ij} + c^{\leftrightarrow}_{ij} + r^{\leftrightarrow}_{ij}}{w_j\tau_{ji} + c^{\leftrightarrow}_{ij} - r^{\leftrightarrow}_{ij}}\right)^{1-\epsilon} \tag{2.10}$$

Using Eq. (2.9) and (2.10), I find that any exogenous shock to empty outflows will adjust the import-export ratio in the same sign direction for trade route ij.

For example, should US preferences for goods from China rise, the existing trade deficit would increase $\left(\Delta\frac{X_{ij}}{X_{ji}} > 0\right)$ and the associated scale of empty container redistribution originating from the US would rise ($\Delta E_{ji} > 0$).[9]

2.4 Data

The main data set of the paper combines monthly US port samples of containerized trade and associated container traffic flows, both for empty and loaded units. Auxiliary tariff and wage data is used for the calibration of exogenous parameters throughout the counterfactual analyses of this study.

2.4.1 Containerized Goods

I use monthly trade data from the US Census Bureau, which details the imports and exports of containerized goods at the US port level by value and weight for each US trade partner. The available sample period begins with January 2003 and provides commodity-level stratification down the to six-digit Harmonized System (HS) level. Using this data, I form a balanced panel of the top 14 port locations for containerized trade flows.[10] In cases of port alliances, I assume that port infrastructure is jointly utilized between ports. The ports of Seattle & Tacoma as well as New York & Newark are each combined into two unique port authorities, the NWSA and PANYNJ, respectively.

2.4.2 Container Traffic

Using this informed shortlist of the top containerized US ports, I approached each respective port authority individually and retrieved monthly 20-foot equivalent unit (TEU) traffic flow data. I received four separate series: (i) inbound loaded containers, (ii) outbound loaded containers, (iii) inbound empty containers, and (iv) outbound empty containers. To my knowledge, this is the first study in international economics to document and use novel empty container repositioning data. Unlike containerized goods flows, I do not observe the origin or ultimate

[9] I test this identity empirically in Subsection 5.1 and find significance at a monthly frequency.

[10] These individual ports include New York (NY), Los Angeles (CA), Houston (TX), Long Beach (CA), Norfolk (VA), Savannah (GA), Charleston (SC), Oakland (CA), Newark (NJ), Seattle (WA), Tacoma (WA), Baltimore (MD), New Orleans (LA) and Jacksonville (FL).

destination of container traffic flows. A 40-foot intermodal container is counted as two TEUs. To ensure a balanced and representative panel of data, I have limited container traffic flows to those observed between January 2012 and December 2021 of 12 key ports, which represents approximately 80% of national container unit thruflows. For more details on the wider time series of port data made available for this study, see Appendix III.

2.4.3 Auxiliary Data

For the quantitative exercises detailed in Section 6, I calibrate observable parameters of wages and tariffs through the use of monthly manufacturing wages and specific tariff rates data. Time series of monthly wages between 2012 and 2021 are sourced from the International Labor Organization (ILO), which specifies annual averages of manufacturing wages in USD value. To account for unreported wage values for specific years of the data, I use OECD annualized growth rates of average monthly manufacturing wages and infer the associated level amounts. I use the U.S. Bureau of Labor Statistics' "Consumer Price Index for All Urban Consumers", which excludes contributions made by food and energy, to deflate these series. I leverage use of the UNCTAD Trade Analysis Information System (TRAINS) database for effective tariff rates on manufactured goods between the US and its trade partners. 'Manufactures' are an SITC 4 product group predefined on the World Integrated Trade Solution (WITS) platform of the World Bank.

2.5 Stylized Facts

In this section, I present two stylized facts which test the validity of the balanced container flow constraint and the hypothesized negative relationship between the share of empty container outflows and the export-import value ratio of containerized goods. While many of these facts have previously been theorized, this study is the first to directly document the responsiveness of the empty container redistribution problem to variation in the US trade balance. Additionally, I provide port-level evidence which suggests that the volume of container traffic at a given port is a strong predictor of whether said port acts as a net inflow or net outflow in terms of its contribution to nationally balanced container flows. I use this third stylized fact to motivate my treatment of the European Custom Area as a single entity, which at only this scale of operations maintains balanced container

redistribution comparable to the US.

2.5.1 Empty Repositioning & Trade Balance Asymmetry

Stylized Fact 1. *A positive deviation in country j's export-import ratio with country i is correlated with a negative deviation in the volume of empty container units shipped from j to i as a share of total container units shipped from j to i.*

When combined, Eq.(2.9) and Eq.(2.10) imply that a higher export-import ratio of a net importer, the US in this case, implies lower empties as a percentage of total container outflows. As US imports from a net exporter country rises ($X_{ji}/X_{ij} \downarrow$), the asymmetry in trade volumes between these two countries grows, which implies that the logistical burden in servicing imbalanced trade – through the repositioning of empty container units – has grown ($E_{ji} \uparrow$).

$$E^*_{ji} = 1 - \left(\frac{X^*_{ji}}{X^*_{ij}}\right)\left(\frac{w_j\tau_{ji} + c^{\leftrightarrow}_{ij} - r^{\leftrightarrow}_{ij}}{w_i\tau_{ij} + c^{\leftrightarrow}_{ij} + r^{\leftrightarrow}_{ij}}\right) \tag{2.11}$$

Given that I do not observe container flows between the US and individual countries, I instead aggregate across US ports and I test this negative relationship empirically through variation in trade and container flows between the US (j) and the rest of the world (i),

$$E^*_{jit} = \alpha + \beta\left(\frac{X^*_{jit}}{X^*_{ijt}}\right) + \mu_{jit} \quad , \quad E^*_{ijt} = \alpha + \beta\left(\frac{X^*_{ijt}}{X^*_{jit}}\right) + \mu_{ijt}, \tag{2.12}$$

where $\beta < 0$ is my proposed null hypothesis. I use four measures of trade balance skewness: the export-import ratio, $\frac{\text{Exports}}{\text{Imports}}$, a net-gross ratio featured in Brancaccio et al. (2020), $\frac{\text{Exports - Imports}}{\text{Total Trade}}$, and their respective opposites of $\frac{\text{Imports}}{\text{Exports}}$ and $\frac{\text{Imports - Exports}}{\text{Total Trade}}$ when addressing inflows of empties. As displayed in Table 2.1, a relatively smaller US trade deficit is associated with a lower scale of empty redistribution. This highlights adjustments in the empty repositioning burden that transport operators face, given variation in bilateral trade volumes across round trips. In Table 2.2, I use the Net-Gross ratio featured in Brancaccio et al. (2020), and observe further support for this proposed relationship between the prevailing trade imbalance and the size of the empty container redistribution problem.

I next examine co-movement between empty container outflows and opposite-direction US imports of containerized goods. As featured in Table 3.2, empty

Table 2.1: Trade Flow Ratio & Empty Shares

Dependent Variable: Empty Container Share of Total Flows				
	Outbound		Inbound	
Model:	(1)	(2)	(3)	(4)
Export/Import (USD)	-0.9575***			
	(0.0687)			
Export/Import (kg)		-0.3909***		
		(0.0288)		
Import/Export (USD)			-0.0253***	
			(0.0062)	
Import/Export (kg)				-0.0327***
				(0.0097)
Mean Dep. Var	43.51%		7.47%	
Mean Regressor	0.322	0.711	3.143	1.427
n-obs	120	120	120	120
Within R^2	0.58	0.68	0.30	0.15

Heteroskedasticity-consistent 'White' standard-errors. Codes: ***: 0.01, **: 0.05, *: 0.1. Examines variation empty containers as a share of total container outflows, given variation in the skewedness of the trade balance. I use month and year fixed effects to control for influences of the US business cycle and seasonality.

Table 2.2: Net-Gross Ratio & Empty Shares

Dependent Variable: Empty Container Share of Total Flows				
	Outbound		Inbound	
Model:	(1)	(2)	(3)	(4)
$\left(\frac{\text{Net Exports}}{\text{Gross Trade}}\right)^{\text{USD}}$	-0.8510***		0.2322***	
	(0.0703)		(0.0428)	
$\left(\frac{\text{Net Exports}}{\text{Gross Trade}}\right)^{\text{KG}}$		-0.5756***		0.1121***
		(0.0514)		(0.0308)
Mean Dep. Var	43.51%		7.47%	
Mean Regressor	-0.514	-0.172	-0.514	-0.172
n-obs	120	120	120	120
Within R^2	0.57	0.65	0.37	0.21

Heteroskedasticity-consistent 'White' standard-errors. Codes: ***: 0.01, **: 0.05, *: 0.1. Examines variation empty containers as a share of total container outflows, given variation in the net-to-gross trade balance. I use month and year fixed effects to control for influences of the US business cycle and seasonality.

container flows are highly correlated with opposite-end flows of US trade. My results suggest that a 1 percent rise in US imports is, on average, associated with a 1.45% increase in outflows of empty container units from the US. In sharp contrast, significant unilateral responses are not detected for given roundtrips between the

US and the rest of the world. I assume this co-movement is primarily driven by exogenous variation in route-specific unobservables such as preference parameter shifts across consumer bases, wage variation, container unit handling costs and tariff rate adjustments. Examining the robustness of these results in Appendix IV, I find that variation in the weight of opposite-end trade flows is also predictive of adjustments in empty container repositioning. Additionally, upon disaggregating to *within-port* variation I find similar patterns of positive co-movement between trade flows and the opposite-end empty container repositioning problem.

Table 2.3: Empty Container Elasticity with Respect to Trade Flows

Dependent Variable: Empty Container Flows (TEU)				
	ln(Outbound)		ln(Inbound)	
Model:	(1)	(2)	(3)	(4)
ln(Inbound Trade)	1.450***		-0.0903	
	(0.0917)		(0.2267)	
ln(Outbound Trade)		0.3229		0.8409***
		(0.2489)		(0.2559)
n-obs	120	120	120	120
Within R^2	0.59	0.02	0.002	0.16

Heteroskedasticity-consistent 'White' standard-errors. Codes: ***: 0.01, **: 0.05, *: 0.1. US empty container flows are regressed on US containerized trade flows, expressed in terms of deflated USD. For example, a one percent increase in 'Inbound Trade' is associated with a 1.45% rise in outbound empty container flows. I use month and year fixed effects to control for influences of the US business cycle and seasonality.

2.5.2 Balanced Container Flows

Stylized Fact 2. *A positive deviation from the total container units transported from i to j is correlated with a positive deviation from the total container units transported from j to i.*

Thus far I have shown that trade balances are strongly indicative of the scale of the empty container redistribution. Upon aggregating across US ports, evidence suggests that national levels of container inflows and outflows appear largely balanced, but only when incorporating contributions made by empty container redistribution. This lends strong support for the balanced container flow constraint, which underpins my partial equilibrium model of empty container redistribution. In Table 2.4, I regress the total number of inbound container units on the total number of outbound containers at the national level. These results suggest that

a system of balanced container exchanges exists even within a given month of containerized transport, as highlighted by the reported coefficient not statistically differing from 1 at a 99% confidence level. In contrast, when focusing on only loaded container exchanges, a far more commonly reported measure of container traffic at the port level, this balance in the exchange of transport equipment is left completely obscured.

Table 2.4: Balanced National Container Flows

Dependent Variable: ln(Inbound Container Flows)			
Model:	Total (1)	Loaded (2)	Empty (3)
ln(Total Outbound)	1.012***		
	(0.0210)		
ln(Loaded Outbound)		-0.0913	
		(0.2841)	
ln(Empty Outbound)			-0.4641***
			(0.0314)
Observations	120	120	120
Within R^2	0.94	-0.007	0.62

Heteroskedasticity-consistent 'White' standard-errors. Codes: ***: 0.01, **: 0.05, *: 0.1. Container flows inbound to the US are regressed on outbound container flows. Results are consistent with estimates using month and year fixed effects.

Figure 2.1 suggests that container flows remain balanced across widenining windows of time. As I expand the relevant time interval, through backward sums of loaded and empty container unit flows, noise surrounding these estimations lessens and levels remain approximately balanced at the 1-to-1 percentage point ratio. Although larger aggregations of container flow statistically deviate from the 1-to-1 ratio of balanced container flows, these deviations are low in power, only ranging between 1 to 2 percent in size.[11]

Container unit measures have largely been focused on loaded traffic flows and often rely on imputed measures available through third-party private entities such as S&P Panjiva (Flaaen et al., 2021; Steinbach, 2022; Ardelean et al., 2022). Fo-

[11]This is likely a symptom of my sample of ports being based on the largest ports in the US. As I highlight in my next stylised fact, although my container flow data represents over 80% of total container traffic in the US, the smaller ports that I exclude from my sample most likely function as net outflows of container units. With their inclusion, and a full representation of the population of container flows, I hypothesize that my mild deviations from the 1-to-1 balanced container exchange would reduce in size.

Figure 2.1: Balanced National Container Flows by Time Window

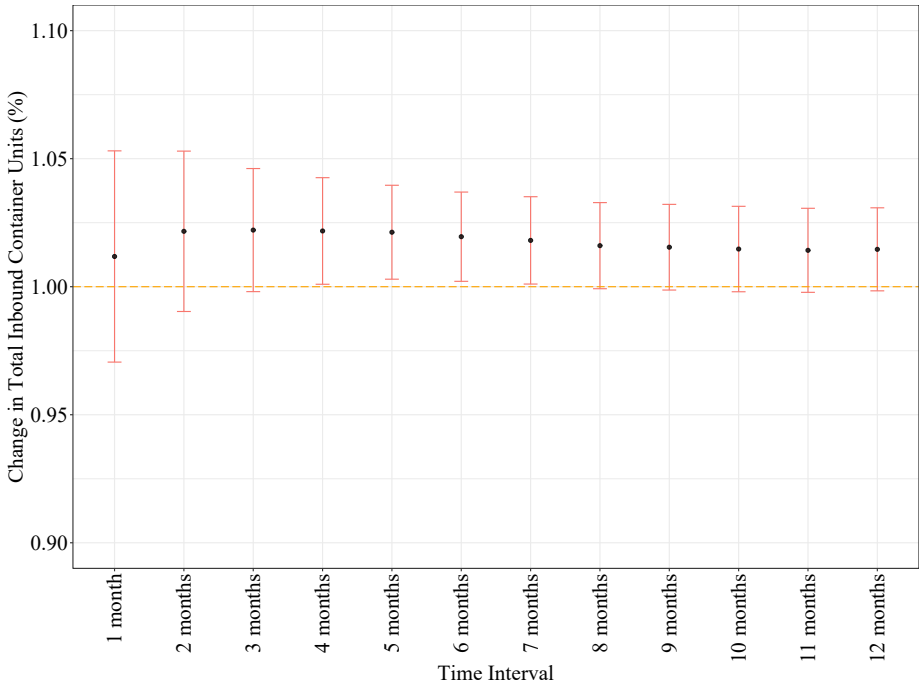

Heteroskedasticity-consistent 'White' standard-errors. Both the dependent variable and regressor are log-transformed. Total inbound containers are summed across a balanced panel of 12 US ports and represent both loaded and empty containers, is regressed on total outbound containers for these same set of ports. Sums are taken across windows of varying lengths of time, ranging from bilateral exchanges within a single month to exchanges across 12 month backward sums.

cusing only on loaded container units – whether reported directly by ports or estimated using Bill of Laden Records from the U.S. Customs and Border Protection (CBP) agency – conceals logistical efforts between the US and the rest of the world. No semblance of balanced container flow patterns are present when excluding empty container repositioning and focusing only on loaded container flows (Figure 2.2).

These findings, when jointly considered, suggest that the system of intermediate transport equipment present in the US achieves a balanced exchange of transport equipment, only when taking into account empty units. In the next subsection, I consider how individual ports contribute to nationwide balanced container flows.

2.5.3 Port Heterogeneity

Stylized Fact 3. *A positive deviation in the total volume of container inflows and outflows of port p is correlated with a positive deviation from the net volume in container inflows less outflows of port p.*

Figure 2.2: Imbalanced National Loaded Container Flows by Time Window

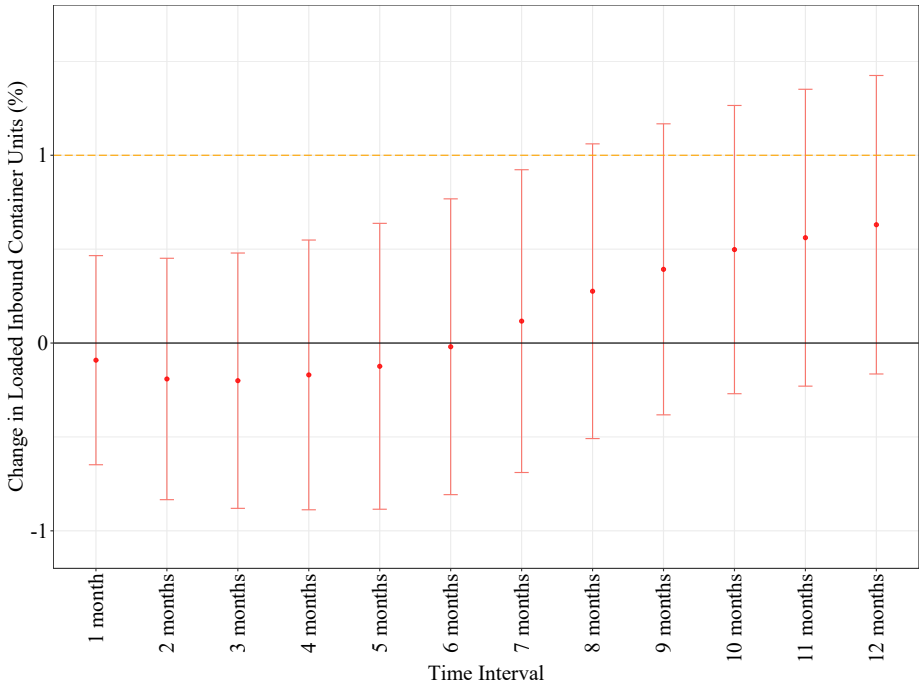

Heteroskedasticity-consistent 'White' standard-errors. Both the dependent variable and regressor are log-transformed. Total inbound containers are summed across a balanced panel of 12 US ports and represent both loaded and empty containers, is regressed on total outbound containers for these same set of ports. Sums are taken across windows of varying lengths of time, ranging from bilateral exchanges within a single month to exchanges across 12 month backward sums.

Although total container flows – both loaded and empty containers – are balanced at the national level, patterns in port-level container flows highlight that the largest ports in the US function as net inflows of total containers, while mid-tier sized ports act as net outflows of total container units. This suggests that an interdependence exists across ports, which maintains balanced container flows at a national level. To the best of my knowledge, these statuses across ports have not yet been documented in the transport economics literature. In Figures 2.3a and 2.3b, I display annual net differences in total container flows by port for 2017 along with the geographic dispersion of these key entry and exit points for container equipment.

These statuses are consistent across time. Los Angeles, Long Beach, PANYNJ, and NWSA act as net inflows whereas the remaining set of mid-tier ports are net outflows. As displayed in Figure 2.4, the total thruflow of loaded and empty containers at a given port is highly predictive directional status. This pattern likely relates to comparative advantages in handling vessels of varying sizes. Larger ports may attract net inflows due to their relatively higher efficiency in handling arriving

Figure 2.3: Port Specialization by Net Inflow Status (2017)

Panel A: Net Inflow of Total Container Units by Port

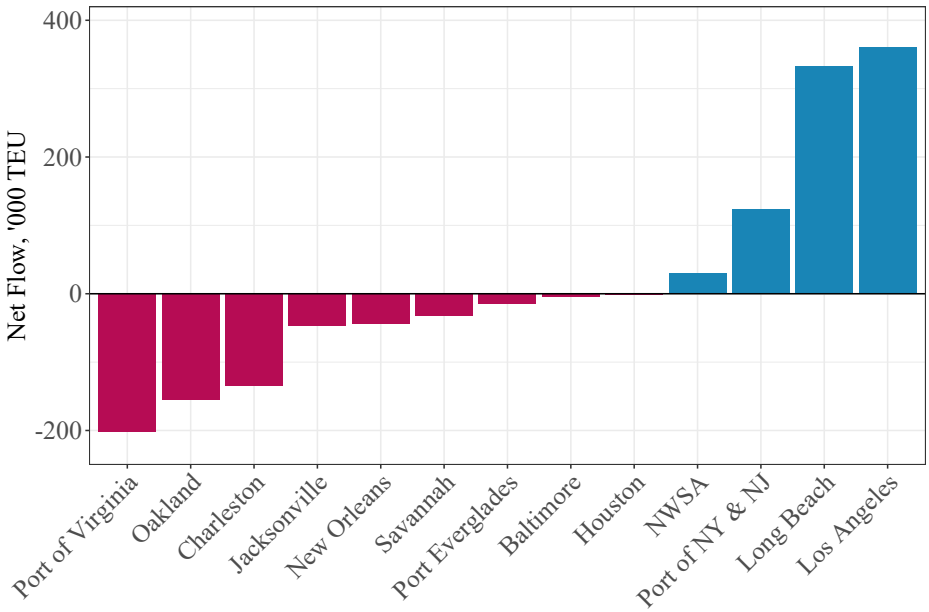

Panel B: Geographic Dispersion of Net Inflows

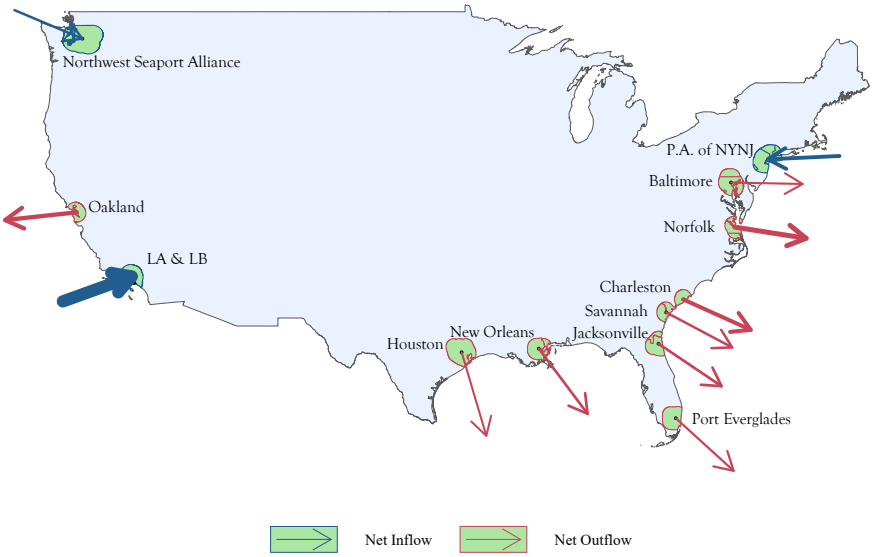

goods (Blonigen and Wilson, 2008). This pattern may also be partly explained by the 'hub and spokes' mechanism in which larger vessels travel between port hubs in

order to exploit lower per-unit transport costs (Ganapati et al., 2021). Additionally, one may levy use of a proximity-concentration argument, in which case the best of both worlds would be for imports to arrive at ports positioned closely to high density population centers such as California and New York (Ducruet et al., 2018). Upon examining average vessel sizes between these port groups, I find that larger vessels arrive at larger net inflow ports, where per-unit import prices are likely cheaper (Table 2.5).

Table 2.5: Average Containership Gross Tonnage by Port Size

Ports	2014	2015	2016	2017	2018	2019
Major Ports	31,558	32,990	34,790	36,569	38,141	39,241
Mid-tier Ports	26,564	27,999	29,639	31,637	32,784	33,407

Note: Reports the average gross tonnage, a nonlinear measure of a ship's overall internal volume, weighted by the number of vessel visits in each port. *Source:* US Army Corp of Engineers, Port Clearance data.

Given that national bilateral container flows are balanced, yet individual ports act as either net inflows or outflows of container units, I suggest that an interdependence across ports which has persisted since at least January 2003. As highlighted in Wong and Fuchs (2022), shipments arriving at major ports see some portion of goods, along with intermodal transport equipment, be transported across the US hinterland. While some container units may return to their US port of origin, my findings suggest that many units of equipment depart from the US through alternative ports around the country, particularly through mid-tier sized ports. Rather than treating each port's trade with the world as an isolated bilateral set of roundtrip trade routes, this container traffic data exhibits signs of a national-level round trip effect which permeates across ports. Containers are redistributed across US ports and collectively form a balanced container flow system necessary to support round trip containerized trade. This motivates my counterfactual analysis of balanced container flow trade at the country rather than port level.

The intensity of involvement in empty container repositioning also varies widely across ports. In 2021, while larger ports adjacent to net exporter countries – such as Los Angeles or Long Beach – shipped out 70–80% of containers completely empty, the southern ports of Houston (TX), New Orleans (LA) and Jacksonville (FL) have maintained historical averages of 6–22%. As displayed in Table 2.6, while differences in these shares are longstanding, many of the larger ports and their respective transport operators have been shouldering an increasing burden of the growing US trade deficit and resulting rise in empty container repositioning.

Figure 2.4: Port Specialization by Total Container Thruflow (2012-2021)

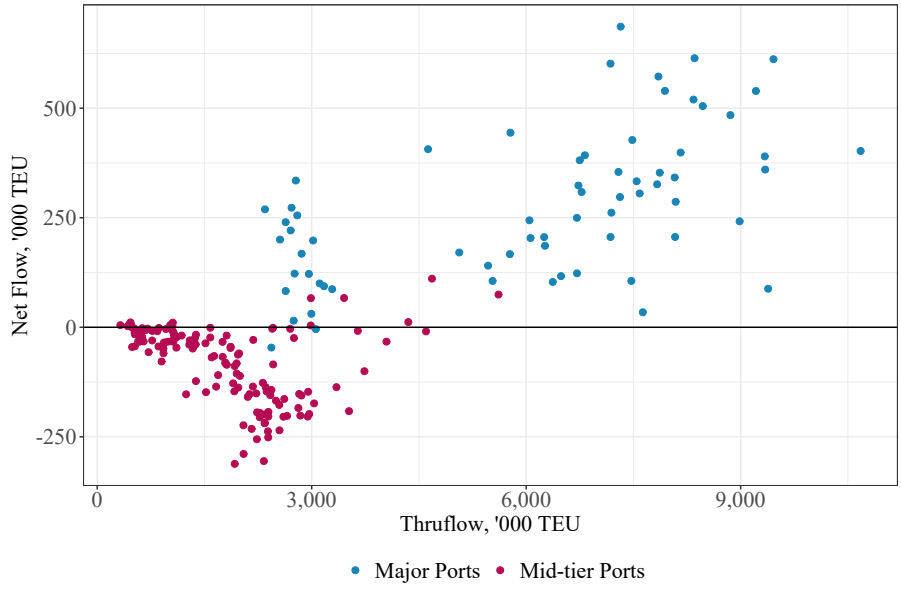

Table 2.6: Average Empty Share of Container Outflows by Port-Year (%)

Port	2013	2015	2017	2019	2021
Los Angeles, CA	48.69	56.87	57.55	60.61	76.94
Long Beach, CA	46.70	55.52	58.77	61.11	69.05
Port of NY & NJ	44.68	55.34	56.96	60.31	68.89
Savannah, GA	21.91	34.61	32.50	36.00	49.93
Norfolk, VA	15.82	27.93	33.14	37.56	41.18
Charleston, SC	23.19	30.32	30.32	36.61	41.09

2.6 Counterfactual

I use the quantitative model featured in Section 3 to consider the policy implications of OSRA22. I first outline a simple two-country baseline scenario of US-RoW (Rest of the World) round trip containerized trade. I then illustrate the flaws associated with this approach, and motivate the estimation of bilateral loaded container flows by US trade partner. By separately representing countries, I include two key features of round trip containerized trade; (i) bilateral flows of empty container units between the US and RoW, and (ii) heterogeneity across trade partners' varying extensive and intensive margins of reliance on empty container outflows from the US. I provide a diagnostic assessment of these estimates, identify the key set of restrictions and assumptions necessary to yield the most compelling fit

to UNCTAD regional container traffic data and proceed with a calibration and estimation of model primitives. Upon establishing this multi-country baseline scenario, I then introduce the counterfactual policy measure – an empty container outflow (ECO) quota, applied through a specific per-unit tax on outgoing empty containers. Accounting for trade partners' varying degrees of reliance on empty containers provides the same qualitative result of policy backfiring on the import leg of US round trips, but introduces quantitatively larger bilateral adjustments in containerized trade.

2.6.1 US-RoW Baseline

In a simple two-entity representation of US containerized trade, a single round trip services all of US containerized trade. Given that I do not observe the origin or destination of port-level container traffic in the US, this is a natural starting point for examining how market intervention would affect containerized trade outcomes. According to the *no excess capacity* constraint featured in Equation (2.4), empty container flows can only be present on one leg of a round trip route. However, as displayed in Figure 2.5, the US maintains positive bilateral flows of empty containers with the rest of the world. For example, at the height of the COVID-19 supply chain crisis approximately 63% of outbound containers left the US empty and less than 4% of incoming container units were empty. In order to reconcile this disparity between observed data and a baseline scenario of containerized trade, I use the net difference in empty container flows to represent the scale of the empty container repositioning problem.

In this setting, I establish a baseline scenario of the model using trade and container traffic data specific to average monthly levels reported in 2017.[12] Using a generalized method of moments (GMM) estimator in which a system of trade and container flow equations, $\{X_{ij}, X_{ji}, l_{ij}, l_{ji}\}$, featured in Equations (2.7) and (2.8), I can represent the endogenous set of moments in the data and exactly identify four unknown model primitives. I reduce the number of unknown exogenous parameters to four by calibrating observable parameters based on a trade-weighted average of tariffs on manufactures, a trade-weighted average of monthly manufacturing wages, and an elasticity of demand of 20.96, represented by ϵ in Eq. (3.1) and estimated using monthly data by Wong (2022).[13]

[12]This choice of year avoids any complications that later periods associated with the China-US Trade War and COVID-19 epidemic would introduce.

[13]See Appendix section V for a detailed description of baseline estimation, as well as an

Figure 2.5: Empty Share of Container Movement by Year-Month

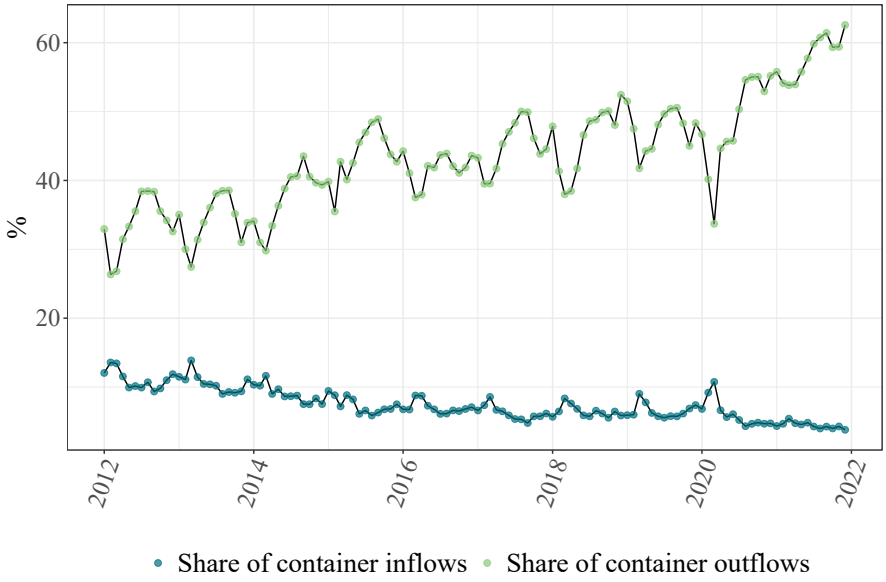

While this remedy simplifies a representation of US round trip trade, the use of net empty flows in a single round trip setting also introduces three drawbacks; (i) an under-representation of the scale of the empty repositioning problem, (ii) no distinguishing between net exporter and net importer statuses across US trade partners, and (iii) no acknowledgement of differences in degrees of reliance on the return of empty containers across net exporters. If this first point is left unaddressed, my estimates may under–report both the substitution of transport services from empty repositioning to US exports and the associated contraction of vessel capacity. Secondly, no accounting of trade partners' extensive margin of reliance on empty container inflows from the US leads to policy effects being spread across all participating countries. In order to determine where vessel capacity will retract, these effects must instead be focused on the net exporter subset of trade partners, which rely on these equipment flows. Lastly, the intensive margin of trade partners' reliance on empty container redistribution also needs to be represented in this baseline scenario. Particular net exporters maintain notably more skewed trade imbalances relative to other US trade partners, which deepens the effect of ECO quotas on these round trips in particular. By accommodating for these last two factors, adjustments in vessel capacity and consequential contractions in import levels will be better reflective of particular vulnerability that net exporter trade partners would exhibit.

assessment of model fit and depiction of the broad backfiring effect of ECO quotas under a US-RoW setting.

To incorporate these key features of containerized trade, I prepare a multi-country baseline scenario, which uses observed country-level containerized goods flows by value and estimated volumes of container unit flows to identify a full set of unobserved exogenous parameters via GMM. In the next section, I detail how I estimate loaded container flows by US trade partner.[14]

2.6.2 Multi-Country Container Flows

To establish a baseline scenario of multiple countries, I require two components; (i) a set of calibrated parameters for each country's round trip with the US, which consists of the real wage and tariff rate for 2017, $\{w_j, w_i, \tau_{ij}, \tau_{ji}\}$, and (ii) a set of observable trade outcomes of each round trip, which reports levels of US imports, exports, loaded container inflows and loaded container outflows with each country, represented by $\{X_{ij}, X_{ji}, l_{ij}, l_{ji}\}$, respectively. Given that I do not observe country-specific flows of loaded container units, I estimate these values using variation in commodity-specific weights of containerized goods exchanged between specific US-country pairs.[15]

2.6.2.1 Assumptions

Container units used in shipping include a set of operational characteristics which define the maximum weight that each individual unit can carry. Therefore, a positive relationship exists between the number of loaded container units used in transport and the weight of goods shipped to a given country. This fact is well-documented in Ardelean et al. (2022), which finds a consistent synchronization of variation in per-unit freight rates of containerized goods imported to Chile across per-kilogram and per-TEU measures. In support of this evidence, I find that a simple log-log regression of US loaded container inflows on the weight of containerized US imports yields a 1-for-1 co-movement between the two measures.

Individual container units not only feature an explicit weight limit, but also report cubic volume capacity. Both the weight and the cubic volume of a particular set of goods determines how many container units are needed for transport.

[14]The results of the simple US-RoW baseline setup and counterfactual exercise are detailed in Appendix V.

[15]The number of countries for which I can estimate container flows is larger than the set featured in my baseline calibration of the model. This is due to only a subset of individual countries having average monthly manufacturing wage data available from 2012 to 2021.

As Holmes and Singer (2018) demonstrates, the binding constraint for a given container unit is almost always volume, rather than weight. This introduces the possibility that differences in the dimensionality of specific products may alter the rate at which variation in weight contributes to the number of necessary container units used. For example, a kilogram of wooden products may utilize more of a given container's cubic volume capacity when compared to a metallic product of similar weight.

To estimate the number of TEU units utilized on a given US-trade partner round trip, I exploit monthly commodity-level variation in the weight of containerized goods, which is observed at the US port to country-level. I incorporate both weight and volume considerations in the decomposition of port-level US container using

$$l_{pt}^{f} = \sum_{j=1}^{J} l_{pjt}^{f} = \sum_{j=1}^{J} \sum_{k=1}^{K} \beta^{fjk} w_{pjkt}^{f}, \;\; f \in \{\text{Imports}, \text{Exports}\}, \tag{2.13}$$

where at US port p, in year-month t, the total number of loaded container units l_{pt} is the sum of containerized weights of country j for commodity k, w_{pjkt}^{f}, times respective loading factors, β_{jk}. Superscript f indicates the direction that containerized goods and their associated loaded containers are moving from the US perspective. Using these population parameters, the data generating process for a loaded container flows between the US and country j is

$$l_{US-j,t}^{f} = \sum_{p=1}^{P} l_{pt}^{f} = \sum_{p=1}^{P} \sum_{k=1}^{K} \beta^{fjk} w_{pjkt}^{f}, \tag{2.14}$$

where combinations of observed w_{pjkt}, and estimated $\hat{\beta}^{fjk}$ allows me to construct fitted values of national container units flows in each direction across J countries. Using this proposed identity would imply a JK number of regressors, which is infeasible even at the HS-2 commodity level aggregation. I assume that the manner in which cubic volume capacity determines commodity-specific loading factors does not vary across countries. For example, should workers at the port of Mumbai fit three metric tonnes of furniture into a single container unit, I assume that, on average, they use available cubic volume as efficiently as workers loading containers in Rotterdam. Given my assumption of loading factor invariance with respect to

the country of origin, my estimation is represented as

$$l_{pt}^{f} = \sum_{k=1}^{K} \beta^{fk} \sum_{j=1}^{J} w_{pjt}^{f} + \varepsilon_{pt}^{f} \tag{2.15}$$

For a given commodity traded between the US and partner countries, the use of available volume capacity may differ on either leg of a round trip, leading to differences in commodity-specific loading factors. While restricting loading factors β to be invariant by direction f would double the associated observation count of this exercise and allows me to exploit wider variation in commodity-specific volumes, this restriction may also inadvertently pool within-commodity variation in too aggregated a manner. For example, consider HS item 68 which includes articles of stone, plaster and similar materials. The US may be exporting particularly low quality stone masonry (low loading factor) while more delicate, higher mineral quality articles may originate from Japan (high loading factor). Should these high quality materials be associated with relatively low volumes of kilogram weight, while low quality US exports of stone articles are associated with high volumes of weight, this restriction would inadvertently yield a negative coefficient in which for HS-68, as weight increases, the loading factor associated with this shipments lowers.[16]

Lastly, while I do estimate loading factors across 97 HS2 commodity-level goods, I use only the 72 HS2 products featured in the UNCTAD's Trade Analysis Information System (TRAINS) SITC product group of 'manufactures' in establishing a multi-country baseline scenario of the model. This is due to my reliance on manufacturing wage data in the calibration of the model.

2.6.2.2 Loading Factor Estimates

Under these assumptions, I regress Eq.(2.15) to generate loading factor estimates across a variety of fixed effects combinations, which control for differences in the scale of container flow operations at each port, local industry compositions in each port's surrounding area and potential biases in loading factors attributed

[16]To address these potential sources of bias, I have explored country-groupings for a given commodity which potentially limits product differentiation, reducing the influence the differences across quality within a product group may have on the estimation of an appropriate loading factor. These geographic and income-based country groupings for specific commodity weights have been evaluated in Appendix VI and generally contribute little towards improving loading factor estimates.

to the seasonality of within-commodity variation. To assess the importance of composition differences in commodities by direction at HS2 level, I have estimated both direction-invariant (joint) and f-specific (separate) loading factors.

Across both 'joint' and 'separate' loading factor exercises, I find that port fixed effects are key in minimizing the number of negative coefficients that crop up among the 97 HS2 products included. These negative coefficients would suggest that, all else controlled for, the higher the weight of goods loaded into containers, the lower the number of containers necessary to ship said goods. A rather salient objective therefore is to use the specification which yields the most plausible set of coefficient estimates.

Figure 2.6: Loading Factor Estimates by Commodity

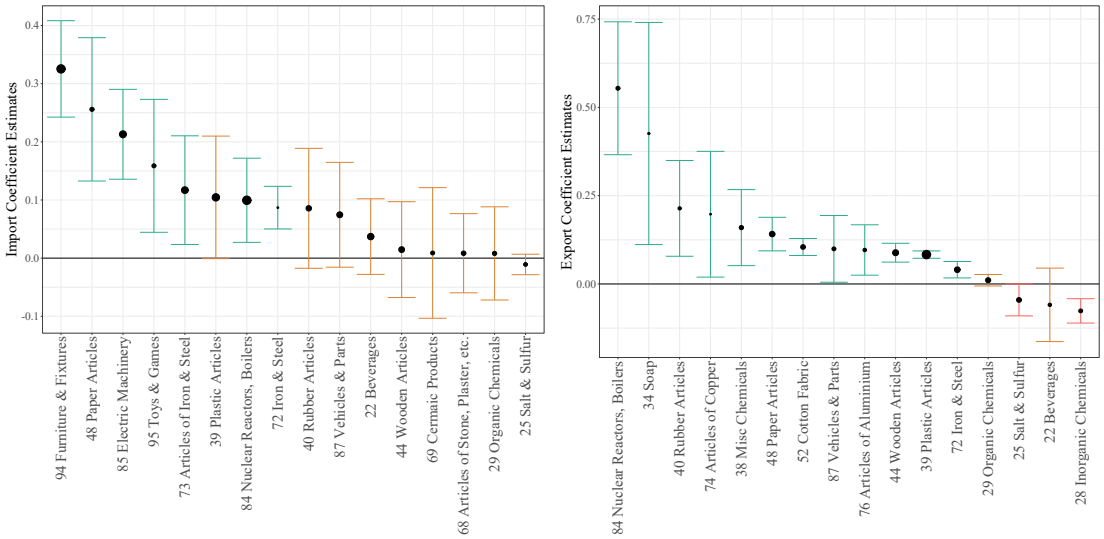

Clustered (port) standard-errors. Regresses monthly port-level total loaded container inflows (outflows) on a set of commodity-specific weights of containerized US imports (exports), expressed in metric tons. Each coefficient can be interpreted as the average loaded container unit volume occupied by a metric ton of commodity k. Results displayed for top 16 manufactured commodities by value. Observed total container levels and associated containerized weights of goods are observed between Jan-2012 and Dec-2021 and use port & year-month fixed effects. Point sizes vary based on share of associated trade flow.

These estimates are generally significant and positive in value.[17] Combinations of port, year and month fixed effects yield within R^2 values ranging from 0.78-0.97 for imported goods and 0.59-0.98 for goods exports. Furniture, paper articles and electrical machinery are found to be the most demanding commodities on incoming container volumes. For example, a single metric ton of furniture is estimated to

[17]Appendix VI provides diagnostic tables which highlights that commodities associated with negative loading factors are generally traded in particularly low volumes. Given that each exercise estimates 97 commodity coefficients under varying combinations of fixed effects, it us unsurprising that some false-positive findings of negative coefficients would populate overall results.

take up one third of a container unit whereas a metric ton of iron & steel is estimated to take up only a tenth of a container unit. US exports of nuclear reactors, boilers, soap and rubber articles are estimated to be the most demanding on container volumes whereas plastic articles, iron & steel occupy far less loaded container unit volume.

Upon predicting port-level container flows & aggregating across US ports, I compare these US estimates to observed national loaded container flows. I find that predicted values using 'separate' loading factors are associated with lower root mean square error values and higher correlation score compared to 'joint' estimates.[18] I therefore focus attention on loading factor estimates specific to the direction in which goods are flowing and generate country–level loaded container flows,

$$\begin{aligned} \text{Container Inflows: } \hat{l}_{j-US,t} &= \sum_{p=1}^{P} \hat{l}_{jpt} = \sum_{p=1}^{P} \sum_{k=1}^{K} \hat{\beta}^{\text{Imp},k} w_{jpkt}, \\ \text{Container Outflows: } \hat{l}_{US-j,t} &= \sum_{p=1}^{P} \hat{l}_{pjt} = \sum_{p=1}^{P} \sum_{k=1}^{K} \hat{\beta}^{\text{Exp},k} w_{pjkt}, \end{aligned} \tag{2.16}$$

where these bilateral volumes are determined by the product of commodity k's containerized weight at time t and a corresponding time-invariant estimated loading factor, β^{fk}, summed across P ports and K commodities.

2.6.2.3 Container Flow Estimates

Estimates of loaded container flows are sensitive to the assumptions and methods used in identifying loading factors across commodities. While the 'separate' estimation of loading factors by direction yields far stronger results, the precise set of fixed effects appears open to multiple combinations, so long as port fixed effects are included. To determine which fixed effects yield the best match and quantify differences in performance, I compare estimated volumes and bilateral ratios of loaded container flows to UNCTAD records of annual loaded containers exchanged on US-East Asian & US-European routes (UNCTAD, 2022).

As highlighted previously, product quality likely plays a role in determining the container volume capacity required for the transport of a given metric ton of a specific commodity. To address this concern, I have also estimated loading fac-

[18] See Table 5.10 in Appendix VI for further details.

tor estimates for each commodity specific to groupings of countries by continental boundaries and by income per-capita. Product quality may be correlated across the imports and exports of countries that share close proximity with one another. Similarly, countries of similar wealth levels may trade in goods of a comparable quality levels. Country-groups' commodity-specific loading factors, each representing a regressor, would introduce a far more substantial extent of sparseness data used for estimation. I address this concern by removing any country-group commodity specific-regressor if less than 40% of its monthly port-level weight flows are reported as positive values. This introduces a trade-off between added precision for key, actively traded commodities across each country-group at the loss of broader commodity representation upon aggregating across port data. Following a series of container flow diagnostics – outlined in Appendix VI – I use port & year fixed effects with no geographic or income-based groupings. These relatively less restricted empirical approaches often introduced greater uncertainty in loading factor estimates without any notable improvement in fits to untargeted UNCTAD measures of two of the US's busiest bilateral lanes of regional loaded container flows. This fit is depicted in Figure 2.7.

Figure 2.7: Model Fit – Loaded Container Ratios by Region (2012-2021)

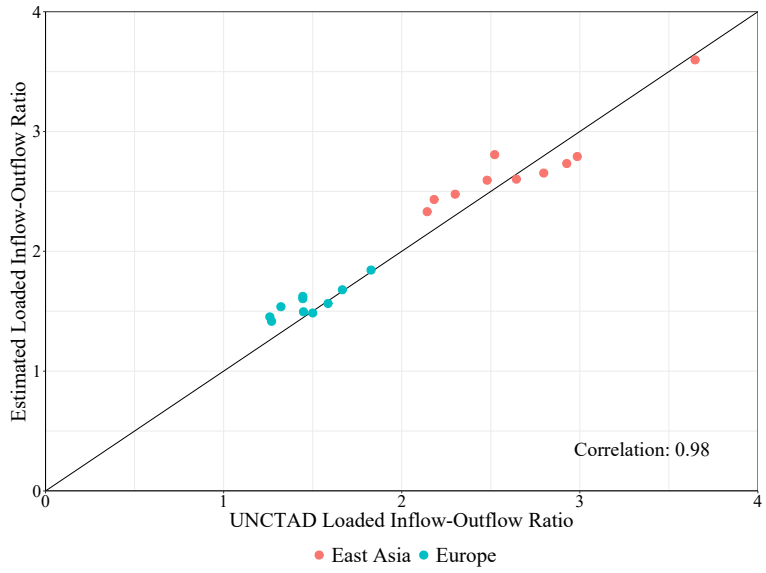

Note: Observed levels originate from UNCTAD records on regional total loaded container flows by year and were untargeted in the estimation of individual country container flow estimates.

While the loading factors and resulting country-level container flow estimates are available across a wide range of countries, I limit the use of these estimates to the subset of countries that report manufacturing wage measures needed for model calibration between 2012 to 2021. Additionally, I introduce balanced container

flow system that incorporates the entire European Single Market and exclude both Mexico and Canada due to land borders with the US potentially limiting the degree to which bilateral flows of containerized trade are fully serviced by maritime transport operators.[19] Lastly, given that the model is calibrated on manufacturing wages, I restrict container flow estimates to levels associated with the weight of containerized manufactures travelling between the US and its respective trade partners.[20]

Upon accounting for these product and multi-country constraints, I generate loaded container flow estimates specifically for manufactured goods across the countries featured in Figure 2.8. This limits my use of multi-country estimated bilateral container flows to represent 70% (50%) of containerized import (export) value.

Figure 2.8: Estimated Container Flows by Country and Direction

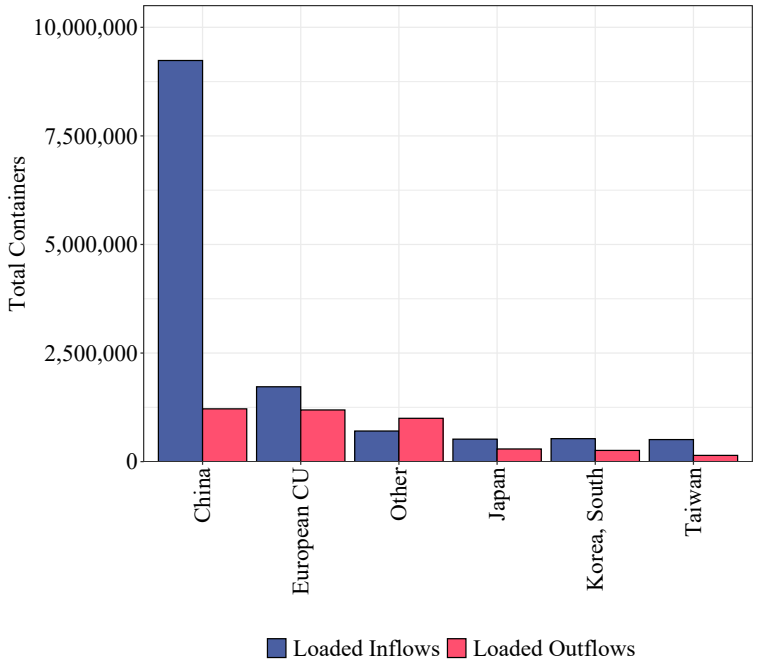

Note: Compared total US container traffic in 2017 across my 12 sampled ports, these disaggregated estimates of manufactured goods flows across the choice subset of trade partners represents 70% (50%) of containerized goods imports (exports) and 65% (43%) of loaded container inflows (outflows). The country group of "other" represents 10 additional lanes of round trip container traffic with the US – consisting of Argentina, Australia, Chile, Columbia, Dominican Rep., Ecuador, Malaysia, the Philippines, Singapore and Turkey.

[19] See Appendix VII for evidence of balanced container flows only at the Single Market level.

[20] The contributing commodities are those featured in the TRAINS SITC-based product group known as 'Manufactures'. I use the United Nations Statistics Divisions' correspondence tables, HS - SITC/BEC, to convert SITC 4 codes belong to the manufactures product group on TRAINS into a set of relevant HS 2017 codes. https://unstats.un.org/unsd/classifications/Econ Last accessed as of March 17th 2023.

2.6.3 Solution Method and Model Calibration

To establish a baseline set of exogenous parameters, I first calibrate a select subset of model primitives and then estimate the remaining set of unknown model primitives using a Generalized Method of Moments (GMM) approach. For a given ij round trip containerized shipping route, the set of unknown exogenous parameters ρ is equal to $\left(a_{ij}, a_{ji}, w_i, w_j, \tau_{ij}, \tau_{ji}, c^{\leftrightarrow}_{ij}, r^{\leftrightarrow}_{ij}\right)$ and the elasticity of substitution measure is represented by ϵ.

For wages, I use an OECD index of monthly manufacturing income growth rates and the International Labor Organization (ILO) annual measure of monthly manufacturing income levels, which are available for a subset of trade partners. For tariffs, I use the UNCTAD Trade Analysis Information System (TRAINS) database on effective manufactured goods' tariff rates, all of which are reported across US trade partners.[21] I deflate the value of trade flows and USD-converted wage levels for each trade partner using the Bureau of Labor Statistics Consumer Price Index for all urban consumers, which considers all final good items less food and energy, averaged across major US cities.[22] Lastly, I include an estimate of price elasticity of demand provided by Wong (2022) and specific to containerized trade, where $\hat{\epsilon} = 20.96$ is assumed to be common across individual trade routes.

Using these calibrated parameters and a vector of country-level endogenous trade outcomes, represented by $Y^{\text{data}} = \{X_{ij}, X_{ji}, \hat{l}_{ij}, \hat{l}_{ji}\}$, I estimate the remaining set of unobserved preference parameters and route-specific per unit handling costs of containers, $\tilde{\rho} = \left(a_{ij}, a_{ji}, c^{\leftrightarrow}_{ij}, r^{\leftrightarrow}_{ij}\right)$, via GMM.[23] I minimize the object function,

$$R = \text{dist}' \times \bar{W} \times \text{dist}, \tag{2.17}$$

where dist represents the log difference in vectors of 'observed' and model-guess trade outcomes between the US and a given trade partner, $\log(Y^{\text{data}}) - \log(Y^{G})$, and $\bar{W}$ is a weight matrix that assists in speeding the identification of $\tilde{\rho}$. I use measures from 2017 to estimate these parameters of underlying long-run primitives of containerized trade. This specific year allows me to avoid any complications or

[21] Upon establishing a login for http://wits.worldbank.org/, select 'Advanced Query' and then the 'Tariff and Trade Analysis' subsection. I use the SITC 4 product group labelled 'manufactures' and the effective tariff rate measure.

[22] U.S. Bureau of Labor Statistics, Consumer Price Index for All Urban Consumers: All Items Less Food and Energy in U.S. City Average [CPILFESL], retrieved from FRED, Federal Reserve Bank of St. Louis; https://fred.stlouisfed.org/series/CPILFESL, November 1st, 2022.

[23] The respective outcome variables used are observed average monthly containerized imports & exports (USD value) and estimated loaded container inflows and outflows.

concerns that the use of data from the proceeding China-US trade war or period of COVID-related port congestion could introduce. Given that for each round trip, I estimate four unknowns across a system of four equations, my model is just-identified and I exactly match the observed trade values and estimated loaded container flows.

To assess the performance of this exercise on untargetted features and moments in the data, I provide three means of assessing model fit for this baseline scenario; (1) the empty container redistribution share of container fleet management costs averages between 14.9–21.3%, depending on the given year, which places US-related costs of empty container redistribution relatively close to 15% share reported by Rodrigue (2020); (2) the difference in pairs of preference parameters on round trip routes attributes stronger tastes on the larger volume importing lane, with ratios of tastes being highly predictive of the skewness prevailing in trade imbalances; (3) using marginal costs of handling loaded, $c_{\underset{ij}{\leftrightarrow}}$, and empty container flows, $r_{\underset{ij}{\leftrightarrow}}$, implied freight rates are greater for portions of US round trips that feature a full set of loaded containers, which is reflective of empirically documented freight rate asymmetries under imbalanced trade (Hummels et al., 2009).

In order to address the importance of specifying country-specific container flows, I also prepare a US-RoW calibration and estimation of exogenous model primitives using these same inputs. This second baseline scenario, which represents trade through a single round trip, under-represents empty container redisitribution and effectively spreads the reliance on the return of this transport equipment from the US across all trade partners. By introducing both the US-RoW and multi-country baseline scenarios to the same counterfactual change, I quantify the importance of accounting for variation in extensive and intensive margins of dependencies on empty container redistribution from the US.

2.6.4 Counterfactual Policy Background

In this subsection, I discuss recent changes to liner shipping regulation through the Ocean Shipping Reform Act of 2022 (OSRA22), a portion of which aims to limit empty container redistribution in favor of stimulating greater US exports. To examine the consequences of restricting empty container outflows, I outline a simplified version of this policy in which the policymaker has capped the share of empty container outflows relative to total outflows from the US through a per-unit tax rate.

2.6.4.1 Pre-policy Conditions

Between October 2021 and November 2022, vulnerabilities in US transport services became notably tangible. A resurgence of economic activity in the US contributed to elevated import demand, which resulted in a widening of the US trade deficit. The associated increase in the asymmetry of bilateral containerized trade volumes coincided with record-high rates of empty container outflows. For example, according to container traffic levels provided by the Port Authority of Los Angeles, the percentage of empties featured on container outflows originating from LA increased from a pre-COVID historical average of 50 percent to over 80 percent in the latter half of 2021. As of 2022, for every five containers that entered the US laden with goods, three of these containers leave the US empty.

These signs of elevated empty redistribution are the result of a sudden shift in market conditions. For example, if US demand for Chinese manufactured goods suddenly increased, a greater number of loaded container units would be transported to the US from China. Upon redistributing containers back to China – to service subsequent Chinese exports – the percentage of empties featured on outbound voyages from the US would rise. Log-jams of vessels and transport equipment also made empty repositioning relatively more appealing. They require less handling due to less time spent transporting goods within a given destination country's hinterland area, are readily usable upon arrival at a destination port and relatively cheaper to transport due to their lower weight. These factors suggest that in certain cases, it may be more profitable for a firm to transport an empty container unit rather than service an additional loaded container unit that cannot be repurposed as quickly.

These opportunity costs and existing differences in import demand between two regions determine the scale of the empty container redistribution problem. Due to the relatively higher opportunity costs of servicing loaded container units and the increased volume of import traffic to the US, a greater percentage of shipping capacity was reassigned to service empty container transport. However, short-run adjustments to a new empty-loaded outflow equilibrium and the increased difficulty for exporters in securing vessel allocated space contributed to a swift bipartisan response from US policymakers.

2.6.4.2 Ocean Shipping Reform Act 2022

In December 2021, the House of Representatives passed H.R.4996, the Ocean Shipping Reform Act of 2021. This bipartisan bill sought to empower the Federal Maritime Commission (FMC) by introducing legislation that prohibits the 'unreasonable' refusal of vessel capacity from US exports. The stated intention of this bill is to ensure fair trade by supporting good-paying American manufacturing jobs and agricultural exports. Upon passing this proposed legislation on to the Senate, lawmakers were explicit in further emphasizing the intent of this bill.

> *"The rulemaking under paragraph (1)*[24] *shall address the unreasonableness of ocean common carriers* ***prioritizing the shipment of empty containers*** *while excluding, limiting, or otherwise reducing the shipment of full, loaded containers when such containers are readily available to be shipped and the appurtenant vessel has the weight and space capacity available to carry such containers if loaded in a safe and timely manner."*
>
> H.R.4996, the Ocean Shipping Reform Act of 2021

In February 2022, the Senate passed OSRA22, which maintained this prohibition. This bill has since entered into public law as of June 16th 2022. However, the bill did not specify how this restriction on prioritizing empties must be imposed and instead delegated this task to the Federal Maritime Commission (FMC). The first challenge for the FMC involves defining cases of 'unreasonable refusals of vessel capacity' and then it must devise measures by which to punish any violators. The FMC has since issued a Notice of Proposed Rulemaking (NPRM), which has suggested that 'unreasonable' refusals must be determined on a case-by-case basis (FMC, 2022). To judge reasonability, the FMC would require that ocean common carrier provide a documented export strategy that enables the efficient movement of export cargo.[25]

In response, the World Shipping Council (WSC), an association that represents 90% of transport operators, has clarified some of the operational and commercial

[24] This relates to Section 9 of the proposed bill, Prohibition on Unreasonably Declining Cargo, where transport operators are warned against *"engaging in practices that unreasonably reduce shipper accessibility to equipment necessary for the loading or unloading of cargo".*

[25] No connection is provided in the NPRM between an "export strategy" document requirement and how this establishes a definition of how a transport operator may unreasonably refuse to negotiate or deal with respect to vessel space accommodations. This has led to a second round of public discourse by the FMC and an extension to these deliberations.

realities that contribute to empty repositioning. A static export strategy is suggested to not align with the business practices of the industry, which is "volatile with rapidly changing factors that impact space availability on a daily basis." Most notably, the WSC goes on to highlight that "export trades cannot be considered in isolation from import trades". This important facet of containerized shipping acts as the cornerstone of my container redistribution model.

> *Carriers use the same containers, ships, and marine terminals to handle both import and export containers, and vessels operate on continuous loops, not distinct import and export legs disconnected from one another. Additionally, the proposed regulatory language does not address in any way the basic reality that imbalanced trades (as reflected on in the preamble) require the repositioning of equipment, which adds an additional dimension to planning and operating vessel networks. It defies the reality of ocean transportation to ignore these complexities and to treat the export and import legs of a trade as unrelated.*
>
> World Shipping Council response to FMC (2022)

While the FMC continues to deliberate over these key details, I propose an exercise which embodies policymakers' intent of limiting empty redistribution in favor of greater capacity allocation towards US exporters. To capture the potential effects of this unconventional policy approach, I introduce a per-unit tax on empty container outflows to the baseline model, where the tax rate is calibrated to target a capped share of empties as a percentage of total container outflows. I consider a restriction to transport equipment use by the US policymaker, where the expressed goal is to return empty activity back to its historical share of 40% of total container outflows.

To establish this counterfactual scenario, the US policymaker sets a per-unit empty tax rate of γ on the outbound channel of round trip transport, which targets the historical average of empty container share of container gross outflows, $\bar{E}_{ji} = 0.4$. This moderate ECO quota scenario represents a case in which policymakers are content with the prior long run average of the empty container redistribution problem.[26] Using the same tax rate, $\gamma_{\bar{E}_{ji}=0.4}$, on the US-Row version of the baseline

[26]I have also examined an 'extreme' ECO quota, in which $\gamma_{\bar{E}_{ji}=0}$ is targeted and the practice of empty container redistribution is eliminated. Similarly to the main results described in the next section, I find that the policy contributes to a decline in vessel capacity on net exporter trade routes and reduction in overall trade value and volume.

scenario, I highlight the benefits of accounting for heterogeneous dependencies on empty container redistribution from the US.

2.6.5 Main Results

As displayed Table 2.7, a moderate ECO quota stimulates export activity. US exporters flock to relatively cheaper freight rates for round trip services to net exporter countries, which results in a substitution from empty container redistribution to additional loaded container servicing. The US containerized trade deficit, represented by the import-export ratio, also declines by 37.3%. However, a focus only on this outbound leg of US round trip transport ignores further market developments, known as round trip effects, which may also be of interest to the policymaker. Relative to the baseline scenario, a multi-country model of US containerized trade sees a 17.7% decline in the real value of imports. This is attributed to the greater cost associated with returning the empties, which passes through entirely to the price of US imports under this perfectly competitive setting. As a result, the price of imported goods rises by 1.7% while US exporters see their goods' prices decline by 4.3%. The overall capacity of TEU services for round trips between the US and individual countries declines by 18.6% due to policy introducing an added friction servicing imbalanced volumes of trade. This leads to a reduction in container redistribution. The scale of the empty container redistribution problem as a percentage of total US container outflows falls by 37.4%.

Table 2.7: Disaggregated Counterfactual Outcomes

U.S. Measures	Imports	Exports	Imp. Price	Exp. Price	Value	Vol.	Capacity
$\Delta\%$	-17.7	31.1	1.7	-4.3	-8.5	-4.4	-18.7

Note: These results reflect percentage changes from their respective 2017 baseline scenarios of the partial equilibrium model and are based on estimates of loaded container flows & observed levels of associated trade in containerized manufactured goods.

While adjustments in individual flow measures and the trade balance are of interest, understanding changes to the scale of overall trade activity is of the greatest importance in this setting. Should overall trade activity decline, so too would the associated gains from trade. In the case of the multi-country setup, a moderate ECO quota contributes to an 8.5% (4.4%) decline in the value (volume) of containerized trade, which suggests a degradation in the gains to trade the US and its trade partners would have otherwise been able to accrue.

Across the subset of net exporters which engage in containerized trade with the US, the pre-existing scale of the empty container repositioning problem acts as a strong predictor of this policy's effectiveness. Using US outflows of empties to country i as a percentage of total US container outflows to country i, I find that countries particularly reliant on empty repositioning yielded the largest declines in imports. East Asian trade partners maintained the high empty container shares in the predefined baseline scenario (Figure 2.9). Upon the introduction of a per-unit tax on empty repositioning, these particularly asymmetric trade routes faced the greatest contractionary pressure. Transport operators servicing these routes respond by introducing larger contractions in vessel capacity, which in turn lowers the value and volume of imports shipped from East Asia to the US. The greater each country's intensive margin of reliance on empty containers, represented by the empty share term, the greater the decline in import levels.

Figure 2.9: US Import Value by Net Exporter (2017)

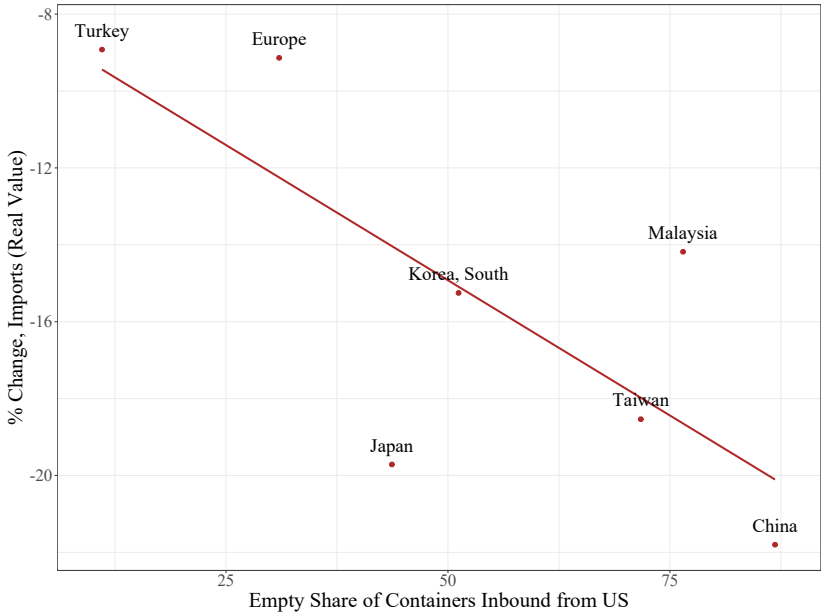

Note: The real value of imports is used, deflated by US CPI for urban areas, less food and energy. The empty share represents $100 * \frac{\text{US-Country Empty Outflows}}{\text{Total US-Country Outflows}}$, and reflects pre-policy shares of total container outflows.

Given that the repositioning of empties has become more expensive, the underlying costs of loaded container services are relatively more appealing. This is reflected by a decline in the US-net exporter freight rate and a substitution into increased US export activity across net exporter round trip trade routes. Countries such as China and Japan yield greater changes due to their particularly significant reliance on empty containers and greater declines in export prices (Figure 2.10).

Figure 2.10: US Export Value by Net Exporter (2017)

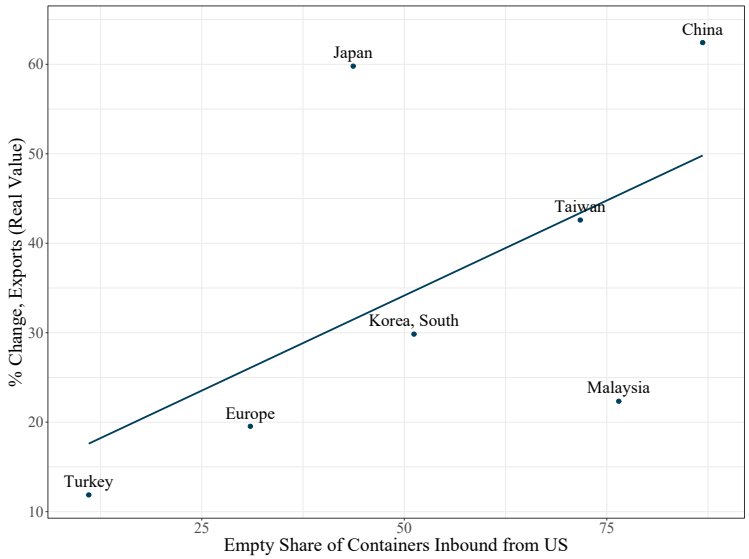

Note: The real value of exports is used, deflated by US CPI for urban areas, less food and energy. The empty share represents $100 * \frac{\text{US-Country Empty Outflows}}{\text{Total US-Country Outflows}}$, and reflects pre-policy shares of total container outflows.

Lastly, the inflationary pressure generated by a tax on empty container units appears to have particularly pronounced effects on endogenous import prices across the net exporters that exhibit a greater reliance on empties. As displayed in Figure 2.11, Turkey and Europe yield relatively low pass-through of this new tax burden on prevailing market prices. However, East Asia yet again yields evidence of greater exposure to this form of protectionism, in which percentage point increases in price levels are almost threefold larger.

The sizable loss in transport equipment accessibility and the acuteness of this decline on routes with a particularly high dependencies on empty repositioning leads to noteworthy changes in country shares of the US import market. As displayed in Figure 2.12, in some cases net exporters gain market shares despite being reliant on empty container repositioning. China, which receives approximate four empty returns for every five loaded containers shipped to the US, suffers a two percentage point loss in its share of containerized US imports. Given Europe's relatively weaker dependency on empty container repositioning, although imports do decline, the overall decline in total US containerized imports of manufactures falls by a greater margin. This results in the European Custom's Area developing a larger share of overall US imports, despite being negatively affected by an ECO quota.

Figure 2.11: US Import Price Inflation by Net Exporter (2017)

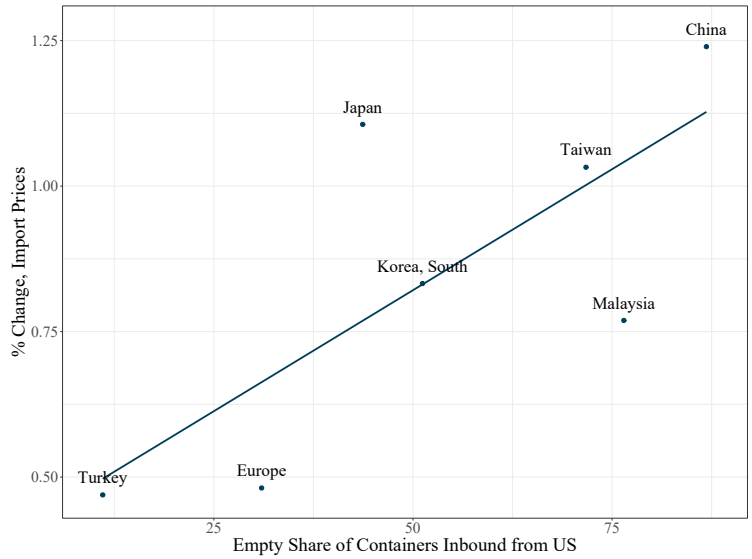

Note: Real prices are reflective of the average value of containerized goods per loaded TEU. Deflated using US CPI for urban areas, less food and energy. The empty share represents $100 * \frac{\text{US-Country Empty Outflows}}{\text{Total US-Country Outflows}}$.

Figure 2.12: Change in Trade Partner Shares of US imports (2017)

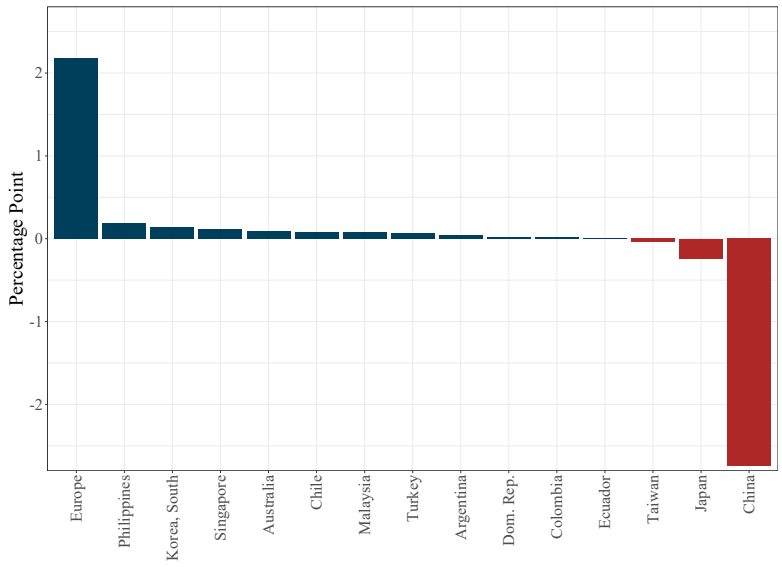

Note: Real values of imports are deflated using US CPI for urban areas, less food and energy.

2.7 Conclusion

This paper provides a quantitative approach towards understanding the novelties of containerized trade and its reliance on the repositioning of physical transport equipment. The first contribution of this study identifies how variation in the avail-

ability of transport equipment may feed into trade outcomes on the opposite leg of a given round trip, and enriches means of incorporating endogenous transport costs. In this particular case, I internalize the cost of repositioning container units to associated transport operators and highlight how variation in such costs may result in adjustments to the available transport capacity devoted to a particular origin-destination pair. Using novel container traffic data provided by the largest ports in the US, representative of 80% of gross container unit traffic, I directly connect theory and empirics. Through this connection, I document a round trip effect taking place in which adjustments in the prevailing trade balance of the US, through larger trade deficits, enlarges the scale of the empty container repositioning problem. Through supportive evidence, I argue that it is opposite-leg trade outcomes that drives variation in the empty container repositioning problem of the US.

I also contribute theoretically to the literatures of international trade and transport economics through my partial equilibrium model of container repositioning. This model that yields positive bilateral freight rates under a setting of perfectly competitive transport operators with perfect knowledge, which as highlighted by Demirel et al. (2010), normally introduces unintuitive and troublesome model predictions. By representing container units physically in the joint profit maximization problem of transport operators, I circumvent a persistent challenge in modelling imbalance round trip trade in which the lower volume leg of a given route yields a freight rate of zero. Additionally, this challenge is not unique to maritime commerce and can be considered applicable across multiple modes of transport. In future work, it would be of interest to understand how this phenomenon interacts with recent developments in market concentration across the global fleet of transport operators. For example, does a greater extent of coordination through cooperative shipping alliances across the global fleet limit container shortages?

Lastly, I quantitatively evaluate how interfering in the use of this transport technology can affect trade flows. Although studies of trade conventionally consider protectionism to occur through adjustments to tariff rates, goods quotas, and other means of applying non-tariff measures, little is understood of how policymakers' targeting of transport equipment could influence trade outcomes. I highlight how a modern and unconventional form of protectionism may backfire and negatively affect broader public. This specific form of policy is motivated by the recently passed Ocean Shipping Reform Act of 2022 (OSRA22), in which restrictions to empty container outflow activities were introduced in an effort to

stimulate US exports. My findings suggest that government intervention in the repositioning of empty container units may lead to unanticipated and adverse effects, in which overall vessel capacity servicing the US reduces due to the relatively greater expense associated with servicing trade imbalances. Within trade lanes, exports grow, but this minor boon are outscaled by a reduction in import activity and increased price inflation for US consumers. Great care should be taken in considering the joint-effects of liner shipping regulation, rather than focusing on an export lane of round trip traffic in isolation. To quote the World Shipping Council's response to OSRA22, "It defies the reality of ocean transportation to ignore these complexities and to treat the export and import legs of a trade as unrelated."

These considerations are important to consider, not only in maritime shipping, but across trucking, rail and airline services. Each of these forms of round trip service accommodate differences in trade volume. As I highlight, particularly asymmetric round trip volumes are the most subject to malaise effects, given the introduction of empty container repositioning regulation. Should we wish to fully embrace trade flows, irrespective of differences in bilateral flows, this requires particularly low costs of handling empty containers. According to these comparative statics, developments in foldable container technology would dramatically cut required dock space for storage and further expand global trade opportunities.

Going forward, I believe this study adds emphasis toward more granular data on port traffic and container shipping details. I welcome the data provision requirements introduced through OSRA22, which enables the Federal Maritime Commission to publish a quarterly report detailing the total import and export tonnage and the total loaded and empty 20-foot equivalent units per vessel operated by ocean common carriers. Upcoming container tracking technology would be of great interest and enable studies such as this paper to directly connect port container traffic through the US hinterland. As my estimation country-specific container flows may indicate, further studies of maritime transport would also be enhanced by a greater knowledge of container origins, routes travelled upon and ultimate destinations. These improvements in data availability would enhance the identification of key transport bottlenecks, allow for the accounting of transshipping activity and better our understanding of countries' joint dependency on efficient transport equipment usage.

Bridge

In this essay, I isolated the 'backhaul problem' faced across multiple transport sectors, in which empty equipment needs to be returned to a location of relatively greater transport demand. While asymmetries in trade are one means of influencing the formation of endogenous transport costs, one must not only consider the container but also the vessel carrying these containers. In the next substantive essay of my dissertation, I explore the evolution of containership services in the US, documenting patterns associated with individual US port visits between January 1977 and December 2023. Underlying container handling costs shaped asymmetries in my first substantive essay. In this next piece, the efficiency of handling containers will be influenced both by the size of incoming vessels and the surrounding port conditions they are exposed to.

Bibliography

Allen, T. and C. Arkolakis (2022). The Welfare Effects of Transportation Infrastructure Improvements. *Review of Economic Studies 89*(6), 2911–2957.

Ardelean, A. T., V. Lugovskyy, A. Skiba, and D. M. Terner (2022, April). Fathoming Shipping Costs : An Exploration of Recent Literature, Data, and Patterns. Policy Research Working Paper Series 9992, The World Bank.

Armington, P. S. (1969). A Theory of Demand for Products Distinguished by Place of Production. *IMF Staff Papers 16*(1), 159–178.

Atkin, D. and D. Donaldson (2015). Who's Getting Globalized? The Size and Implications of Intra-national Trade Costs. NBER Working Papers 21439, National Bureau of Economic Research, Inc.

Behrens, K. and P. Picard (2011). Transportation, freight rates, and economic geography. *Journal of International Economics 85*(2), 280–291.

Bernhofen, D., Z. El-Sahli, and R. Kneller (2016). Estimating the effects of the container revolution on world trade. *Journal of International Economics 98*(C), 36–50.

Blonigen, B. and W. Wilson (2008). Port Efficiency and Trade Flows. *Review of International Economics 16*(1), 21–36.

Bombardini, M., B. Li, and F. Trebbi (2023). Did US Politicians Expect the China Shock? *American Economic Review 113*(1), 174–209.

Bonadio, B. (2022). Ports vs. Roads: Infrastructure, Market Access and Regional Outcomes. Technical report, Working Paper.

Bown, C. P. (2021). The US–China Trade War and Phase One Agreement. *Journal of Policy Modeling 43*(4), 805–843.

Brancaccio, G., M. Kalouptsidi, and T. Papageorgiou (2020). Geography, transportation, and endogenous trade costs. *Econometrica 88*(2), 657–691.

Brooks, L., N. Gendron-Carrier, and G. Rua (2021). The local impact of containerization. *Journal of Urban Economics 126*(C), S009411902100070X.

Carreras-Valle, M.-J. (2022). Increasing Inventories: The Role of Delivery Times. Technical report, Working Paper.

Cooks, C. and P. Li (2023). Value Pricing or Lexus Lanes? Winners and Losers from Dynamic Toll Pricing. Job Market 2024 Paper, Institute for Economic Policy Research (SIEPR), Stanford University, Work in Progress.

Crainic, T. G., M. Gendreau, and P. Dejax (1993). Dynamic and Stochastic Models for the Allocation of Empty Containers. *Operations Research 41*(1), 102–126.

Demirel, E., J. van Ommeren, and P. Rietveld (2010). A matching model for the backhaul problem. *Transportation Research Part B: Methodological 44*(4), 549–561.

Drewry (2006). Annual Container Market Review & Forecast 2006/07. Technical report, Drewry Shipping Consultants Ltd: London.

Ducruet, C., S. Cuyala, and A. El Hosni (2018). Maritime networks as systems of cities: The long-term interdependencies between global shipping flows and urban development (1890–2010). *Journal of Transport Geography 66*(C), 340–355.

Fajgelbaum, P. D., P. Goldberg, P. J. Kennedy, and A. Khandelwal (2020). The Return to Protectionism. *The Quarterly Journal of Economics 135*(1), 1–55.

Fajgelbaum, P. D. and A. K. Khandelwal (2022). The economic impacts of the us–china trade war. *Annual Review of Economics 14*, 205–228.

Flaaen, A., F. Haberkorn, L. Lewis, A. Monken, J. Pierce, R. Rhodes, and M. Yi (2021). Bill of Lading Data in International Trade Research with an Application to the COVID-19 Pandemic. Finance and Economics Discussion Series 2021-066, Board of Governors of the Federal Reserve System (U.S.).

FMC (2022). Definition of Unreasonable Refusal To Deal or Negotiate With Respect to Vessel Space Accommodations Provided by an Ocean Common Carrier. *Federal Register 87*(182), 57674–57679.

Ganapati, S., W. F. Wong, and O. Ziv (2021). Entrepôt: Hubs, Scale, and Trade Costs. NBER Working Papers 29015, National Bureau of Economic Research, Inc.

Grossman, G. M. and E. Helpman (2021). Identity politics and trade policy. *Review of Economic Studies 88*(3), 1101–1126.

Hayakawa, K., J. Ishikawa, and N. Tarui (2020). What goes around comes around: Export-enhancing effects of import-tariff reductions. *Journal of International Economics 126*(C), S0022199620300787.

Heiland, I., A. Moxnes, K. H. Ulltviet-Moe, and Y. Zi (2022). Trade From Space: Shipping Networks and The Global Implications of Local Shocks. (Work in Progress).

Holmes, T. J. and E. Singer (2018). Indivisibilities in Distribution. Working Paper 24525, National Bureau of Economic Research.

Hummels, D. (2007). Transportation Costs and International Trade in the Second Era of Globalization. *Journal of Economic Perspectives 21*(3), 131–154.

Hummels, D., V. Lugovskyy, and A. Skiba (2009). The Trade Reducing Effects of Market Power in International Shipping. *Journal of Development Economics 89*(1), 84–97.

Ignatenko, A. (2023). Price Discrimination and Competition in International Transportation. Working paper, Norwegian School of Economics.

Irarrazabal, A., A. Moxnes, and L. D. Opromolla (2015). The Tip of the Iceberg: A Quantitative Framework for Estimating Trade Costs. *The Review of Economics and Statistics 97*(4), 777–792.

Ishikawa, J. and N. Tarui (2018). Backfiring with Backhaul Problems. *Journal of International Economics 111*(C), 81–98.

Juhász, R. (2018). Temporary Protection and Technology Adoption: Evidence from the Napoleonic Blockade. *American Economic Review 108*(11), 3339–76.

Lee, C.-Y. and D. Song (2017). Ocean container transport in global supply chains: Overview and research opportunities. *Transportation Research Part B-methodological 95*, 442–474.

Levinson, M. (2016). *The Box: How the Shipping Container Made the World Smaller and the World Economy Bigger* (REV - Revised, 2 ed.). Princeton University Press.

Notteboom, T., A. Pallis, and J.-P. Rodrigue (2022, January). *Port Economics, Management and Policy*. Routledge.

Rodrigue, J.-P. (2020, May). *The Geography of Transport Systems*. Fifth edition. — Abingdon, Oxon ; New York, NY : Routledge, 2020.: Routledge.

Sampson, T. (2017). Brexit: The Economics of International Disintegration. *Journal of Economic perspectives 31*(4), 163–84.

Samuelson, P. A. (1952). The Transfer Problem and Transport Costs: The Terms of Trade When Impediments are Absent. *The Economic Journal 62*(246), 278–304.

Song, D. (2021). A Literature Review, Container Shipping Supply Chain: Planning Problems and Research Opportunities. *Logistics 5*(2), 1–26.

Song, D.-P. (2007). Characterizing optimal empty container reposition policy in periodic-review shuttle service systems. *Journal of the Operational Research Society 58*(1), 122–133.

Song, D.-P. and J.-X. Dong (2015). Empty Container Repositioning. Chapter 6, pp. 163–208. Springer.

Steinbach, S. (2022). Port congestion, container shortages, and U.S. foreign trade. *Economics Letters 213*, 110392.

UNCTAD (2022). *Review of Maritime Transport 2022, Navigating Stormy Waters*. United Nations Publications.

Williamson, O. E. (1966). Peak-load pricing and optimal capacity under indivisibility constraints. *The American Economic Review 56*(4), 810–827.

Wong, W. F. (2022). The Round Trip Effect: Endogenous Transport Costs and International Trade. *American Economic Journal: Applied Economics 14*(4), 127–66.

Wong, W. F. and S. Fuchs (2022). Multimodal Transport Networks. FRB Atlanta Working Paper 2022-13, Federal Reserve Bank of Atlanta.

Chapter 3

Container Ports

Container Ports

Philip Economides*, Simon Fuchs† and Woan Foong Wong*

April 29th, 2023

Abstract

The majority of international trade is transported by ocean-going ships, where ports serve as important interchanges facilitating the flow of these goods. We study the long run interaction between containerships and top US ports over the past 47 years by compiling and combining three data sets. We establish that while the number of ship visits have more than tripled and the average ship size quadrupled, the average amount of time a ship dwells at a port has stayed roughly the same at about 2.5 days. Ongoing work includes developing a shift-share instrument to identify the impact of port traffic on ship dwell times and a model of capacity reallocation at ports, in order to quantitatively study the impact of changing shipping technologies on port traffic and wait times.

JEL Codes: D62, F18, F64, L51, Q52, Q53, R41
Keywords: transport externalities, port logistics, vessel queues, congestion, maritime trade.

*Department of Economics, University of Oregon.
†Federal Reserve Bank of Atlanta.
Contact: economi@uoregon.edu, simon.fuchs@atl.frb.org, and wfwong@uoregon.edu. The views in this paper are solely the responsibility of the authors and should not necessarily be interpreted as reflecting the views of the Board of Governors of the Federal Reserve System or of any other person associated with the Federal Reserve System. All errors are our own. We thank the NBER/NSF/DOT for project support.

The essay below originated from a project I contributed to as a research assistant for Professor Woan Foong Wong. While Professor Wong and our co-author, Dr Simon Fuchs, suggested the topic of the paper and provided initial points of reference in the literature, I have refined the research questions addressed in this essay and developed supporting geo-spatial algorithms used to clean and merge three separate large datasets on vessel positioning at ports in order to conduct the analyses in this essay. Following consistent meetings with my co-authors, I have also been supported in compiling an extensive review of existing data sources on maritime trade and transportation that is suitable for the analysis in this essay, which has allowed us to pursue access to these data sets. Referring to the outlined specifications I discussed with my co-authors, I have prepared each of the appropriate estimations in the empirical section of this essay and implemented a preliminary methodology for applying an instrumental variable of interest. Going forward, I expect further changes in future iterations of this study, attributable to my co-authors and I. These changes include further refinement of our empirical approach, the introduction of a theory model, combining our empirical results with counterfactual analysis to examine the influence of port infrastructure adjustments and technological innovations in vessel technology on US trade outcomes. While both Professor Wong and Dr Fuchs have contributed to various parts of this project, I have contributed strongly to the progress of this research. From the data collection, cleaning, initial analysis, up to the current draft, I have worked directly on each of the sections of this study.

3.1 Introduction

The majority of international trade is transported via ocean on ships. This places a great deal of importance on the state of port facilities, both with respect to each port's scale of operations and efficiency in servicing vessels. Over recent years, increasingly larger and larger containerships are built to take advantage of scale economies in transportation (Cullinane and Khanna, 2000; Tran and Haasis, 2015). A concerted effort to pursue these benefits has contributed to an effective arms race across the merchant fleet, in which container ship capacities have increased nearly six-fold. As a result, ports and terminals – seeking to remain competitive destinations for waterborne commerce – are incentivized to make "large and rapid investments in infrastructures" to meet the needs of larger vessel sizes (Imai et al., 2006; Parola et al., 2017). While these large ships carry significantly more vol-

ume, vessels are also consequentially spending longer times at ports unloading and loading. These longer ship dwell times, all else equal, introduce increased negative externalities for other vessels using the same port. However, larger ships does also translate into fewer port visits overall, since these ships are able to transport much more goods each visit.

Using historical records of ship tracking and port call data, we capture the long-run evolution of ship visits and dwell times at US ports and examine the factors that contribute to ship dwell times. We compiled and combined datasets from four different sources in order to put together 47 years of panel data on container port visits across the US. From 1977-2002, we use private data from Lloyds List Intelligence, which at the time employed numerous agents across the world to manually track vessel arrivals and departures from ports through on-site observations and paper-based port records. From 2002-2016, we obtained port entrance and clearance records from the US Army Corps of Engineers. From 2016-2023, we obtained automatic identification system (AIS) data for ships in US waters which captures ship movements down to the minute-level. For each of these datasets, we observe the unique vessel identifiers for each ship which we merge to their characteristics including containership capacity (in twenty-foot equivalent units, TEUs) and year they were built using a fourth dataset.

Although port operations are key to securing access to foreign goods for many countries, there is a dearth of port performance measures. To address this need, experts in maritime transport and international trade have sought to estimate port efficiency. Both survey responses (Clark et al., 2004) and estimates using fixed effects models using variation in handling costs (Blonigen and Wilson, 2008; Ducruet et al., 2020) have been used to yield port efficiency measures. We provide a relatively more disaggregated measure of performance, which allows for the assessment of individual berth locations within port facilities at minute-level intervals.

Furthermore, this growing volume of maritime transport services has incentivized the construction of larger containerships and development of complex shipping networks that exploit the increasing returns of scale that larger vessels provide. Ganapati et al. (2021) documents a hub-and-spoke system of global trade, finding that 80% of trade is shipped indirectly via entrepôts – major hubs that facilitate trade between many origins and destinations. In particular, routes with lower per-unit trade costs feature larger ships. A 10% decrease in estimated iceberg trade costs is associated with 6% larger ship sizes. Carballo et al. (2023) finds evidence that reduced processing time for shipments at the border contributes sig-

nificantly to elevated trade outcomes. While larger vessels are associated with efficiency through lower costs, we ask whether the increase in size could also contribute to faster rates of TEU handling. Our study focuses on port-level container handling and vessel berth use across US ports, allowing us to incorporate potential negative spillovers of prevailing port congestion on surrounding vessel services. By identifying dwell events at the individual vessel level, we are able to track the adoption of larger containership classes over time and identify granular adjustments in vessel services of specific berth locations within ports. This also allows us to decompose how adjustments in technology and congestion contribute to the efficient use of port resources.

Our results show that there have been large increases in the amount of containership traffic at US ports: the total number of containership visits has increased by about three times since 1977 while the total TEU capacity of these ships has increased sevenfold. Second, the average size of these containerships has increased dramatically as well: average TEU capacity of containerships have increased by about 5 times, from averages of approximately 1,300 TEUs in 1977 to almost 8,000 TEUs by 2023. Third, these large containerships have been making less port visits: the average number of annual port visits per containership have halved from 24 in the 1970's to 12 in recent years. At the same time, the average amount of time a ship spends at port has stayed steady at around 2.4 days (with large spikes during strike times and during the pandemic period). We categorized vessels using their time invariant characteristics of year built, length, container capacity and gross tonnage to document increasing container handling efficiencies as vessels scale up in size. Our analysis suggests that a one percent increase port traffic contributes to a 0.09–0.17 percent increase in vessel dwell times per TEU, suggesting that elevating congestion at port leads to negative spillovers for surrounding vessels.

The rest of this chapter proceeds as follows. In Section 3.2, we describe our data and provide key details that have guided our choice set of US ports. Section 3.3 provides stylized facts on the evolution of container shipping for 1977–2023 servicing the US. In Section 3.4, we outline empirical strategies for identifying the effect of vessel size and congestion on port dwell times. Section 3.5 concludes.

3.2 Data

In this section, we describe the multiple data sources we utilize to capture traffic activity at US container ports between January 1977 and December 2023. We then discuss how we compile and combine 47 years of port visits and vessel-positioning data. Next, we explain how we match this data to ship registries, geographic areas of ports, and international trade flows using the unique International Maritime Organization (IMO) code assigned to each vessel. Lastly, we describe some general summary statistics.

3.2.1 Ships and Port Data

Port Visits We utilize two sources of data to construct the first 39 years of port visits data. For the first 25 years, 1977–2002, we utilize data from Lloyd's List Intelligence (Lloyds). Lloyds collected details on port visits at the day-level through on-site agents situated at ports and paper records of vessel activity. This data reports the unique ship IMO code, arrival date, departure date, gross tonnage and name of each visiting vessel. For the next 13 years, We use Port Entrances and Clearances data from the United States Army Corp of Engineers (USACE). In addition to the details in the LLoyds data, these records has information on the type of vessel, which allows us to identify which of these are containerships (International Classification of Ships by Type, ICST).

Vessel-Positioning Data Our most granular data is based on an automatic identification system (AIS) of vessels in which transponders fixed to ships reports the geo-location, speed, status, vessel name and unique identifier for each vessel present in US waters. These signals are stored and updated every minute by the US Coast Guard and made publicly available on the MarineCadastre platform. We observe minute-level individual vessel movements between January 2016 and December 2023. Prior to 2016, usage of AIS transponders was not mandatory for commercial vessels in US waters. Due to this limitation, we elect use port call data for 1977–2015 which yields less precise durations of port visits – by calendar date count – across vessels.

Each individual vessel location is tracked across time at a minute-level resolution. We pair these geo-spatial coordinates with spatial polygons of port statistical areas. Any vessels observed within or in close proximity to a port is retained in

the data set. The focus of this study is placed specifically on containerships. We therefore limit our use of AIS coverage to the top containership ports in the US.[1] An individual port dwell event begins the moment a vessel stops within a port polygon (signals a speed of zero) and begins broadcasting that it is engaged in the loading/unloading of cargo (a status code of 5). The moment the vessel switches to a positive speed and updates its status code back to being underway, we note this as the end of a port dwell event. The passage of time between the start and end of this time spent mooring at port represents the duration a vessel dwells at port, loading and unloading cargo. Upon arriving at a resulting set of port dwell events, we apply post-processing filtration to mirror procedures applied by the Bureau of Transport Statistics.[2] We provide a full account of the steps we have devised in the Data Appendix for this chapter.

Ports In order to define the geographic areas of the 28 ports, we use geospatial data from the U.S. Army Corps of Engineers.[3] After some modifications, this allows us to use polygon regions of US port areas and interact them with vessel position data. In combination, these items allow us to identify the exact minute at which port entrances and departures occur across key port areas of interest.

International Trade We source US trade data from the USACE and US Census Bureau. The USACE provides records of US waterborne commerce between 1940–2021, which details the volume of imports and exports by US port and year. The US Census Bureau provides monthly containerized trade flows from January 2003 to December 2023 by port, country, and commodity type in both weight and value.

Vessel Registry We use the VesselTracking platform to update our historical record of port calls with further information about individually identified vessels. Using the IMO code of each vessel, VesselTracking provides the year built, max-

[1]These ports include the Port Authority of New York and New Jersey (NY, NJ), Savannah (GA), Virginia (VA), Oakland (CA), Everglades (FL), the North Western Sea Alliance (WA), Los Angeles (CA), Miami (FL), Long Beach (CA), Charleston (SC), Jacksonville (FL), Philadelphia Regional Port Authority (PA), San Juan (PR), Baltimore (MD), Mobile (AL), Tampa Port Authority (FL), Boston (MA), Wilmington (NC), Gulfport (MS), Wilmington (DE), Palm Beach (FL), Hueneme (CA), San Diego (CA), and Everett (WA).

[2]For further details on the Bureau's methodology in recording vessel dwell times, see https://www.bts.gov/PPFS-Tech-Docs

[3]Our selection of ports is informed by 2020 Panjiva rankings of container handling volumes. See https://www.logisticsmgmt.com/article/top_30_u.s._ports_big_ports_got_bigger_in_2020, last accessed on May 30th 2024.

imum container (TEU) capacity and length of each vessel. Given that this data covers both existing and decommissioned vessels, we are able to apply full coverage across our sample. We limit our sample to vessels associated with non-zero container capacities, if not already flagged as a containership by USACE port call data.

3.2.2 Port Composition

Our study focuses on the top-ranked ports for containerized shipping activity, as displayed in Table 4.1. In cases of close geographic proximity, aggregated data reporting for sets of ports, or strategic alliances across individual port authorities, we combine port areas together into single entities.[4] In total, these ports represent 90.7% (88.4%) of the value (volume) of US containerized trade over the past two decades. The 17 trillion USD amount of containerized trade we account for represents 23% of trade value upon including all modes of transportation.

Table 3.1: Port Rankings by Containerized Trade Value (2003-2023)

Rank	Port	Value ($bn)	Rank	Port	Value ($bn)	Rank	Port	Value ($bn)
1	Los Angeles	4685.75	10	Seattle	573.96	19	Mobile	106.82
2	New York	2973.94	11	Baltimore	443.37	20	Boston(USA)	90.70
3	Long Beach	1617.12	12	Miami	418.82	21	Gulfport	47.60
4	Savannah	1376.86	13	Port Everglades	317.64	22	Palm Beach	35.29
5	Norfolk	1177.66	14	New Orleans	200.29	23	San Diego	28.33
6	Houston	1134.07	15	Philadelphia	195.86	24	Everett(WA)	26.23
7	Charleston	1096.86	16	Jacksonville	149.51	25	Port Hueneme	23.49
8	Oakland	797.44	17	Wilmington(NC)	123.75	26	Tampa	17.61
9	Tacoma	694.93	18	Chester(PA)	113.80	27	Freeport(Texas)	14.59

Source: US Census Bureau, HS Port-level Data. Values reflect total imports and exports summed across 2003 to 2023.

By region, Gulf and East coast ports have been increasing their shares of overall waterborne commerce between 2003 and 2023. This is attributed to factors such as the widening of the Panama Canal, which lessened East Asia's reliance on the

[4]We have combined Tampa and Manatee ports. Similarly, we have also merged Seattle & Tacoma ports into a single North Western Alliance (NWSA) entity and New York & Newark ports, which are maintained by the Port Authority of New York and New Jersey (PANYNJ). Lastly, due to LLoyd's records combining Los Angeles and Long Beach, we have maintained this combination throughout our sample into a single port category. In practice, the two San Pedro Bay ports share strong competition between one another and unique business models for securing long-term warehouse use/leasing.

US West Coast for major vessel operations, and the spatial market appeal of transhipping to the US through highly modernized European ports. In recent years, this attrition faced by the US West Coast has been accelerated by contentious rail and port labor negotiations alongside severe challenges in port congestion.

Figure 3.1: Coastal Shares of Containerized Trade Value (2003-2023)

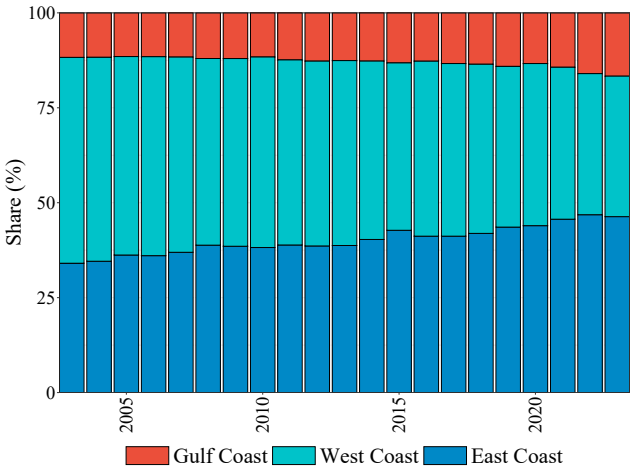

3.3 Stylized Facts

In this section, we document a series of stylized facts regarding container shipping activity trends at US ports over the past 47 years. Overall, we observe 4,522 unique containers making a total of 624,570 port visits at the top 28 US container ports over this time period.

Frequency of Port Visits We find that the total number of port visits by containerships per month has risen steadily, almost quadrupling in count between 1977 and 2010 (Figure 3.2). However, this trend stagnates after the Great Recession and starts to decrease afterwards to around 1200 ships per month.

These port visits could be made by the same ship visiting more than once in a month, or they could be made by multiple different ships. This distinction is important since the frequency of port visits is often influenced by vessel size, wherein smaller vessels normally service shorter distance routes and therefore are more likely to repeatedly visit the US within a given month. Restricting our number of visits to unique port-vessel events, Figure 3.3 shows that the increasing

Figure 3.2: Total Number of Port Visits by Containership

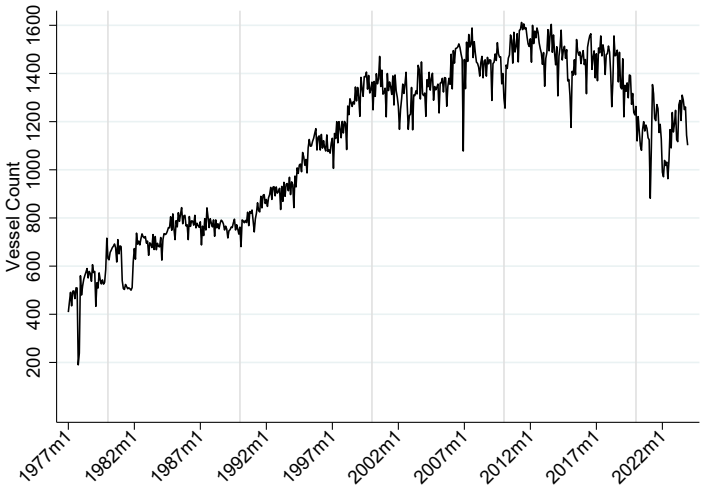

***Notes*:** This figure presents the total number of port visits by each containership per month-year in our combined data set for the top 28 US ports spanning 47 years.

trend of port visits are not solely driven by the same ships visiting ports with higher frequency, although the overall magnitude is down by more than half. The total number of unique port visits by ships still increased by approximately three times from 1977 to a peak of 600 visits around 2007 onwards. This allows us to put together our first stylized fact:

Figure 3.3: Total Number of Unique Port Visits by Containers

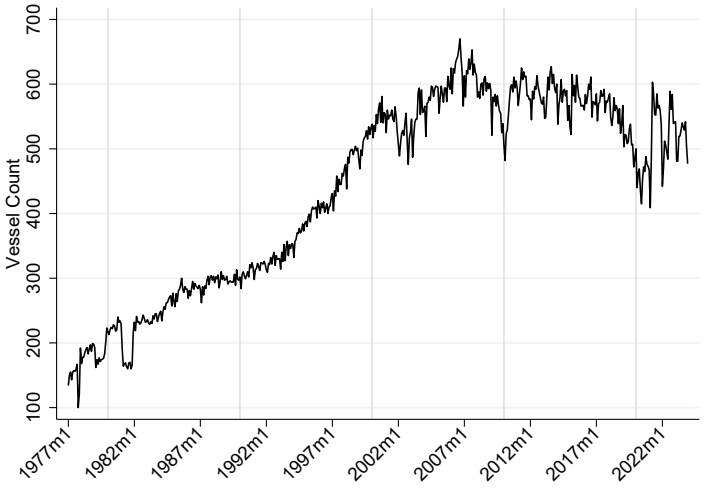

***Notes*:** This figure presents the total number of unique containership-port visits per month-year in our combined data set for the top 28 US ports spanning 47 years.

Stylized Fact 1. *The number of port visits by containerships has increased by more than three times over the past 47 years. The number of visits quadrupled at its peak around the Great Recession and then declined after that. The increase in port visits is driven by both the increase in visit frequency by the same ships, as well as the increase in the introduction of new ships.*

Variation of Ship Sizes Next, we examine how the sizes of containerships have evolved over this period (Figure 3.4). We first define the size of a ship by its container capacity, the maximum number of twenty-foot equivalent unit containers each vessel can load (total TEU). Figure 3.4a shows that the average capacity of individual containerships has increased almost eight fold across our sample. This steady increase continues even though there was a decline in the total number of containership visit between 2010 and 2017 (Figure 3.2). The utilization of larger vessels at top US ports can explain the stagnating number of port visits since these larger vessels do not need to visit as frequently. Figure 3.4b shows that the total TEU volume of containership mass continues to increase over our period, with a more recent decline in total capacity around the pandemic period. As the building of newer and larger vessels require better technology, we can trace the introduction of each of these new ship classes in our data period (Figure 3.4c). We also show that this increasing trend in ship capacity is robust when restricted to unique containerships (Figure 3.4d). This allows us to summarize our second stylized fact:

Stylized Fact 2. *The containerships visiting US ports are getting much larger. Average capacity has increased by almost eight times over the past 47 years.*

While both stylized facts highlight a broad acceleration in the evolution of vessel technology from the mid-2000's, we can delve deeper into these insights through the observed vessel characteristics in our data. Given our knowledge of each vessels' capacity, length and build year, we assign classes to individual containerships based on the classifications outlined in Rodrigue et al. (2017). The smallest class of vessels, "Micro and Early Builds", maintained a prominent share of the US market until May 1988 (Figure 3.5). From 1988 to 2015, "Panamax" vessels functioned as the primary means of transportation for containerized goods. By September 2016, "post-Panamax" containership technology had quickly ascended to support the majority of US shipping. It has only been in recent years that "Neo-Panamax" vessels and, on rare occassions, some of the largest vessels on the global fleet, have begun servicing US ports.

Figure 3.4: Variation in Containership Capacity

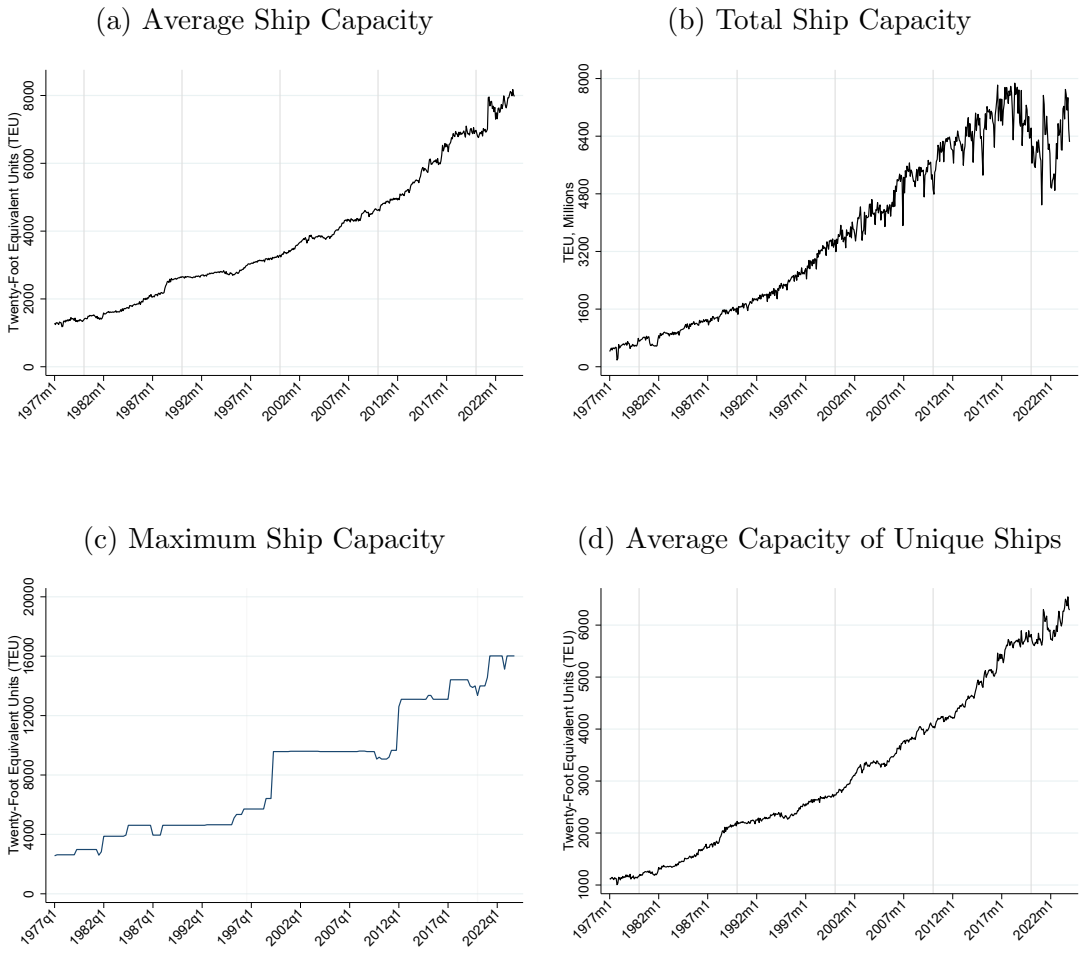

***Notes*:** In panel (c) values at the tails of the distribution are windsorized by year to less extreme values $(0.05, 99.95)$ of TEU capacities (red). We do so to moderate the influence of once-off large vessel visits, normally conducted to promote a port expansion event.

The top five container ports across the US have grown their service of containership mass ten fold by the peak year of 2017. Despite this impressive growth, particularly in the cases of Norfolk and Savannah, this group of ports' total market share of containership services has waned since heights of 60% between 2002–2008. Top five shares have since decline steadily to a range 51–54% in 2023, which suggests a less concentrated market with respect to cargo handling services.

As containerized transport became increasingly reliant on larger vessels, shipping distances and transit durations have grown, contributing towards a downward trend in the number of vessel visits occurring per containership servicing the US (Figure 3.7). This evidence is strikingly similar to Far East–North Europe patterns

Figure 3.5: Changes in Container Capacity Shares

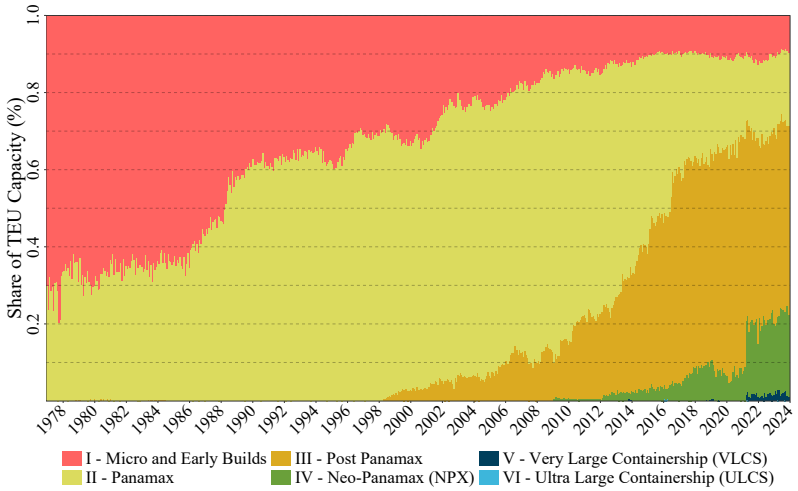

***Notes*:** This figure presents the trends in TEU capacity shares of different vessel-types over the 47 year period.

Figure 3.6: Port Volumes of Vessel TEU Capacity by Year-Month

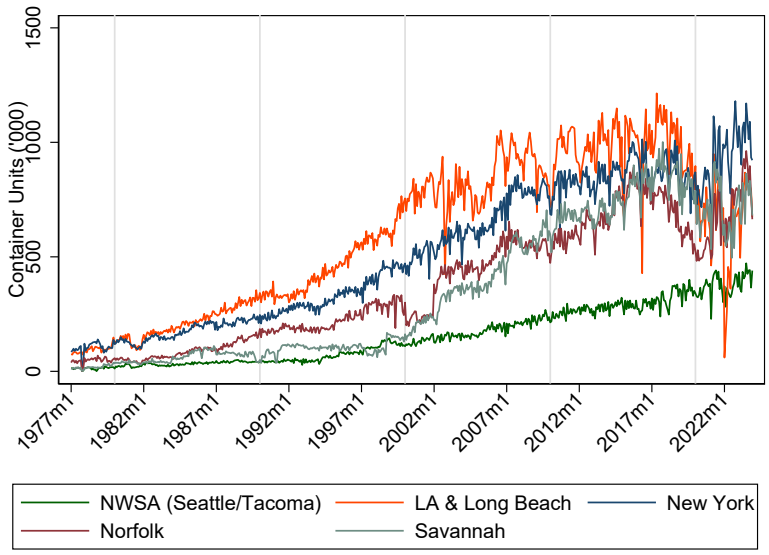

outlined in Ducruet and Notteboom (2012) in which the number of port calls per round trip decreased from five in 1989 to three in 2009.

Time Spent at Ports As the number of port visits has increased, along with the sizes of ships making these visits, we are interested in how both these factors contribute to the amount of time ships spend at ports. We calculate ship dwell

Figure 3.7: Average Visits per Containership by Year

times as the time it takes a ship to enter and clear a port. Perhaps surprisingly, average dwell times of containerships have stayed relatively stable at a 2.25 day average, even in the presence of larger ship sizes and increased visits (Figure 3.8). There are a number of deviations from this relatively stable number, like the accumulated levels of traffic during COVID-19 post 202 where average dwell times increase to more than three days. As we highlight in Figure 3.9, these challenges were particularly pressing at the ports of Los Angeles and Long Beach, but persist in other key areas to a lesser extent. Similarly to patterns in concentration of container mass across ports, we find that the top five ports' share of dwell times has lessened from a 60% peak in 2002–2007 down to a modest 48% share in 2023. This leads to our third stylized fact:

Stylized Fact 3. *The average dwell times of containerships at ports have remained relatively flat over time at an average of 2.25 days per visit, despite the increase in number of port visits along with the sizes of ships making these visits.*

With each period comes added reductions in per-unit handling costs of containerized goods as the global fleet further intensifies the use of improved vessel technology. Vessel mass continues to accumulate at ports limited in space and resources. These details invite two questions; (i) How were existing shipping services' access to port resources affected by these increasingly larger entrants to the containerized market, and (ii) What are the implications of increased vessel mass for the handling efficiency of container units at port? We explore these items in ongoing work.

Figure 3.8: Average Dwell Times of Containership Visits

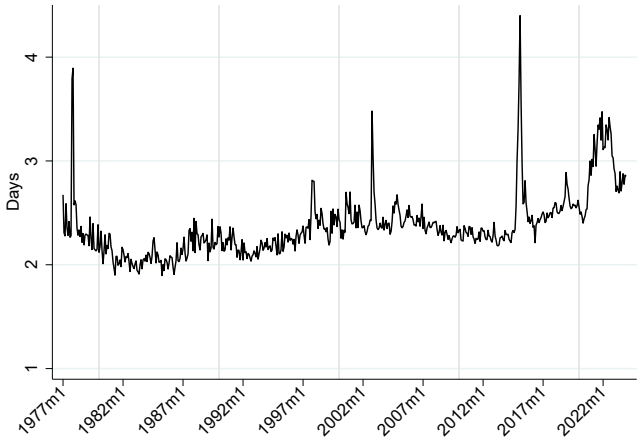

Figure 3.9: Average Dwell Times of Containership Visits by Port

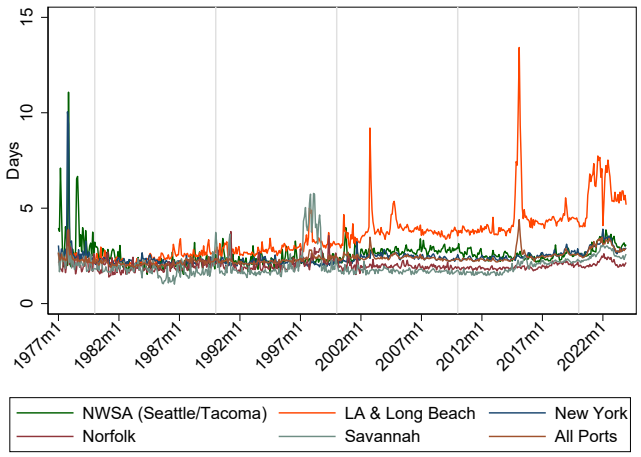

3.4 Empirical Strategy

In this section, we examine patterns in dwell time durations across individual vessels visiting US ports. We capture average differences in dwell times across the ship class categories to examine how a given ships' time-variant mass influences expected dwell times. Additionally, we consider the effects of existing port traffic, its vessel type composition and the concentration of larger vessels on vessel dwell times. Our findings suggest improved vessel technology can be a burden on the existing global fleet servicing US trade.

3.4.1 Dwell Time on Vessel Size

In this subsection, we examine differences in average vessel dwell times across specific containership categories, each of which is associated with increasingly large attributes in terms of vessel length, gross tonnage and maximum TEU capacity. We estimate the following regression:

$$\text{ln Ship Dwell Time}_{spdmyr} = \sum_{c=2}^{C} \beta_{\text{c}} \text{ Ship Category}_{s} + \delta_{dmy} + \alpha_{pym} + \gamma_{r} + \varepsilon_{spdmyr}, \tag{3.1}$$

where ln Ship Dwell Time$_{spdmyr}$ is the number of calendar days ship s spent at port p, along coastline r, on day of the week d, month m, and year y. Ship Category$_{s}$ denotes the ship-specific size classification of vessel s, based on a series of guidelines detailed in Rodrigue et al. (2017). Should a vessel be built at a particularly length, width, maximum TEU capacity and gross tonnage to match these traits, we assign the vessel a time-invariant categorization. δ_{dmy} is day-month-year fixed effects, α_{pym} is port-year-month fixed effects and γ_{r} is a regional fixed effect based on which coastline vessel s is servicing. We use the smallest category – micro, early build and Panamax vessels – as our reference group. As a result, β_{c} coefficients should be interpreted as relative differences in dwell times, compared to the smallest category of containerships.

The day-month-year fixed effects control for aggregate events that impacts all ships. The port-year-month fixed effects control for fixed and time-varying characteristics at the port level. Time varying port characteristics account for potential technology changes over time that ports can undertake that might affect ship dwell times, for example technology upgrades at ports over time to accommodate larger ships. Fixed regional characteristics include time-invariant comparative advantage differences for coastlines that result in larger ships being received at these areas which mechanically take longer time to unload, for example coastlines with deeper natural harbors or regions adjacent to larger transport network hubs. We vary the fixed effects in our model to also address fixed port characteristics like its geography, and seasonality broadly applicable across US waterborne commerce, and find relatively similar results.

We find that vessel size categories are highly predictive of port dwell times across vessels. The larger a vessel is, the longer the duration of time it will spent at port filling a berth-zone area while goods are unloaded and loaded. Relative

differences in Neo-Panamax and Very Large & Ultra Large Container ships exhibit dwell times almost 50% larger in magnitude. Despite larger vessels introducing a greater burden on port resources, in total volume, there may be economies of scale to benefit from with respect to servicing one large vessel rather than two vessels that, when combined in max TEU capacity, represent the same level of container handling volume.

Table 3.2: OLS Vessel Dwell Time by Ship Category

Dependent Variable:	Vessel Dwell Time (Days)			
	(1)	(2)	(3)	(4)
Post Panamax	0.1981**	0.2215***	0.2214***	0.1989**
	(0.0782)	(0.0764)	(0.0764)	(0.0784)
Neo-Panamax (NPX)	0.4308***	0.4755***	0.4757***	0.4315***
	(0.0967)	(0.1084)	(0.1081)	(0.0956)
Very & Ultra Large Containerships	0.4760***	0.5951***	0.5938***	0.4715***
	(0.0819)	(0.1270)	(0.1264)	(0.0834)
Vessel Age	-0.0017	-0.0016	-0.0016	-0.0018
	(0.0066)	(0.0061)	(0.0061)	(0.0066)
Day–Month-Year FE	✓	✓	✓	✓
Port–Year FE	✓			
Port FE		✓		
Port–Month FE			✓	
Port–Year–Month FE				✓
Observations	613,385	613,385	613,385	613,385
R^2	0.39	0.35	0.35	0.42

Notes: Clustered port standard-errors in parentheses. Codes: ***: 0.01, **: 0.05, *: 0.1. Examines variation in the average dwell time of individual vessels relative to our reference group of early-build/micro vessels and Panamax category containerships.

To address economies of scale, we use ratios of dwell time to container capacity of each ship and repeat the regression specified in Equation 3.1. Assuming vessels of varying size exchange similar proportions of container volume at port, relative to their respective capacities, this regression details how efficient container handling is across vessel size categories. We find that economies of scale are detectable under this specification (Table 3.3). Efficiency improves across larger vessel categories. At the extreme, modern vessels of very large and ultra large' proportions are associated with 65–80% greater container handling efficiency relative to our reference group of smaller ships. Controlling for size categories, we also find that a one-percentage increase in vessel age is associated with a 0.13% higher dwell time per container handled.

One important caveat of this exercise is the fact that the denominator of our measure is time-variant and relies upon relative similarities across vessel classes

with respect to the proportion of handled container units relative to capacity. To address this concern, we utilize Panjiva data which details individual vessel records of container offloading. Matching Panjiva records of vessel activity to our existing data, we are able to display similar results in which greater vessel size is associated with higher container handling efficiency. These results are available in Appendix A.3.

Table 3.3: OLS Vessel Efficiency by Ship Category

Dependent Variable:	Dwell Time per Container Unit (Days per TEU)			
	(1)	(2)	(3)	(4)
Post Panamax	-0.5649***	-0.5187***	-0.5188***	-0.5645***
	(0.0932)	(0.0917)	(0.0918)	(0.0935)
Neo-Panamax (NPX)	-0.6814***	-0.5844***	-0.5844***	-0.6806***
	(0.1270)	(0.1361)	(0.1359)	(0.1263)
Very & Ultra Large Containerships	-0.8085***	-0.6510***	-0.6525***	-0.8141***
	(0.1169)	(0.1572)	(0.1564)	(0.1192)
Vessel Age	0.1271***	0.1277***	0.1277***	0.1268***
	(0.0137)	(0.0129)	(0.0129)	(0.0136)
Day–Month-Year FE	✓	✓	✓	✓
Port–Year FE	✓			
Port FE		✓		
Port–Month FE			✓	
Port–Year–Month FE				✓
Observations	613,385	613,385	613,385	613,385
R^2	0.53	0.50	0.50	0.54

Notes: Clustered port standard-errors in parentheses. Codes: ***: 0.01, **: 0.05, *: 0.1. Examines variation container handling efficiency of individual vessels relative to our reference group of early-build/micro vessels and Panamax category containerships.

3.4.2 Instrumental Variable Approach

A caveat of regressing vessel times on port traffic is the issue of simultaneity bias. In a given period t, vessel i could choose observed port p due to mitigating congestion issues elsewhere. As a result, the traffic conditions at port p partly contribute to the observed duration of vessel i's port dwell event.

To address this concerns about reverse causality, we intend to implement an instrumental variable which projects exogenous variation in port traffic using variation in each port's measure of trade exposure. This demand-shifter of port traffic is uncorrelated with unobserved ship dwell times determinants ϵ_{spdmyr}. Our current IV strategy uses aggregate changes for trade (imports and exports) at the national level and our top port shares of historical containerized commerce, by weight, to predict demand for traffic at each port:

Table 3.4: OLS Elasticity of Vessel Efficiency with respect to Port Traffic

Dependent Variable:	Dwell Time per Container Unit (Days per TEU)			
	(1)	(2)	(3)	(4)
Port Gross Tonnage	-0.0132	-0.0337	-0.0334	-0.0039
	(0.0123)	(0.0349)	(0.0350)	(0.0151)
Port Vessel Count	0.1709***	0.0895*	0.0899*	0.1124***
	(0.0272)	(0.0438)	(0.0440)	(0.0240)
HHI	-0.0415***	-0.0824***	-0.0826***	-0.0207***
	(0.0044)	(0.0097)	(0.0098)	(0.0040)
Vessel Age	-0.0017	-0.0065	-0.0065	-0.0019
	(0.0094)	(0.0085)	(0.0084)	(0.0093)
Large Vessel Share (%)	0.0855**	0.0682	0.0687	0.0705*
	(0.0342)	(0.0611)	(0.0612)	(0.0382)
Ship FE	✓	✓	✓	✓
Day–Month-Year FE	✓	✓	✓	✓
Port–Year FE	✓			
Port FE		✓		
Port–Month FE			✓	
Port–Year–Month FE				✓
Observations	613,385	613,385	613,385	613,385
R^2	0.84	0.83	0.83	0.84

Notes: Clustered port standard-errors in parentheses. Codes: ***: 0.01, **: 0.05, *: 0.1. All variables are in logs excluding 'large vessel share' which reports the percentage of visiting vessels in the 4th and 5th quintiles of vessel size across ports and time. 'Efficiency' is dwell time per TEU, where the denominator uses each vessel's maximum container capacity. 'Port Tonnage' reports the weekly tonnage of containership vessels present at port p, excluding ship i's contribution. 'Port Vessel Count' reports the number of containership vessels present at port for a given week. 'HHI' reports a Herfindahl–Hirschman index of vessel tonnage concentration. The higher the value, the more densely concentrated total weekly mass is across visiting containerships at a given port p. 'Vessel Age' reports the difference in year and build year of ship i. New entrant vessels are those built in the same year they are actively servicing US ports. We apply an age of 0.5 to new entrants to preserve them in the sample. These vessels are potentially key drivers of spillover variation in surrounding vessel dwell times.

For port p year y

$$\text{Port Trade Exposure}_{py} \equiv \omega_{py^0} \sum_{P} \Xi_{pym}$$

where the lagged weighted sum of total cargo tonnage into each port from year y^0 during the historic period of 1959–1976.[5] The shift is the nominal value of current-year-month total trade across the US, non-seasonally adjusted, where trade flows date back to January 1987.[6] In future work, we will leverage the parameters generate from this exercise, combined with a micro-model of containership port dwell events, to evaluate counterfactuals related to the introduce of additional berth space and improved vessel technology. This latter goal of our seeks to enhance policy guidance on port infrastructure investment following turbulent congestion and maritime bottlenecks oscillating between the US East and West Coasts.

[5]Source: USACE Waterborne Commerce in the United States, Parts 1–5.

[6]Going forward, we will use undisclosed historical commerce flows, which vary by port–year–commodity, and introduce improved granularity to our analysis.

3.5 Conclusion

This paper examines the evolution of containership technology and how it has influenced both containership dwell times and port spillover effects for the surrounding vessels. Using this evidence, we are able to characterize the length of port dwell events as being subject to two key competing aspects; (i) each vessel's size influencing their own length and efficiency of port visits, and (ii) congestion externalities associated with the introduction of improved vessel technology.

Upon accounting for size differences across vessel classes we find that efficiency gains outscale the longer durations that larger vessels are subject to, suggesting that vessels may be subject to economies of scale while processing goods at port. This evidence is corroborated by insights from Panjiva Bill of Lading data, which provide an added caution that US ports may not yet be capable of handling some of the largest vessels in the global container fleet in an efficient manner.

To examine traffic effects, we consider how amassing volumes of vessel presence, in a given port–week, influences prevailing dwell times of individual vessels accessing these same port resources. Both our OLS and instrumental variable specifications suggest that increased vessel mass extends individual dwell times, which suggests that the broader evolution of vessel technology may have adversely influenced the performance of the existing container fleet on the intensive margin (congestion effect). However, one must also consider the fact that ports are now far more concentrated in mass as a result of these innovations. Using a Herfindahl–Hirschman Index of vessel mass concentration, find that as port resource use becomes more saturated by individual vessels, resulting dwell times of vessels present at port diminishes (efficiency effect).

One aspect of an increased concentration of vessels in US transport services that we do not address is the potential trade-offs between greater economies of scale in container handling and mitigated gains as a result of weaker market competition. Hummels et al. (2009) suggests that price discrimination intensifies as vessel counts narrow on a given lane of transport services. Extending this logic to transport operators' respective shares of leased port storage facilities, the cost reducing elements of the efficiency gains we document may be somewhat undermined by greater market power among choice mega-ships. We encourage further research in this direction to evaluate how ownership compositions of arriving vessels influence on-site container handling costs and pass-through to US importers.

In future work, we aim to quantitatively explore these competing effects of improvements in technology both diminishing existing fleet performance on the intensive margin while enhancing it on the extensive margin. This would allow us assess the impact of pandemic port congestion, adjustments to port infrastructure and continued improvements in containership sizes. Our future pursuits will develop a tractable general equilibrium framework to be able to quantify welfare effects across counterfactual scenarios of this nature.

Bridge

While these essays up to this point have shed light on how logistical practices and vessel characteristics influence the ebb-and-flow of maritime trade outcomes, one big question arises from both of these forms of activity. What influence do vessels have on environmental outcomes? While goals of vessel and port decarbonizations have remained objectives of the IMO and US Department of Transportation, respectively, the footloose nature of vessel traffic makes the detection of associated environmental externalities difficult to apply pinpoint analysis towards. As I will highlight in the subsequent chapter, even a reliance on air quality monitoring devices adjacent to port areas can lead to a compounding of issues that limit this for policy analysis. To mitigate these issues, I use vessel position data, allowing me to dissect individual voyages towards US ports into their various stages and evaluate the effect of the new San Pedro Bay vessel queuing system on both local and global emissions.

Bibliography

Blonigen, B. and W. Wilson (2008). Port Efficiency and Trade Flows. *Review of International Economics 16*(1), 21–36.

Carballo, J., A. Graziano, G. Schaur, and C. Volpe Martincus (2023). Import Processing and Trade Costs. IDB Publications (Working Papers) 12716, Inter-American Development Bank.

Clark, X., D. Dollar, and A. Micco (2004). Port efficiency, maritime transport costs, and bilateral trade. *Journal of Development Economics 75*(2), 417–450.

Cullinane, K. and M. Khanna (2000). Economies of scale in large containerships:

optimal size and geographical implications. *Journal of transport geography 8*(3), 181–195.

Ducruet, C., R. Juhász, D. Nagy, and C. Steinwender (2020). All aboard: The effects of port development. NBER Working Papers 28148, National Bureau of Economic Research, Inc.

Ducruet, C. and T. E. Notteboom (2012). Developing Liner Service Networks in Container Shipping.

Ganapati, S., W. F. Wong, and O. Ziv (2021). Entrepôt: Hubs, Scale, and Trade Costs. NBER Working Papers 29015, National Bureau of Economic Research, Inc.

Hummels, D., V. Lugovskyy, and A. Skiba (2009). The Trade Reducing Effects of Market Power in International Shipping. *Journal of Development Economics 89*(1), 84–97.

Imai, A., E. Nishimura, S. Papadimitriou, and M. Liu (2006). The Economic Viability of Container Mega-Ships. *Transportation Research Part E: Logistics and Transportation Review 42*(1), 21–41.

Parola, F., M. Risitano, M. Ferretti, and E. Panetti (2017, January). The Drivers of Port Competitiveness: A Critical Review. *Transport Reviews 37*(1), 116–138.

Rodrigue, J., C. Comtois, and B. Slack (2017). *The Geography of Transport Systems*. Routledge.

Tran, N. K. and H.-D. Haasis (2015). An empirical study of fleet expansion and growth of ship size in container liner shipping. *International Journal of Production Economics 159*(C), 241–253.

U.S. Army Corps of Engineers (2021). Ports and port statistical areas. data retrieved from U.S. Army Corps of Engineers Geospatial, https://geospatial-usace.opendata.arcgis.com/datasets/b7fd6cec8d8c43e4a141d24170e6d82f_0/explore.

Chapter 4

Cargo Ships & Coastal Smog: A Case Study of San Pedro Bay

Cargo Ships & Coastal Smog: A Case Study of San Pedro Bay

Philip Economides*

June 2, 2024

Abstract

This paper examines the effect of a new port queuing system at San Pedro Bay, California, on local and global maritime emissions using data from the Environmental Protection Agency, MarineCadastre and MarineTraffic. I find evidence which suggests that an estimated time of arrival based queue port queue system encourages a slowdown of vessel voyages. Furthermore, this added travel certainty lessens idling time in the local port vicinity – despite deeper water waiting experiences contributing positively to overall fuel consumption. Taking the voyage and queuing legs of 2,111 vessel transits into account across over 2,000 distinct journeys, I associate the policy with a 30.2% reduction in these vessels' CO_2 emissions.

JEL Codes: D62, F18, F64, L51, Q52, Q53, R41
Keywords: local environmental policy, transport externalities, local air pollution, port logistics, vessel queues, congestion, maritime trade.

*Department of Economics, University of Oregon.
I am indebted to Woan Foong Wong, Bruce Blonigen, Anca Cristea, and Nicole Ngo for their advice and guidance. I would like to thank Mark Colas, Grant McDermott, Ed Rubin, and seminar participants at the University of Oregon for suggestions and comments. All remaining errors of this initial draft are my own.

4.1 Introduction

According to the World Bank, international trade in 2022 represented 62 percent of global GDP – a remarkable ascension from a 24 percent share in 1970. With goods more commonly sourced from abroad, the average transportation distance of intermediate and final goods has also grown. From 1965 to 2020, the cargo weight of short-distance trade rose by 45 percent, while longer-distance voyages more than doubled their cargo volumes (Ganapati and Wong, 2023). Given these trends, the maritime shipping industry has developed a significant carbon footprint.[1]

This form of activity – in which 70 percent of maritime emissions occur within 400 km of coasts (Corbett et al., 2007) – has been attributed to harmful health outcomes for nearby populations (Capaldo et al., 1999; Liu et al., 2016; Gillingham and Huang, 2021; Zhang et al., 2021). Reductions to the shipping industry's global emissions footprint face two distinct challenges; (i) vessel ownership is well distributed across countries, highlighting a need for concerted global governance efforts, and (ii) much of the available tools for reducing emissions are indirect in nature, which allows for strategic responses by key stakeholders.

Both the International Maritime Organization (IMO) and US Department of Transportation (DOT) have pursued policy seeking to decarbonize ports and the maritime transport sector. For example, the IMO has member states targeting reductions in total greenhouse gas (GHG) emissions of maritime transport by 20–30 percent as of 2030 and 70–80 percent by 2040. Their main goal is net-zero GHG emissions by 2050. Furthermore, a recent preview of the "US National Blueprint for Transportation Decarbonization" by the DOT outlines how the US government seeks to accelerate the transition to clean options in maritime shipping through zero-emission fuels, technologies, energies, and new vessels.[2]

[1] Maritime shipping represents 2.89 percent of global CO_2 emissions (IMO, 2021).

[2] Available at https://www.transportation.gov/priorities/climate-and-sustainability/us-national-blueprint-transportation-decarbonization. Last accessed on May 30th 2024.

This paper examines how a logistical intervention by port authorities contributes to decarbonization in the maritime transportation sector. I consider a case study of the ports of San Pedro Bay, which sought to mitigate a large increase in vessel emissions through the introduction of a new port queuing system. Under the prior system, queue positions at the ports of LA and Long Beach were issued on a first-come first-serve basis upon entering within 25 nautical miles of the San Pedro Bay port complex. Vessel operators' choice of voyage speed influenced their assigned queue position. Should a port be at full capacity, vessels could either drop anchor in close proximity to the cities of Los Angeles and Long Beach or drift nearby, and begin contributing to local port emissions.

The US economic recovery from the COVID-19 epidemic led to a dramatic increase in import demand, reflected by record numbers of commodity-laden containers entering the US between October 2020 and November 2021.[3] This increase in maritime trade activity caused historic levels of congestion across US ports, leading to prolonged vessel queues and abnormally high GHG emissions. For example, recent findings from the Los Angeles Port Authority's Inventory of Air Emissions (2021) suggest a 69 percent annual increase in port emissions of PM_{10} and PM_{25} between 2020 and 2021, with the rate as high as 143 percent specifically for ocean-going vessels. Contributions through the anchorage and queuing stages of vessel operations represented the majority of these emissions (Figure 4.1) and were driven primarily by containerships (Figure 4.2). This period of congestion led to numerous cases of environmental damage. In October 2021, just a month prior to policy introduction, a crude oil spill occurred. This was later attributed to anchor damage caused to a nearby pipeline by two containerships, which resulted in losses and clean-up costs worth an estimated 160 million USD.[4]

[3]2021 represented an 15.4 percent annual increase in container traffic, as opposed to a long run average of 3.5 percent across the prior decade of activity.

[4]See National Transportation Safety Board, Project Summary: Marine Investigation - 130 Docket Items - DCA22FM001 and Report MIR-24-01, "Anchor Strike of Underwater Pipeline and Eventual Crude Oil Release". Last Accessed 03/09/2024.

Figure 4.1: 2005-2021 POLA OGV NOx Emissions (tons), by mode

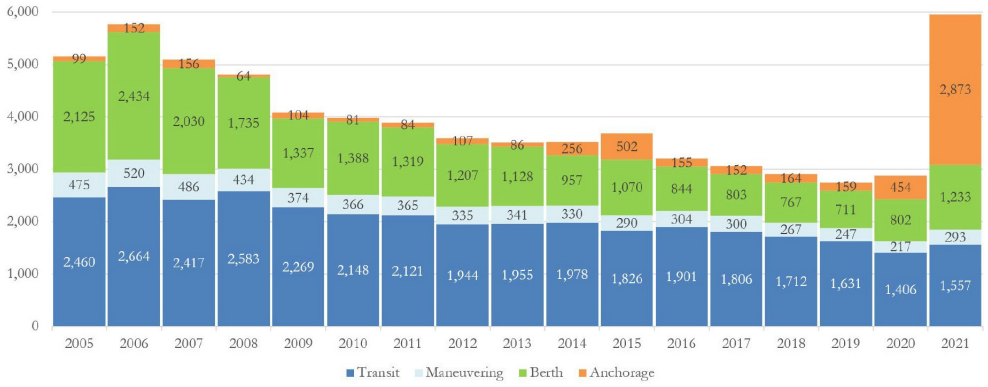

Source: Los Angeles Port Authority's Inventory of Air Emissions (2021)

Figure 4.2: 2020 & 2021 POLA OGV NOx Emissions (tons), by mode

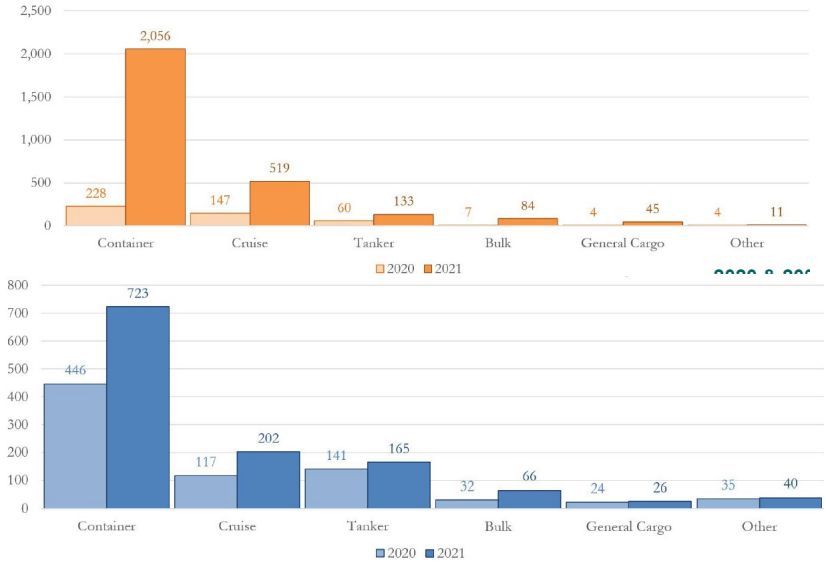

Source: Los Angeles Port Authority's Inventory of Air Emissions (2021)

To address the ports' escalating levels of pollution and prevailing environmental damage, the vessel queuing system was updated. On November 11th 2021, the ports of LA and Long Beach jointly announced a new procedure in which vessels would be assigned queue positions by Pacific Maritime Management Services. Rather than the prior "first-come first-serve" process, a queue position would instead be determined by an estimated time of arrival (ETA) from a prior port of departure, assuming a constant travel speed. Furthermore, arriving ships are re-

quired to wait outside the 'Safety and Air Quality Area', 150 nautical miles out at sea, rather than within the anchorage zone. Although the policy may reduce travel speeds through guaranteed queue positions, the added requirement to remain adrift further out at sea introduces an ambiguous global vessel emissions effect. Should it be the case that vessels hardly changed their speeds and fuel consumption while adrift off the continental shelf is particularly taxing on emission levels, this policy could be considered a form of environmental NIMBY-ism, similarly to cases featured in Morehouse and Rubin (2021) and Zou (2021).[5] In this case, ports would be reaping the commercial benefits of their property rights while exporting the cost of any resulting air pollution. Alternatively, if speed reductions are considerable or vessels spend less time idling due to improved certainty on port admittance, the greater fuel expended during the queuing process may be negligible in comparison. Under such circumstances, this logistical practice may offer oversight bodies, such as the International Maritime Organization or the US Department of Transportation (DOT), an additional policy tool through which to meet long-term goals of a decarbonized maritime transport sector.

I quantify the local and global effect of this policy on vessel-related carbon emissions. First, I use a difference-in-difference approach to estimate the new system's effect on areas in proximity to the ports, using the EPA's local air quality measures, where relevant controls consist of (i) port areas of Oakland, Seattle and Tacoma, and (ii) nearby inland regions.[6] While Figure 4.3 suggests a rather dramatic reduction in local emissions, given the subsequent decline in ships in anchorage, I find evidence to suggest that countervailing effects offset any potential improvement in local air quality. I also ask whether this decision simply shifted emissions elsewhere or functioned as a tool to reduce global vessel emissions. I

[5] "Not In My BackYard", a term coined by Mitchell and Carson (1986). Often associated with cases in which a property owner wants a beneficial economic activity to occur on her property while expelling the negative externalities of production elsewhere.

[6] This data has previously been used to highlight how local vessel emissions contribute negatively to health outcomes (Gillingham and Huang, 2021; Hansen-Lewis and Marcus, 2022).

resolve this ambiguity by weighing changes in both voyage & queuing behaviour and estimate a 30.2% decline in the global emissions of containerships inbound for San Pedro Bay, due to the new vessel queuing system.

Figure 4.3: POLA Number of Container Ships at Anchorage, Daily

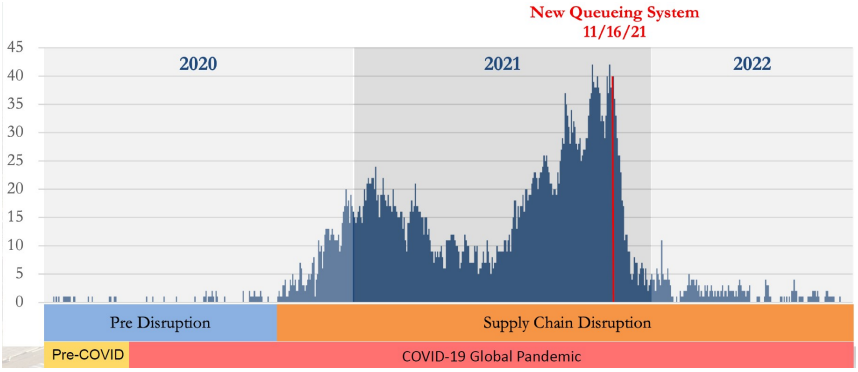

Source: Marine Exchange of Southern California

This paper contributes to several strands of literature. Firstly, it adds to a recent selection of studies leveraging use of relatively modern transportation data. I rely on automatic identification system (AIS) vessel traffic to observe the exact geo-spatial positions of vessels at a one-minute resolution through big data queries (Heiland et al., 2019; Prochazka et al., 2019; Tumbarello et al., 2019; Brancaccio et al., 2020; Wong, 2022; Wong and Fuchs, 2022). As Klotz and Berazneva (2022) highlights, the precision of AIS data allows for granular analysis into coastal movements and berthing at local ports, which is essential for estimating associated emissions levels. I consider vessel–specific, within–route emissions across two stages of vessel transit; (i) voyage – transit between a prior port of departure and US waters, and (ii) queuing – the anchoring and drifting of vessels awaiting port entrance along the US west coast. This study offers a new methodology by which AIS vessel positions can be used to map drifting and anchoring behaviour within port queues and infer individual emission levels across vessels.

I also contribute to topics of transports policy, congestion and environmental conservation (Kinney et al., 2011; Cristea et al., 2013; Ngo et al., 2015; Shapiro,

2016; Rivera, 2021). Gillingham and Huang (2021) finds that emissions from vessels at-berth in US ports contributed to reduced child birth weights. Similarly, Hansen-Lewis and Marcus (2022) concludes that the introduction of US maritime emissions control areas significantly decreased fine particulate matter, low birth weight, and infant mortality. However, strategic responses of transport operators limited these gains to only half of forecasted reductions. I quantify local vessel emissions through queuing activities and quantify global emissions associated with inbound voyages & out-of-port congestion. By holding service lanes fixed across my sample – I mitigate the influence of various strategic responses that transport operators may be availing of. I also document that queuing behaviour, while limited to narrow geographic regions, represents at least 20% of transit time for inbound containerships along the US West Coast.

Third and lastly, this paper advances our knowledge of viable tools for environmental regulatory intervention. Given that an ETA-based policy resulted in global emissions falling and vessels spending less time idling outside of harbor regions, this may not only limit negative externalities associated with the industry but also boost its productivity. My findings suggest that queuing activity has acted has the main driver of emission reductions. Small– to medium–sized ports, less subject to excessive queuing behaviour, may be less likely to capture the environmental benefits of this logistical practice.

The remainder of the paper proceeds as follows. Section 2 provides background and a description of the data before shifting into the means by which I estimate at-sea vessel emissions both at the voyage and queuing stages. Section 3 details the empirical strategy for identifying the local & global policy effects of the new queuing system and discusses results. Section 4 concludes.

4.2 Data & Inference

In this section, I describe the combination of several publicly available datasets and a privately purchased port call data, which allows for the construction of individual vessel emission records between November 2019 to November 2022. The data fall into three broad categories: air quality, vessel, and geographic data. I then outline how I infer associated fuel consumption and emission levels using observed vessel–voyage events. I elaborate on data preparation in Appendix A3, Section I.

4.2.1 Data

Air Quality: To address local emissions levels, I use daily Air Quality Index measures provided by the Environmental Protection Agency (AQI). This data relies on outdoor monitors across the United States. States determine monitor placements based on areas of relatively high population. According to the EPA, each state is responsible for developing its own monitoring plan, which is then reviewed and revised every five years. To include additional monitors, these instruments must follow "stringent siting and quality assurance criteria and are maintained by state and local agencies." Each monitor's report details ozone, particulate matter, carbon monoxide, sulfur dioxide and nitrogen dioxide levels.[7] Each state-county in the dataset contains multiple site locations.

I form separate sets of inland and coastal sites across Los Angeles and Long Beach to compare control and treatment group outcomes, respectively. For robustness, I also use comparable zones in proximity to port regions along the West Coast, untreated by the new ETA–based queuing system.

[7]The reported value identifies the highest concentration of a given pollutant among all of the monitors within each reporting area. It will select two breakpoints that contain the concentration. The index value is calculated as $\mathrm{I}_p = \frac{\mathrm{I_{Hi}} - \mathrm{I_{Lo}}}{\mathrm{BP_{Hi}} - \mathrm{BP_{Lo}}} (\mathrm{C_p} - \mathrm{BP_{Lo}}) + \mathrm{I_{Lo}}$, where $\mathrm{C_p}$ is the truncated concentration of pollutant p, $\{\mathrm{BP_{Hi}}, \mathrm{BP_{Lo}}\}$ are the breakpoints associated with the truncated value, and $\{\mathrm{I_{Hi}}, \mathrm{I_{Lo}}\}$ are their associated AQI values.

Vessels: I have purchased port call data from MarineTraffic (MT), which provides a record of port entrances and exits internationally. I focus on a subset of visits across the US west coast – Seattle, Tacoma, Oakland, Los Angeles and Long Beach – dated between November 2019 and November 2022. MT data details each vessel's prior port of departure and departure time, and port of arrival and arrival time. Each vessel is also uniquely identified by their assigned International Maritime Organization (IMO) codes, which remain invariant to changes in ownership, flag and vessel name. Upon cleaning, this dataset consists of 1,061 uniquely identified vessels servicing 10,035 port visits, where vessels' container capacities range from 200–23,000 twenty-foot equivalent units.

While port call data is helpful in establishing transit routes, distances and durations, this alone would not allow one to distinguish between voyage and queuing stages of transit. To separately these separate stages, I combine MT with records of individual vessel movements in US waters. These US Coast Guard records use vessels' transceivers that signal the IMO code, status, speed, geo-location, and name of a given ship. I use a publicly available provision of this signal data from MarineCadastre (MC) for containership vessel movements at a minute resolution between January 2019 to December 2022. Lastly, I use time-invariant vessel characteristics from VesselTracking (VT) to assign each vessel their gross size and container capacity. These metrics are key in interpreting how vessel speed maps into fuel consumption.

Using unique vessel IMO codes and associated transit timelines, I combine the coordinates and timestamps of vessels' MT port departures with MC reappearances in US waters. This allows for the assignment of exact travel distances and speed to each individual vessel voyage stage. Transit between US waters arrival and eventual admittance into a US port represents the queuing stage of each voyage. Combining these two events represents the full transit experience of an

individual vessel. By joining the two datasets, I can discern which transits in US waters represent international journeys (Figure 4.4).

Figure 4.4: Match Status by Origin and Group

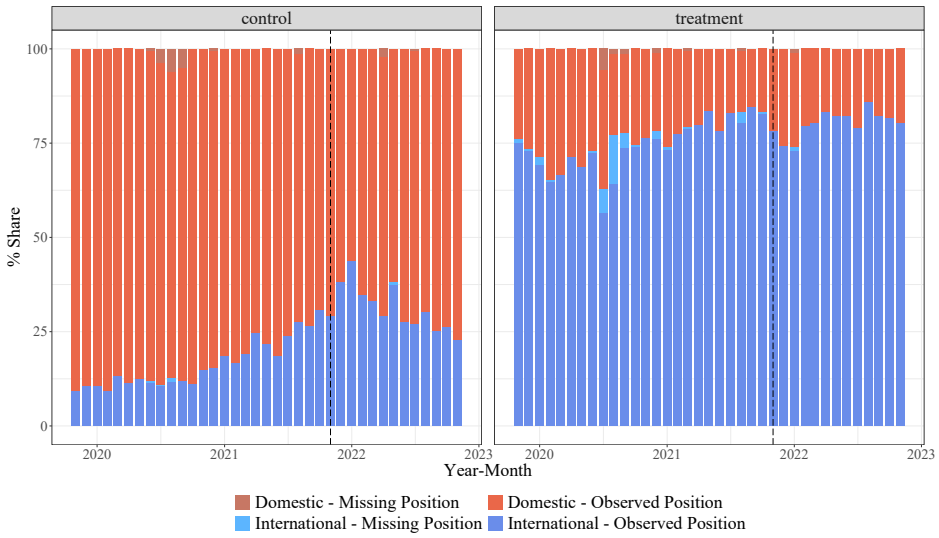

Upon dropping extreme outliers – determined based on average travel speeds of individual voyages – I use a sample of 10,035 vessel voyages serviced by 1,061 distinct containerships.[8] Table 4.1 characterize each included port by period.

Table 4.1: Summary Statistics of Vessel Voyages

Port	Period	Visits	Vessel Age	Max TEU	Dwell Time	Voyage Time	Voyage Speed
Long Beach	pre-	1708	11.45	7705.59	93.97	237.38	17.22
Long Beach	post-	751	12.74	7466.68	100.84	339.94	15.12
Los Angeles	pre-	1890	10.94	7491.60	119.64	259.50	18.22
Los Angeles	post-	800	11.27	7310.79	132.11	385.55	14.62
Oakland	pre-	1906	12.84	7145.26	48.77	36.09	4.01
Oakland	post-	729	16.06	5370.96	67.75	124.45	6.81
Seattle	pre-	706	12.68	6341.05	56.10	75.57	5.60
Seattle	post-	375	13.28	5541.22	52.30	196.03	9.29
Tacoma	pre-	936	18.35	4716.93	49.22	150.26	15.30
Tacoma	post-	412	20.64	4721.33	64.44	172.31	14.72

Columns 4–8 report averages across vessels for their respective port and time period. "Pre-" is defined as prior to November 11th 2021, when the new San Pedro Bay queuing system was announced for LA and Long Beach. 'Vessel Age' is reported in years. 'Max TEU' reports the container capacity of vessels, 'Dwell Time' details how many hours vessels spend handling goods at port. 'Voyage Time' details hours between a departure time and the point at which a vessel reappears in US waters. 'Voyage Speed' is reported in nautical miles per hour.

[8] I follow Davies and Jeppesen (2015), which labels extreme outliers as values outside a specific closed range. The lower bound is the 25th percentile of average travel speeds less three times the interquartile range (75th percentile value less the 25th percentile value). The upper bound is the 75th percentile of average travel speeds plus three times the interquartile range.

As these statistics highlight, there are a considerable number of journeys taking place within proximity to the North American continent. Many cases involve vessels completing subsequent visits at nearby ports upon arriving at the US West Coast. For my empirical approach, I first consider the new queuing system's effect on broader vessel activity, and then limit my evaluations to consider only international journeys.

There is also the potential that transport operators may strategically respond to the policy by switching destination ports from abroad. For example, if I wished to preserve my ability to endogenously influence queue positions, I could elect to switch my initial US entry point to a non-treated port. Upon originating from the non-treated port, my subsequent journey to a treated port has now been reduced dramatically and a far lower percentage of overall transit services is exposed to the new queuing system. To avoid this issue of partial selection out of treatment, I focus my third set of results on the subsample of vessels that maintained services to their original pre–policy destinations after the implementation of the policy. Any vessels that no longer serviced the West Coast, as well as newly introduced vessels appearing only after policy implementation are also excluded to avoid concerns of strategic responses that rotate vessels in and out of the West Coast trade network. "Switcher", "Entrant" and "Exit" vessels are excluded from this third empirical approach. The remaining balanced panel of vessel activity occurring consistently prior– and post–policy includes 2,354 port visits serviced by 301 distinct vessels.

Geographic: I use Port Statistical Area data, made available through the United States Army Corp of Engineers (USACE). After some modifications, this allows me to represent polygon regions of key port areas. Using these boundaries, I identify the exact minute at which port entrances and departures occur across US ports, which spells the end of the queuing stage for a given vessel.

4.2.2 Fuel Consumption

To study variation in vessel emissions, I require a measure of fuel consumption. I infer these levels by inputting vessel's travel speeds and ship sizes (TEU capacity) into fuel consumption functions featured in Figure 4.5 from Rodrigue (2020).[9] I interpolate across these TEU-specific functions and generate a bi-variate, polynomial function through OLS.[10]

Figure 4.5: Fuel Consumption by Speed and TEU Capacity

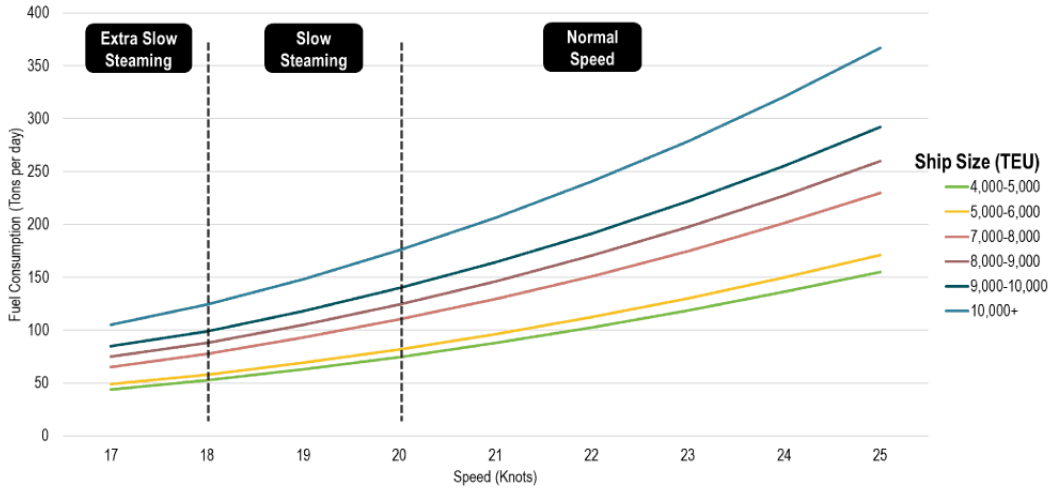

Source: Rodrigue (2020). The Geography of Transport Systems, Chapter 4, Transportation and Energy.

For static berth activity, I recommend the use of a scaling factor proposed by Hulskotte and Denier van der Gon (2010) which receive frequent use in the maritime logistics literature (Jalkanen et al., 2012; Ju and Hargreaves, 2021; Schwarzkopf et al., 2021). This is a linear function of the gross tonnage of vessels times the hours spent stationary (Table 4.2). For the purposes of this study, assessing voy-

[9]Since I do not observe engine types across vessels, I do not use an alternative naval engineering formula featured in Corbett et al. (2009) and Lugovskyy et al. (2023), which combines speed and engine types across main and auxiliary units. Ship size is recognized as a strong predictor of emissions and has sufficed in applied studies of vessel emissions (Walsh and Bows, 2012).

[10]Assessing the model fit of this exercise, the function appears to best perform at standard cruising speeds of 10–25 nautical miles (knots) per hour. However, at slower speeds, inferred functions of fuel consumption levels do not behave reliably. I introduce a conditional estimation of fuel consumption in which levels below cruise speed (10 knots) receive additional adjustments based on prevailing studies of vessel emissions at slow movement stages. See Appendix A3 (II.) for further details.

age and queuing stages of transit, I do not include berthing activity in broader analysis.

Table 4.2: Estimate of Fuel Consumption by GT-Dwell Hours

Type of ship	Fuel Consumption Rate (kg fuel/1000 GT h)	Average hotelling time at berth (hours)
Oil Tankers	19.3	28
Chemical and other tankers	17.5	24
Bulk Carriers	2.4	52
Containers	5.0	21
General Cargo	5.4	25
Ferries and RoRo	6.9	24
Reefers	24.6	31
Other	9.2	46

Source: Hulskotte and Denier van der Gon (2010). Fuel Consumption and Associated Emissions from Seagoing Ships at Berth Derived from Onboard Survey, Atmospheric Environment, Vol. 44(9), pp 1229–1236.

Upon calculating fuel consumption for each stage of transit, I use assumptions detailed in the proceeding subsection to generate associated emissions levels for each vessel's various stages of transit.

4.2.3 Vessel Emissions

I refer conversion rates provided by Czermanski et al. (2021), which converts tons of fuel to CO_2, SO_X, NO_X and $PM_{2.5}$ kilogram emissions. I assume vessels are in accordance with IMO 2020, which mandates an upper limit of 0.5% sulfur content in vessel fuel sources and therefore exclusively use the first row of featured conversion rates (Table 4.3).

Table 4.3: Emissivity Indices for Selected Marine Fuels

	[kg/t of Fuel]			
Fuel	CO_2	SO_X	NO_X	$PM_{2.5}$
MDO 0.5%	3206.00	10.50	50.50	2.30
HFO 1.5%	3114.00	31.50	51.00	3.40
HFO 2.0%	3114.00	42.00	51.00	3.40
HFO 3.5%	3114.00	71.50	51.00	3.40
LSHFO 0.5%	3151.00	10.50	51.00	2.30
LSMGO 0.1%	3151.00	2.10	50.50	2.30
LNG	2750.00	¡0.02	8.40	0.02
Methanol	1375.00	0.00	26.10	0.02
HFO + SCRUBBER + SCR	3176.00	0.84	7.65	0.51

Source: Czermanski et al. (2021), based on the assumptions of the Med Atlantic Ecobonus (MAE) Project, MAE External Cost Calculator Tool.

For a full set of details regarding how vessel emissions are calculated for slow travel speeds in the local port area, see Appendix A3, Section III.

4.3 Empirical Strategy & Results

Variation in local emissions can be represented through two types of measures; (i) observed general measures of air quality from the Air Quality Index, and (ii) estimated vessel-specific emission levels implied by the fuel consumption of containerships reporting AIS signals in the San Pedro Bay area. Using global movement data, I also examine whether this decision shifted the emissions problem elsewhere or reduced the global emissions of vessels. This involves carefully dissecting individual vessel voyages across voyage, queuing and berthing stages of transit. In the proceeding section, I first detail my empirical strategy and then yield policy effects for both local and global vessel emissions.

4.3.1 Empirical Strategy

Vessel position data reports the speed and status codes of each vessel in US waters, allowing me to identify whether vessels are underway (U), maneuvering (M), at anchor (A) or at berth unloading their goods (B). Using local emissions efficiency – represented as an emissions per hour rate $\left(\frac{e^L_{ipt}}{h^L_{ipt}}\right)$ – summed across these four local transit stages,

$$\frac{e^{\mathrm{L}}_{ipt}}{h^{\mathrm{L}}_{ipt}} = \frac{e^{\mathrm{U}}_{ipt} + e^{\mathrm{M}}_{ipt} + e^{\mathrm{A}}_{ipt} + e^{\mathrm{B}}_{ipt}}{h^{\mathrm{U}}_{ipt} + h^{\mathrm{M}}_{ipt} + h^{\mathrm{A}}_{ipt} + h^{\mathrm{B}}_{ipt}}, \tag{4.1}$$

may analysis is capable of focusing on each individual stages of local activity. For simplicity, I combine activity across underway, maneuvering and anchoring activity as the "Queuing Stage" (Q) – which excludes berthing.

To measure global emissions, I take these measures jointly with voyage (V) emissions of each ship from their respective ports of departure, e^{V}_{ipt}. The fuel efficiency of each global voyage is expressed as,

$$\frac{e^{\mathrm{G}}_{ipt}}{h^{\mathrm{G}}_{ipt}} = \frac{e^{\mathrm{V}}_{ipt} + e^{\mathrm{Q}}_{ipt}}{h^{\mathrm{V}}_{ipt} + h^{\mathrm{Q}}_{ipt}} \tag{4.2}$$

To exploit the quasi-experimental nature of this policy change – announced and introduced within a 5-day window – I consider the following specification:

$$Y^{S}_{iodt} = +\delta^{S}_{1} T_d + \delta^{S}_{2} D_t + \delta^{S}_{3} \left(T_d \times D_t\right) + \phi^{S}_{io} + \phi^{S}_{t} + \mu_{irpt}, \tag{4.3}$$

where i identifies the individual vessel, io indicates the vessel–voyage route serviced repeatedly over time, and t represents the associated time period. Dummies T_d and D_t act as treatment and post-period dummies, respectively. Control group ports include Oakland, Seattle and Tacoma which are also exposed to shocks common across the US West Coast, while not treated by this particular policy. The fuel efficiency outcome variable, Y^{L}_{ipt}, is emissions-per-hour on a given transit stage, $S \in \{\mathrm{V}, \mathrm{Q}, \mathrm{G}\}$ and can therefore be decoupled for any particular stage of service within a given vessel-voyage, $iodt$. The coefficient of interest, δ^{G}_{3}, indicates the global emissions effect of the policy, where $\hat{\delta}^{G}_{3} < 0$ would suggest that this new queue system is a tool that could assist in efforts to decarbonize vessels servicing US ports. Key to this identification approach is the assumption of parallel trends. In Figure 4.6, a clear parallel trend exists in the absence of treatment between treated and control port groups.

I suggest that the guaranteed queuing position issued in the post-period portion of the sample may have encouraged a relatively higher percentage of vessels to slow-steam towards their West Coast destination, lowering average emission levels across the voyage length of a given transport service. Referring to Eq. (4.2),

Figure 4.6: Parallel Trends in Average Voyage Speeds

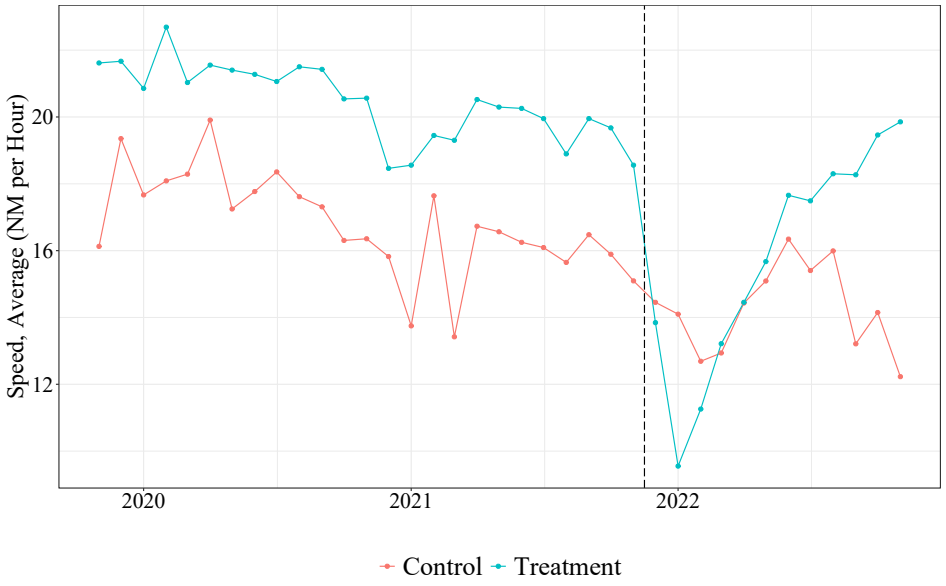

this would suggest that $\frac{e^V_{ipt}}{h^V_{ipt}}$ should decline. Furthermore, if a queue position is known then transport operators would be able to better time their arrivals and minimize unproductive idling near the port area. Counteracting this effect, the increased extent to which vessels must remain idle outside of the treated ports' respective anchorage zones would contribute to greater degrees of drifting and repositioning (distance travelled) relative to being able to lay anchor, which may elevate emission per hour rates among visiting vessels. Examining Eq. (4.2), and supposing we treat drifting as an alternative form of deep-sea anchorage, this would suggest that $\frac{e^Q_{ipt}}{h^Q_{ipt}}$ could rise. This leads to an ambiguity in the values of $\{\delta^G_3, \delta^Q_3\}$ which may be of empirical interest to port authorities that wish to implement environmentally-friendly logistical changes to port management. Should $\hat{\delta}^G_3 < 0$, this would suggest that a simple queuing system change could contribute to existing efforts by the IMO to reduce the carbon footprint of the maritime transport sector. If $\hat{\delta}^G_3 >= 0$, this would implies that the policy is either ineffective in achieving air quality improvements and may possibly be a negative externality generating form of environmental NIMBY-ism.

I also employ use of a difference-in-difference estimator to examine the policy effect on local air emissions in treated and non-treated US West Coast port areas. I estimate the policy effect on local emissions using the following specification:

$$Y_{ipt} = \alpha + \gamma_1 T_p + \gamma_2 D_t + \gamma_3 \left(T_p \times D_t\right) + \varepsilon_{ipt}, \tag{4.4}$$

where i identifies the individual location (or vessel), p indexes a given port region, t represents the associated date. Dummies T_p and D_t act as treatment and post-period dummies, respectively. T_p takes a value of 1 for any given coastal locations along Los Angeles and Long Beach, and is 0 otherwise.[11] D_t takes a value of 1 for any time period from November 11$^{\text{th}}$ 2021 onward. The dependent variable includes the following forms of emissions from AQI data; carbon monoxide (CO), sulfur oxides (SO_X), nitrogen oxide (NO_X), fine particulate matter ($PM_{2.5}$), and coarse particular matter (PM_{10}).

4.3.2 Local Emission Effects

In this subsection, I outline the results of Equation 4.4. In Figure 4.7, I display Zone I – 'port-adjacent' monitors within 25 miles of the centroid of highlighted port areas – and Zone II – monitor groups between 25-50 miles from their respective port centroid. Miles of distance between points are calculated using Vincenty distance, which accounts for oblate spheroid curvature of the earth.

I follow two specifications which alternate the key control group. For the initial set of results, the treatment (control) group consists of monitors within 25 (between 25-50) miles of the San Pedro Bay port complex. In the second set of results, the treatment (control) group consists of monitors within 25 miles of the

[11] To address concerns about vessel pollutants spreading across nearby coastal and inland regions of San Pedro Bay in a similar manner, an alternative treatment indicator compares sites associated with treated ports against sites of non-treated port cities along the West Coast (e.g. Oakland, Seattle, Tacoma).

San Pedro Bay port complex (ports of Seattle or Oakland). Despite a considerable reduction in port traffic in the anchorage and drift zones adjacent to the ports of Los Angeles and Long Beach, a review of variation in local conditions suggests no notable reduction in associated air pollutant concentrations.

Figure 4.7: AQI Monitor Local Sites

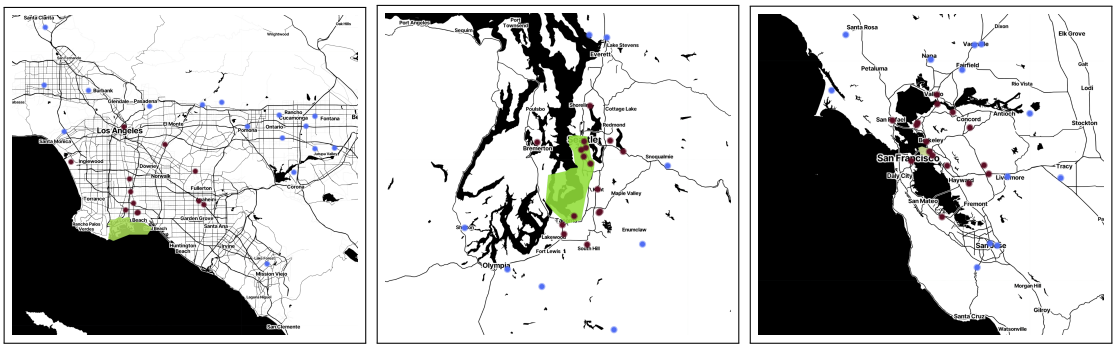

Note: Each polygon depicts a port area. Red sites represent zone I monitors. Blue sites represent zone II monitors.

Upon reviewing the on-site effect, which compares zones I and II within San Pedro Bay, I find a significant increase in local emissions (Table 4.4). I find that the new system contributed positively to port-adjacent emissions through a; (i) 10.9% increase in carbon monoxide, (ii) 12.1% rise in nitrogen dioxide, (iii) 11.2% rise in oxides of nitrogen, and (iv) 3.9% elevation in ozone levels.[12]

Using particulate matter (PM) measures of pollutant concentrates, I find similar evidence of broad increases in emissions across monitors adjacent to the port area, relative to the outer zone of monitors (Table 4.5). PM_{10} emissions rose by a 23% and $PM_{2.5}$ rose by 5.4%. Sulfur emissions showed a slight decline, although not to a statistically significant extent.

In the second specification of this assessment, I contrast outcomes across port-adjacent monitors near the ports of Los Angeles and Long Beach to other port-adjacent monitors positioned along the West Coast (Table 4.6). This may address concerns that particular vessel emissions may struggle to permeate regions beyond

[12]These upward shifts are relative to adjacent inner-city monitor zones distanced between 25-50 miles from the San Pedro port area.

Table 4.4: Difference-in-Difference, Control: San Pedro Bay, Zone-II

Dep. Variable:	CO (1)	NO2 (2)	NOx (3)	Ozone (4)
Post–Period	0.0976 (0.2539)	0.1382 (0.1670)	0.2977 (0.2551)	-0.2403 (0.1635)
Treated	0.0189 (0.0031)	-0.0392** (0.0014)	0.0819*** (0.0012)	-0.1824*** (0.0001)
DiD	0.1089** (0.0019)	0.1213*** (0.0015)	0.1121*** (0.0013)	0.0386*** (4.14×10^{-5})
Day FE Month-Year FE	✓ ✓	✓ ✓	✓ ✓	✓ ✓
Observations R^2	17,804 0.30	21,127 0.33	21,141 0.32	18,294 0.49

Note: ***: 0.01, **: 0.05, *: 0.1. Standard-errors are robust to clustering by monitor zone. Each observation is a distinct day-monitor-port emission type reading. 'Post-Period' is equal to 1 for dates November 11th 2021 to October 30th 2022. 'Treatment' is equal to 1 for air pollutant concentration monitors within a 25-mile radius (Zone I) of the centroid of the San Pedro Bay port complex. The relevant control group consists of monitors within 25-50 miles of the same reference point (Zone II).

Table 4.5: Difference-in-Difference, Control: San Pedro Bay, Zone-II

Dep. Variable:	PM_{10} (1)	$PM_{10-2.5}$ (2)	$PM_{2.5}$ (3)	SO2 (4)
Post–Period	-0.1898* (0.0160)	0.2919 (0.0582)	-0.3486 (0.2103)	0.3764* (0.0311)
Treated	-0.3151*** (0.0018)	-0.5804*** (0.0035)	0.0032 (0.0014)	-0.4552* (0.0370)
DiD	0.2302** (0.0052)	0.1582** (0.0070)	0.0541* (0.0045)	-0.0966 (0.0349)
Day FE Year–Month FE	✓ ✓	✓ ✓	✓ ✓	✓ ✓
Observations R^2	6,949 0.22	1,303 0.40	14,471 0.25	3,853 0.19

Note: ***: 0.01, **: 0.05, *: 0.1. Standard-errors are robust to clustering by monitor zone. Each observation is a distinct day-monitor-port emission type reading. 'Post-Period' is equal to 1 for dates November 11th 2021 to October 30th 2022. 'Treatment' is equal to 1 for air pollutant concentration monitors within a 25-mile radius (Zone I) of the centroid of the San Pedro Bay port complex. The relevant control group consists of monitors within 25-50 miles of the same reference point (Zone II).

25 miles of the US coastline. Results are broadly supportive of findings in Table 4.4, both in terms of direction and relative magnitudes across emission types.

Referring to particulate matter emissions in Table 4.7, port-to-port difference-in-difference comparisons yield further evidence of a statistically significant rise in emissions upon the introduction of the new port queuing system. Notable deviations from the zone-based results listed in Table 4.5 include a near doubling of particulate matter between 2.5 and 10 micrometers in diameter. Additionally,

Table 4.6: Difference-in-Difference, Control: Seattle/Oakland, Zone-I

Dep. Variable:	CO (1)	NO2 (2)	NOx (3)	Ozone (4)
Post–Period	0.3445**	0.3377**	0.5386**	-0.4985**
	(0.0639)	(0.0639)	(0.1071)	(0.0712)
Treated	-0.2141*	0.3427**	0.3074	0.2007***
	(0.0502)	(0.0579)	(0.1054)	(0.0078)
DiD	0.1577***	0.1085**	0.1864***	0.0402**
	(0.0078)	(0.0145)	(0.0019)	(0.0073)
Day FE	✓	✓	✓	✓
Year–Month FE	✓	✓	✓	✓
Observations	17,788	21,738	20,732	17,385
R^2	0.29	0.41	0.36	0.41

Note: ***: 0.01, **: 0.05, *: 0.1. Standard-errors are robust to clustering by monitor zone. Each observation is a distinct day-monitor-port emission type reading. 'Post-Period' is equal to 1 for dates November 11th 2021 to October 30th 2022. 'Treatment' is equal to 1 for air pollutant concentration monitors within a 25-mile radius (Zone I) of the centroid of the San Pedro Bay port complex. The relevant control group consists of monitors within 25 miles of the Port of Seattle and the Port of Oakland.

a somewhat significant decline in sulfur dioxide is detected.

Table 4.7: Difference-in-Difference, Control: Seattle/Oakland, Zone-I

Dep. Variable:	PM_{10} (1)	$PM_{10-2.5}$ (2)	$PM_{2.5}$ (3)	SO2 (4)
Post–Period	0.0164	-0.3332	0.4302	0.1943
	(0.2726)	(0.2562)	(0.3694)	(0.1447)
Treated	0.5940	1.426***	0.5539**	-0.2624**
	(0.2523)	(0.0051)	(0.1093)	(0.0510)
DiD	0.2863***	0.9336***	0.0107	-0.3240*
	(0.0264)	(0.0040)	(0.0113)	(0.1001)
Day FE	✓	✓	✓	✓
Year–Month FE	✓	✓	✓	✓
Observations	3,330	925	27,184	8,802
R^2	0.38	0.71	0.22	0.07

Note: ***: 0.01, **: 0.05, *: 0.1. Standard-errors are robust to clustering by monitor zone. Each observation is a distinct day-monitor-port emission type reading. 'Post-Period' is equal to 1 for dates November 11th 2021 to October 30th 2022. 'Treatment' is equal to 1 for air pollutant concentration monitors within a 25-mile radius (Zone I) of the centroid of the San Pedro Bay port complex. The relevant control group consists of monitors within 25 miles of the Port of Seattle and the Port of Oakland.

Reviewing these local emissions effects jointly, both control groups appear to corroborate the same story; the new port queuing system is associated with elevated emissions. Whether contrasting local emissions to adjacent regions within Southern California or similar coastal port regions along the US West Coast, the system contributed to elevated CO, NO2, NOx, Ozone and particulate matter pollutant concentrations. Reviewing the policy in question, there are less vessels now

using anchorage zones and drifting in the nearby bay area. However, given that these vessels were beyond 20 nautical miles out at sea, it is possible that these emissions did not strongly permeate the US coastline. Additionally, other factors may have offset any negative contributions the policy potentially made via the vessel congestion channel. For example, the en masse departure of these vessels – almost reached 100 containerships at the peak of the congestion crisis – potentially rekindled public interest in visiting coastal areas such as Santa Monica Pier and Venice Beach. Furthermore, the added certainty of vessel arrival times likelihood enhanced the appeal of connective modal services via truck and rail, further intensifying emissions in the region.

For reasons such as these, broad reviews of emissions can be far too subject to confounding factor biases. In the following subsection of this paper, I use vessel movement data to isolate the local and global effects of the policy on vessel emissions and mitigate any local confounding factors concerns.

4.3.3 Voyage Emission Effects

Table 4.8 details the effect of the new queue system on vessel voyage speeds. Column 3 excludes individual vessels that may have switched ports as a result of the implementation of this policy and acts as the main set of results. This restricts strategic responses across vessel operators that otherwise potentially biases results in columns 1 and 2 (Klotz and Berazneva, 2022). I find that the introduction of this new queue system lowered travel speeds by 16.97%.[13]

Using each vessel's voyage speed and their respective mass, I generate a set of emissions across individual vessel–voyages servicing the US west coast. As displayed in Table 4.9, my preferred subsample of international voyages yields a 10.47% reduction in total emissions following the introduction of the new queue

[13]For a log-level regression, I take the exponent of the coefficient and subtract 1.

Table 4.8: Difference-in-Difference Estimates – Voyage Speed

	Nautical Miles Per Hour		
	(1)	(2)	(3)
Post–Policy	0.2206***	0.1828**	0.2400***
	(0.0595)	(0.0776)	(0.0909)
Treatment	0.0796***	0.0414*	0.1080
	(0.0256)	(0.0244)	(0.1013)
DiD	-0.2129***	-0.1540***	-0.1860***
	(0.0321)	(0.0373)	(0.0394)
Vessel–Voyage FE	✓	✓	✓
Year–Month FE	✓	✓	✓
Observations	7,055	5,665	2,354
Average Speed, Pre-Policy	18.98	19.14	19.65
R^2	0.82	0.71	0.63

Note: ***: 0.01, **: 0.05, *: 0.1. Standard-errors are robust to clustering within vessel–voyage lanes of transport service. Each observation is a distinct voyage arriving on the US west coast between Nov 2019 and Nov 2022. Column 1 reports the broad diff-in-diff treatment effect on vessels. Column 2 excludes transshipping activity – short subsequent journeys between US ports after their initial arrival from a foreign port of origin. Column 3 only includes Column 2 vessel voyages that maintained the same international trade routes pre- and post- policy. Each regression uses a logged dependent variable. To limit extreme outlier distortions, I exclude any voyages with travel speeds less than the 25th percentile minus three times the interquartile range (75th percentile - 25th percentile) or higher than the 75th percentile plus three times the interquartile range (Davies and Jeppesen, 2015). "Average Speed, Pre-Policy" refers average vessel voyage travel speed of treated US ports prior to 11/11/2021.

system. Furthermore, per hour and per nautical mile emissions fell by 25.12 and 9.83 percent, respectively.[14] Although I refer to CO_2 emissions in my findings, the linear relationship prescribed by Czermanski et al. (2021) between fuel use and emissivity implies that log changes will be identical across all emission types.

I use an event study design to examine whether these policy effects are permanent or transitive in nature and subset for international journeys that continued maintaining the same service lines following the introduction of the policy. Relative to October 2021, vessels temporarily slow their transit speeds across voyages. As displayed in Figure 4.8, the two-way fixed effects findings suggests that reduced travel speed adjustments eased off by September 2023.

Similarly, emissions across voyages do see a level reduction that shows mean-reversion behaviour after July 2022. These short–lived effects suggest that an ETA-based queuing system may not yield substantial boons to the port's efforts

[14]Relaxing the sample to consider all 5,628 international vessel visits yields similar results.

Table 4.9: Difference-in-Difference Estimates – Voyage Emissions

	CO_2 Emissions			Em. per Hour	Em. per Knot
	(1)	(2)	(3)	(4)	(5)
Post–Policy	0.2929	-0.0503	-0.0895	0.1153	-0.1246
	(0.2917)	(0.0797)	(0.0996)	(0.1422)	(0.0867)
Treatment	1.929***	0.0918**	0.1193	0.1984	0.0900
	(0.3091)	(0.0363)	(0.0823)	(0.1760)	(0.0762)
DiD	-1.159***	-0.1053**	-0.1107**	-0.2894***	-0.1035**
	(0.1411)	(0.0430)	(0.0536)	(0.0777)	(0.0457)
Vessel–Voyage FE	Yes	Yes	Yes	Yes	Yes
Year–Month FE	Yes	Yes	Yes	Yes	Yes
Observations	10,004	5,628	2,346	2,346	2,346
R^2	0.91	0.95	0.91	0.75	0.83

Note: ***: 0.01, **: 0.05, *: 0.1. Standard-errors are robust to clustering within vessel–voyage lanes of transport service. Each observation is a distinct voyage arriving on the US west coast between Nov 2019 and Nov 2022. Column 1 reports the broad diff-in-diff treatment effect on vessels. Column 2 excludes transshipping activity – short subsequent journeys between US ports after their initial arrival from a foreign port of origin. Column 3 only includes Column 2 vessel voyages that maintained the same international trade routes pre- and post- policy. Columns 4 and 5 shift focus to per hour and per nautical mile measures of emissivity, respectively. Each regression uses a logged dependent variable. To limit extreme outlier distortions, I exclude any voyages with hourly emissions less than the 25th percentile minus three times the interquartile range (75th percentile - 25th percentile) or higher than the 75th percentile plus three times the interquartile range (Davies and Jeppesen, 2015).

Figure 4.8: Event Study (TWFE) - Voyage Speed

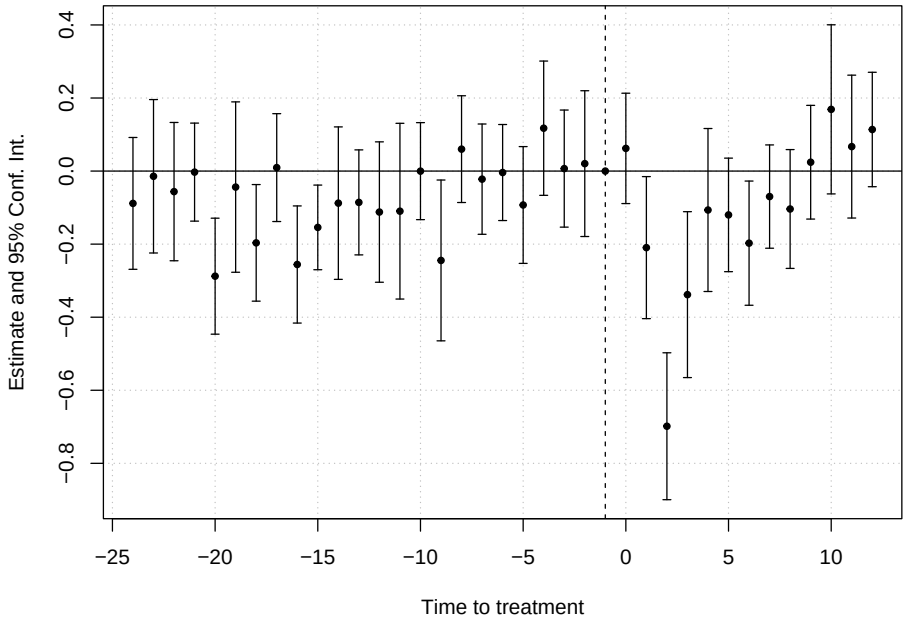

to decarbonize long-distance maritime shipping. However, in the next section I shift focus to the queuing leg of transit and demonstrate a substantial reduction in local vessel emissions. When combined with the queuing stage effect, global emission display a broad-based reduction as a result of this new system.

Figure 4.9: Event Study (TWFE) - Voyage Emissions

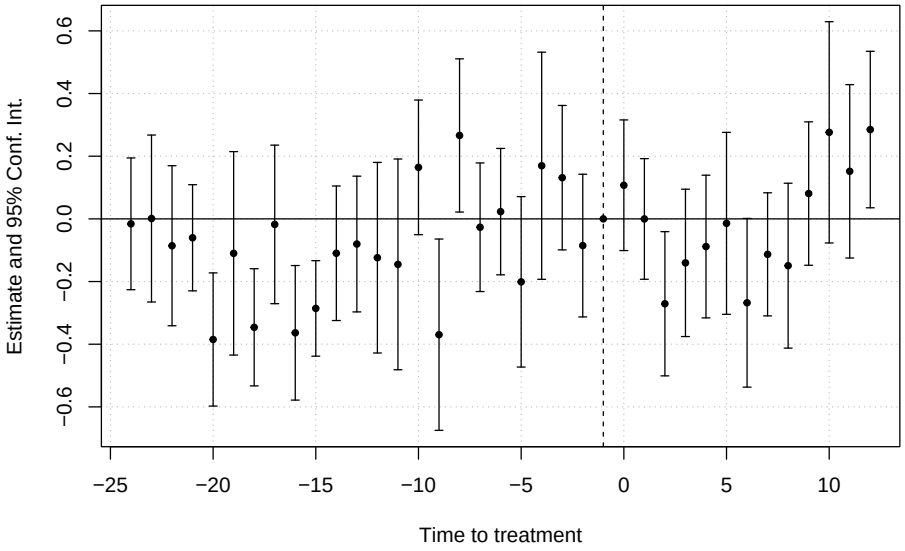

4.3.4 Queuing Emission Effects

In this subsection, I examine changes in queuing emissions, following the introduction of the new vessel queuing system. To measure queuing emissions, I take the subsample of vessels of international origin that maintained consistent service of the same routes pre– and post– policy. For each vessel IMO, I identify four key identifying features to filter for the relevant vessel movement data; IMO, MMSI, timestamp of arrival in US waters and timestamp of arrival at a west coast US port. I then filter the vessel position data for these key dates and unique vessel identifying codes, arranging observations by timestamp. This allows me to map the path of each vessel travelling through US waters. For each observation, I observe the speed (SOG), geospatial location (LAT, LON), and timestamp of the vessel. I calculate the distance, time elapsed and rate of speed for each pinged signal of a given vessel. Using the speed and container capacity, I also determine the associated emissions of each step in the vessels local journey to port in kilograms (CO_2, SO_X, NO_X, and $PM_{2.5}$).

To represent the emissions of each arriving vessels' queuing experience, I sum across emission contributions for a given vessel and the calculate three indicators; (i) total emissions, (ii) per nautical mile rate of emissions and (iii) per hour rate of emissions. In Figure 4.10, I depict changes in emissions by treatment group and period. Additionally, I track the duration, average movement speed and distance coverage of each individual vessel's queuing stage. While there is a distinct reduction in queued vessel emissions among the treated group, the distribution of emissions among control vessels exhibits no directional drift (Figure 4.10a). The increased variance of the control group may be attributed to the particular drop in sample size for the period, as highlighted in Figure 4.10b.

I feature these adjustments in a difference-in-difference specification (Table 4.10) – sampling for vessels operating inbound from foreign origin ports and subject to no lane switching following the queue system's introduction. In Column 1, my findings suggest a 30.21% decline in vessel emissions during the queuing stage of transit. This evidence is supportive of the position that increased certainty of admittance timing, prior to arrival, encourages less loitering around the local port area. Delving deeper into the effect, policy has contributed to a substantial reduction in time spent locally prior to port admittance – supportive of my proposed mechanism of greater certainty for arriving vessels enabling less time spent waiting. Since vessels are no longer idling as much and continuing to emit pollutants into the local area, emissions per nautical mile (knot) travelled decline (Column 3) and relatively more active vessels exhibit higher average travel speeds (Column 4). Columns (5) and (6) address potentially higher emissions resulting from increased exposure to the deep sea, and consequentially greater fuel consumption due to more frequent repositioning while waiting adrift offshore. These relatively less statistically significant findings highlight possible evidence that vessels were travelling slightly greater distances during their queuing stage, likely due to more frequent

Figure 4.10: CO_2 emissions by hour across queued vessels

(a) Distribution of Emissions by Subsample

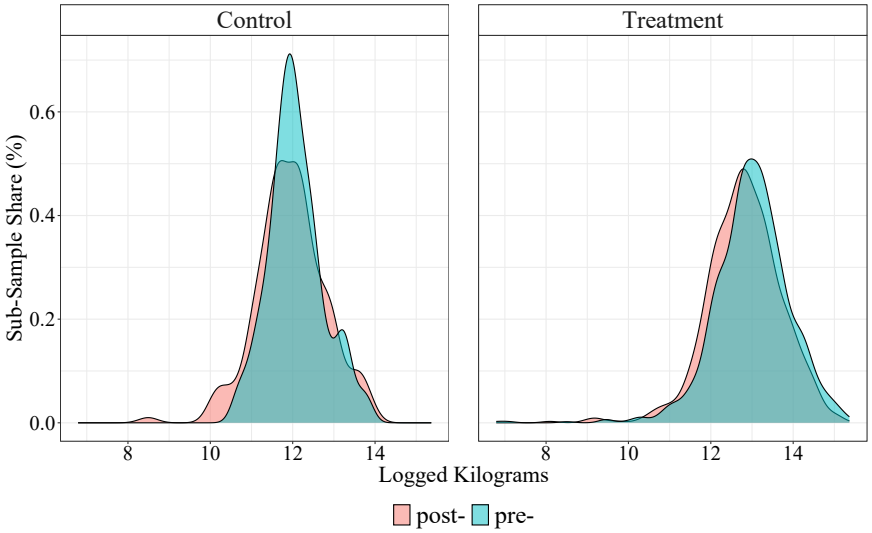

(b) Number of Vessel-Voyages by Subsample

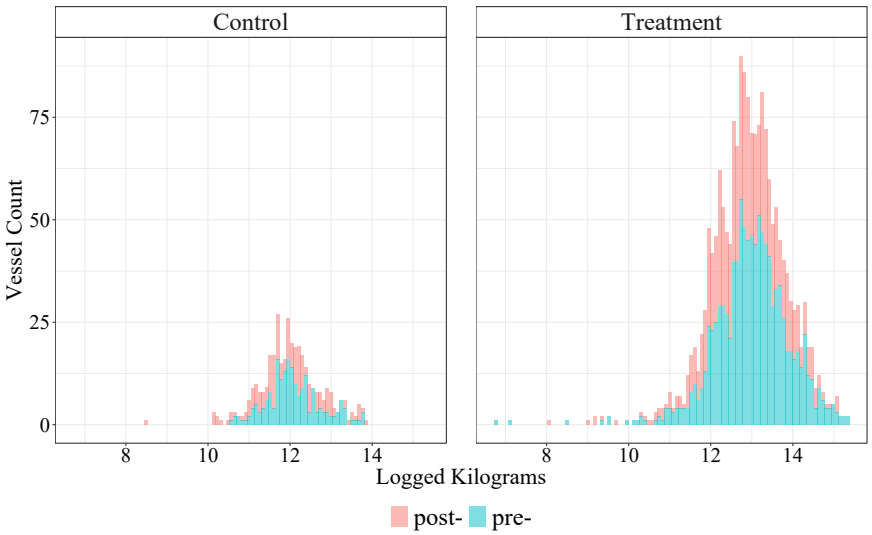

repositioning. Controlling for the shorter wait times, vessels' emissions per hour while queuing also rose by 11%, suggesting a greater degree of exertion following the blanket requirement to wait 150 nautical miles out at sea. Despite these demands though, it appears that improved certainty of queue positions outweighs the slightly worse waiting experience that vessels were exposed to.

Table 4.10: Difference-in-Difference Estimates – Queuing Emissions

	CO_2 Emissions (1)	Duration (2)	Speed (3)	Em. per Knot (4)	Distance (5)	Em. per Hour (6)
Post–Period	-0.3114	-0.3302	0.0325	0.1116	-0.4231*	0.0187
	(0.2384)	(0.2663)	(0.1623)	(0.1685)	(0.2418)	(0.1068)
Treatment	1.299***	1.470***	-0.6342***	-0.4931**	1.792***	-0.1708
	(0.2067)	(0.2370)	(0.1051)	(0.2505)	(0.3774)	(0.1252)
DiD	-0.3021***	-0.4119***	0.4806***	-0.4508***	0.1487	0.1098*
	(0.0820)	(0.1183)	(0.0940)	(0.0871)	(0.1028)	(0.0658)
Vessel–Voyage FE	✓	✓	✓	✓	✓	✓
Year–Month FE	✓	✓	✓	✓	✓	✓
Observations	2,111	2,111	2,111	2,111	2,111	2,111
R^2	0.59	0.57	0.59	0.52	0.45	0.68

Note: ***: 0.01, **: 0.05, *: 0.1. Standard-errors are robust to clustering within vessel–voyage lanes of transport service. Each observation is a distinct queuing experience of a vessel arriving on the US west coast between Nov 2019 and Nov 2022. I filter only for vessel voyages that maintained the same international trade routes pre- and post- policy and drop any observations that lack matching vessel movement data. To limit extreme outlier distortions, I exclude any voyages with emissions less than the 25th percentile minus three times the interquartile range (75th percentile - 25th percentile) or higher than the 75th percentile plus three times the interquartile range (Davies and Jeppesen, 2015).

Given these estimates, I next weigh the contributions of reduced voyage and queuing emissions together and calculate the policy's overall global effect.

4.3.5 Global Emission Effects

In this section, I separately identify the voyage and queuing legs of a given vessel transit. As detailed in Figure 4.11, queuing represents a substantial share of the distance, duration, and associated emissions of international shipping.

Figure 4.11: Queuing Share of Global Containership Transit for US West Coast

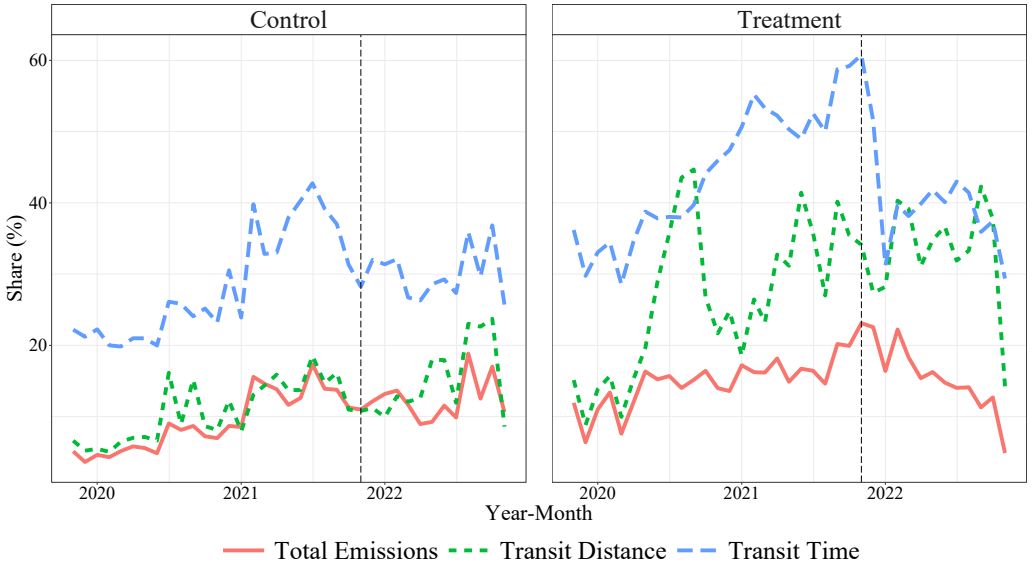

Prior to the introduction of the new queuing system, both port groups experienced a doubling of vessel transit time allocated to the queuing experience across a two year time span. The introduction of ETA-based queue positions among treated ports – issued upon departure from a prior port of laden – was followed by a severe decline in transport operators' time allocated towards queuing. Unlike the control group, upward trends in the share of travel distance attributed to the queuing stage halted. Given the shorter time spells that vessels remain within the port area, the queuing share of global emission contributions has also declined. Meanwhile, the control ports of Seattle, Tacoma and Oakland have largely maintained prior trends.

Referring to Equation 4.2, I assess the broad impact of the policy on global emissions by combining each vessels' voyage and queuing stages of transit. I find that the introduction of the new queuing system contributed to an 11.84% reduction in global vessel emissions servicing the US west coast.

Table 4.11: Difference-in-Difference Estimates – Global Emissions

	CO_2 Emissions (1)	Em. per Hour (2)	Em. per Knot (3)
Post–Period	-0.2081**	0.0891	-0.0954
	(0.0902)	(0.1103)	(0.0909)
Treatment	0.2084***	-0.1481	-0.1223
	(0.0744)	(0.1607)	(0.0865)
DiD	-0.1184***	-0.0372	-0.1560***
	(0.0447)	(0.0682)	(0.0481)
Vessel–Voyage FE	✓	✓	✓
Year–Month FE	✓	✓	✓
Observations	2,111	2,111	2,111
R^2	0.90	0.80	0.72

Note: ***: 0.01, **: 0.05, *: 0.1. Standard-errors are robust to clustering within vessel–voyage lanes of transport service. Each observation is a distinct global transit experience of a vessel arriving on the US west coast between Nov 2019 and Nov 2022. I filter only for vessel voyages that maintained the same international trade routes pre- and post- policy and drop any observations that lack matching vessel movement data. To limit extreme outlier distortions, I exclude any voyages with emissions less than the 25th percentile minus three times the interquartile range (75th percentile - 25th percentile) or higher than the 75th percentile plus three times the interquartile range (Davies and Jeppesen, 2015).

Furthermore, emissions per nautical mile travelled have declined by 15.6%. I do not detect a significant decline in emissions per hour due to increases during queu-

ing offsetting reductions associated with voyage. While vessels have temporarily slowed down while at sea, the opposing effect of being more active during the queuing experience and potentially having to readjust position more frequently while waiting have added a partial upward effect to any broad adjustments in emissions per hour. In other words, vessels have repurposed available time that would have otherwise been allocated to the idling experience towards their voyages.

4.4 Discussion & Conclusion

This study focuses on the medium run environmental effects of an ETA-based vessel queuing system. My results show that the emissivity of containership vessels destined for San Pedro Bay declined, when controlling for prevailing trends along the other major container ports of the US west coast. These new conditions allowed transport operators to learn their queue position prior to arriving in the local port area. As a result, they could adjust speeds and minimize the amount of idling they would perform in the local port vicinity. This contributed to a 41.2% reduction in the duration of queuing times at port and a 30.2% reduction in total local emissions. However, local monitors adjacent to the port areas show signs of a broader elevation in emissions among post-period treated ports. These patterns are possibly a symptom of increased commercial activity in the port areas, following the policy's success in relieving the local logjam in container movements. This and the added certainty of vessel arrivals would likely bolster multimodal transport activity. Additionally, the increased appeal of the coastal area, following the removal of unsightly containership queues, may have also boosted local emissions in the area. In future work, I intend to extend this analysis to incorporate endogenous queuing activity along the US west coast, using weather-related instrumental variables to project against containership traffic within the San Pedro Bay area.

Additionally, my findings suggest that the new queuing system encouraged a slowdown in vessels bound for the ports of Los Angeles and Long Beach. In total, emissions were reduced by approximately 10.48% and travel speeds fell by 16.97%. Coupled with the event study design of this analysis, I posit that these adjustments are transitive in nature and that relative slowdowns in across vessels became statistically insignificant in less than a years time.

To document the relative importance of these two patterns, I combine the international and local effects of the new queuing system to assess global implications. Firstly, I document that despite the small geographic region that queuing is contained within, this activity represents a substantial share of the lifespan of a given vessel–voyage. In duration, it can range between a 20–60% year–month average share of total international transit times between ports. In emissions and distance, year–month averages range from 5–40%. The queuing stage is therefore a very important aspect of containership voyages that carries great weight in efforts to mitigate emissions. Accounting for both legs of transit, I find that the new queuing system of San Pedro Bay is attributable to an 11.8% reduction in total vessel emissions. Vessels in fact speed up during the queuing stage, due to less idling. This combined with the temporary slowdown in voyage speeds leads to a muted effect on average emissions per hour. Despite this fact, a substantial reduction in wait times occurs, which has led to emissions per nautical mile traversed in service of San Pedro Bay falling by 15.6%.

Coupled together, these findings suggest that an ETA-based queuing system offers a substantial decarbonization boon to ports exposed to lengthy wait time and queuing processes. For small or mid-tier ports less likely to exhibit lengthy idling times, further study is required to establish whether the logistical costs of maintaining an ETA-based queuing system would be environmentally beneficial.

Bibliography

Brancaccio, G., M. Kalouptsidi, and T. Papageorgiou (2020). Geography, transportation, and endogenous trade costs. *Econometrica 88*(2), 657–691.

Capaldo, K., J. J. Corbett, P. Kasibhatla, P. Fischbeck, and S. N. Pandis (1999). Effects of ship emissions on sulphur cycling and radiative climate forcing over the ocean. *Nature 400*(6746), 743–746.

Corbett, J. J., H. Wang, and J. J. Winebrake (2009). The effectiveness and costs of speed reductions on emissions from international shipping. *Transportation Research Part D: Transport and Environment 14*(8), 593–598.

Corbett, J. J., J. J. Winebrake, E. H. Green, P. Kasibhatla, V. Eyring, and A. Lauer (2007). Mortality from Ship Emissions: A Global Assessment. *Environmental Science & Technology 41*(24), 8512–8518. PMID: 18200887.

Cristea, A., D. Hummels, L. Puzzello, and M. Avetisyan (2013). Trade and the greenhouse gas emissions from international freight transport. *Journal of Environmental Economics and Management 65*(1), 153–173.

Czermanski, E., G. T. Cirella, A. Oniszczuk-Jastrzabek, B. Pawlowska, and T. Notteboom (2021). An Energy Consumption Approach to Estimate Air Emission Reductions in Container Shipping. *Energies 14*(2).

Davies, R. and T. Jeppesen (2015). Export mode, firm heterogeneity, and source country characteristics. *Review of World Economics (Weltwirtschaftliches Archiv) 151*(2), 169–195.

Ganapati, S. and W. F. Wong (2023). How Far Goods Travel: Global Transport and Supply Chains from 1965–2020. *Journal of Economic Perspectives 37*(3), 3–30.

Gillingham, K. and P. Huang (2021). Racial Disparities in the Health Effects from Air Pollution: Evidence from Ports. NBER Working Papers 29108, National Bureau of Economic Research, Inc.

Hansen-Lewis, J. and M. M. Marcus (2022). Uncharted waters: Effects of maritime emission regulation. Technical report, National Bureau of Economic Research.

Heiland, I., A. Moxnes, K. H. Ulltveit-Moe, and Y. Zi (2019). Trade From Space: Shipping Networks and The Global Implications of Local Shocks. CEPR Discussion Papers 14193, C.E.P.R. Discussion Papers.

Hulskotte, J. and H. Denier van der Gon (2010). Fuel consumption and associated emissions from seagoing ships at berth derived from an on-board survey. *Atmospheric Environment 44*(9), 1229–1236.

IMO (2021). Fourth Greenhouse Gas Study 2020. Full report, International Maritime Organization.

Jalkanen, J.-P., L. Johansson, J. Kukkonen, A. Brink, J. Kalli, and T. Stipa (2012). Extension of an assessment model of ship traffic exhaust emissions for particulate matter and carbon monoxide. *Atmospheric Chemistry and Physics 12*(5), 2641–2659.

Ju, Y. and C. A. Hargreaves (2021). The impact of shipping co2 emissions from marine traffic in western singapore straits during covid-19. *Science of The Total Environment 789*, 148063.

Kinney, P. L., M. G. Gichuru, N. Volavka-Close, N. Ngo, P. K. Ndiba, A. Law, A. Gachanja, S. M. Gaita, S. N. Chillrud, and E. Sclar (2011). Traffic impacts on PM2.5 air quality in Nairobi, Kenya. *Environmental Science & Policy 14*(4), 369–378.

Klotz, R. and J. Berazneva (2022). Local Standards, Behavioral Adjustments, and Welfare: Evaluating California's Ocean-Going Vessel Fuel Rule. *Journal of the Association of Environmental and Resource Economists 9*(3), 383 – 424.

Liu, H., M. Fu, X. Jin, Y. Shang, D. Shindell, G. Faluvegi, C. Shindell, and K. He (2016, November). Health and climate impacts of ocean-going vessels in East Asia. *Nature Climate Change 6*(11), 1037–1041.

Lugovskyy, V., A. Skiba, and D. Terner (2023). Unintended Consequences of Environmental Regulation of Maritime Shipping: Carbon Leakage to Air Shipping. In *SSRN Electronic Journal*.

Mitchell, R. C. and R. Carson (1986). Property Rights, Protest, and the Siting of Hazardous Waste Facilities. *American Economic Review 76*(2), 285–90.

Morehouse, J. M. and E. A. Rubin (2021). Downwind and Out: The Strategic Dispersion of Power Plants and their Pollution. In *SSRN Electronic Journal*.

Ngo, N. S., M. Gatari, B. Yan, S. N. Chillrud, K. Bouhamam, and P. L. Kinney (2015). Occupational exposure to roadway emissions and inside informal settlements in sub-Saharan Africa: A pilot study in Nairobi, Kenya. *Atmospheric Environment 111*, 179–184.

Prochazka, V., R. Adland, and F.-C. Wolff (2019). Contracting decisions in the crude oil transportation market: Evidence from fixtures matched with AIS data. *Transportation Research Part A: Policy and Practice 130*(C), 37–53.

Rivera, N. (2021). Air quality warnings and temporary driving bans: Evidence from air pollution, car trips, and mass-transit ridership in Santiago. *Journal of Environmental Economics and Management 108*(C), S0095069621000371.

Rodrigue, J.-P. (2020, May). *The Geography of Transport Systems*. Fifth edition. — Abingdon, Oxon ; New York, NY : Routledge, 2020.: Routledge.

Schwarzkopf, D. A., R. Petrik, V. Matthias, M. Quante, E. Majamäki, and J.-P. Jalkanen (2021). A ship emission modeling system with scenario capabilities. *Atmospheric Environment: X 12*, 100132.

Shapiro, J. (2016). Trade Costs, CO2, and the Environment. *American Economic Journal: Economic Policy 8*(4), 220–54.

Tumbarello, P., S. Arslanalp, and M. Marini (2019). Big Data on Vessel Traffic: Nowcasting Trade Flows in Real Time. IMF Working Papers 2019/275, International Monetary Fund.

Walsh, C. and A. Bows (2012). Size matters: Exploring the importance of vessel characteristics to inform estimates of shipping emissions. *Applied Energy 98*(C), 128–137.

Wong, W. F. (2022). The Round Trip Effect: Endogenous Transport Costs and International Trade. *American Economic Journal: Applied Economics 14*(4), 127–66.

Wong, W. F. and S. Fuchs (2022). Multimodal Transport Networks. FRB Atlanta Working Paper 2022-13, Federal Reserve Bank of Atlanta.

Zhang, Y., S. D. Eastham, A. K. Lau, J. C. Fung, and N. E. Selin (2021, aug). Global air quality and health impacts of domestic and international shipping. *Environmental Research Letters 16*(8), 084055.

Zou, E. Y. (2021). Unwatched Pollution: The Effect of Intermittent Monitoring on Air Quality. *American Economic Review 111*(7), 2101–26.

Chapter 5

Concluding Remarks

In this dissertation, I have demonstrated the importance of accounting for the logistical practices of transport intermediaries in representing endogenous transport costs, used historical port call data to study the evolution containership technology, and evaluated the environmental implications of vessel queuing systems.

In Chapter 2, I focused on the empty container repositioning practice faced by the United States and its respective trade partners. To pursue this time, I used novel port-level US container traffic data for January 2012 to December 2021 and combined the data with US Census records of port–level monthly containerized imports and exports. I first documented that the US maintains a nationally balanced exchange of transport equipment with the rest of the world, well–timed to support monthly variation in the asymmetries of the US trade deficit. I also established a micro-founded model of transport equipment repositioning, which involved embedding logistical decision making across intermediary container shipping firms into a roundtrip model of transportation and trade. Lastly, I conduct a counterfactual analysis of policy implications for the recently passed Ocean Shipping Reform Act of 2022, which seeks to limit empty container outflows in favor of stimulating US exports. I find that restricting container repositioning stifles the vessel capacity of a given round trip and reduces bilateral trade activity, leading to lower gains from trade. The policy also behaves in a particularly targeted manner, with East Asian trade parterns – most reliant on empty container returns – facing the greatest degrees of loss in exports to the US.

In Chapter 3, we examined how adjustments in the composition of vessels servicing US containerized trade contributed container handling outcomes at the port level. Our depiction of container shipping relies on four key data sets, which allowed us to observe US activity between January 1977 and December 2023. We find that transport operators initially met the increasing volume of demand of trade by simply throwing more vessels at the problem. We documented a five-fold

increase in the average size of vessels for 1977–2023, while in comparison the number of visiting vessels increased three-fold. Upon saturating US ports with vessels in 2012, we posit that tastes for shipbuilding increasingly shifted towards the upgrading of vessel technology and expansion of vast hull sizes. These increasingly larger vessels are associated with longer dwell times, but upon accounting for the scale of containers they are capable of carrying, we identified efficiencies of scale in their use in handling transport equipment. To examine how accumulating traffic and existing congestion influences the outcomes of incumbent visiting vessels at the port, we developed an instrumental variable that acts as a demand-shifter for port traffic. We found that increases in port traffic contribute to negative spillovers for surrounding vessels. We identified these two countervailing effects on container handling efficiency as having contributed to dwell times across ports stabilizing at a 2.4 day average duration across the past 50 years of containerized transport, despite the novel innovations made in individual shipping capacities.

In Chapter 4, I studied the environmental effects of a new containership queuing system introduced in San Pedro Bay that issues vessel queue positions based on an estimated time of arrival (ETA). The prior system had required vessels to join these ports' queues by entering within 20–25 nautical miles of the port vicinity. This effectively encouraged a system of "rat races", in which vessels were collectively incentivized to speed against one another to endogenously secure earlier queue positions. I find that while this slowdown lowered vessel emissions at the voyage stage of transit, the effect was transitive in nature. The substantial reduction in global containership emissions that I document was driven instead by adjustments in behaviour at the queuing stage of transit. By guaranteeing a queue position upon departure from a prior port of origin, transport operators were able to minimize idling time and contribute to a 30.2% reduction in total global emissions.

The results from my dissertation emphasize the importance of maintaining a multidisciplinary approach, which has allows for the dovetailing of studies in maritime transport, trade and environmental economics. In each of my substantive chapters, I leverage use of novel data sets in order to answer key questions of the prevailing literature. For example, in a recent review of academic research of maritime shipping Ardelean et al. (2022) identifies *"...gaps on the policy questions that need further research, such as regulation of liner shipping, a better understanding of the determinants of port efficiency, and the effects of environmental regulation on the transportation sector."* My array of essays makes a serendipitous contribution to each one of these three respective topics of interest by evaluating the consequences of physical transport equipment in liner shipping, providing a historical decomposition of port congestion via vessel technology and port efficiency, and developing an event study of how queuing regulations impact the environmental outcomes of maritime transport. To continue benefiting from global trade, we must better understand the underlying supply–side factors that enable the increasingly large volumes of commerce we aspire to exchange. This requires a deep understanding of how the state and logistical use of transport equipment contributes to trade outcomes, whether that be the ship bearing our goods, the containers they are laden with, or the port infrastructure receiving both items jointly.

Appendix I

A1 (I.) General Equilibrium with Homogeneous Input Prices

The assumption of common input prices across loaded and empty containers is generalizing restriction that yields zero freight rates for transport services originating from net importer countries.Consider equation (3)

$$\max_{l_{ij},l_{ji},e_{ij},e_{ji}} \pi^{\leftrightarrow}_{ij} = T_{ij}l_{ij} + T_{ji}l_{ji} - c_{ij}l_{ij} - c_{ji}l_{ji} - r^{\leftrightarrow}_{ij}(e_{ij} + e_{ji}) \;\text{ s.t. } l_{ij} + e_{ij} = l_{ji} + e_{ji}$$

I adjust this specification to a more general form which sets all container input prices equal to a route specific cost term $\{c_{ij}, c_{ji}, r^{\leftrightarrow}_{ij}\} = c^{\leftrightarrow}_{ij}$. Consider Case II in which a trade imbalance exists between countries i and j such that $l_{ij} = l_{ji} + e_{ji}$ and $e_{ij} = 0$. Under these circumstances, imbalance trade and balanced container flows imply a zero freight rate on route ji.

$$\begin{aligned}\max_{l_{ij},l_{ji},e_{ij},e_{ji}} \pi^{\leftrightarrow}_{ij} &= T_{ij}l_{ij} + T_{ji}l_{ji} - c^{\leftrightarrow}_{ij}l_{ij} - c^{\leftrightarrow}_{ij}l_{ji} - c^{\leftrightarrow}_{ij}(e_{ji}) \quad \text{s.t.} \quad l_{ij} = l_{ji} + e_{ji} \\ &= T_{ij}l_{ij} + T_{ji}l_{ji} - c^{\leftrightarrow}_{ij}(l_{ij} + l_{ji} + l_{ij} - l_{ji})\end{aligned}$$

FOC

$$\frac{\partial \pi^{\leftrightarrow}_{ij}}{\partial l_{ij}} = 0 \implies T_{ij} = 2c_{ij}$$

$$\frac{\partial \pi^{\leftrightarrow}_{ij}}{\partial l_{ji}} = 0 \implies T_{ji} = 0$$

Similarly to Behrens and Picard (2011), I find that both bilateral freight rates of a given round trip route are non-zero only when shipments of loaded containers are balanced. In practice, incoming loaded containers being converted into an input for outgoing transport services involve more time, weight and cleaning relative to incoming empty containers. This suggests higher marginal costs of revenue-

generating loaded container inputs relative to using inbound empties to service outbound transport services.

Upon acknowledging these underlying differences in handling costs between empty and loaded containers through heterogeneous input prices, within route, the general equilibrium model is capable of generating positive freight rates for both sides of an imbalanced round trip trade on $\overset{\leftrightarrow}{ij}$. I use heterogeneous input prices to generate empty container flows in conjunction with positive bilateral tariff rates.

A1 (II.) Balanced Trade Scenario

The perfectly competitive transport operator will yield prices where the marginal benefit of an additional loaded container transport is equal to the marginal cost. Using the implied l_{ji} from equation (4), and setting these quantities equal to one another, we arrive at a case of two equations and two unknowns for $\{l_{ij}, T_{ij}\}$. Setting these equations equal to one another allows for freight rates to be solved.

$$\begin{aligned}
\left(\frac{\epsilon}{\epsilon-1}\frac{1}{a_{ij}}\right)^{-\epsilon}(w_i\tau_{ij}+T_{ij})^{-\epsilon} &= \left(\frac{\epsilon}{\epsilon-1}\frac{1}{a_{ji}}\right)^{-\epsilon}\left(w_j\tau_{ji}c_{\overset{\leftrightarrow}{ij}}+c_{\overset{\leftrightarrow}{ij}}-T_{ij}\right)^{-\epsilon} \\
\frac{1}{a_{ij}}(w_i\tau_{ij}+T_{ij}) &= \frac{1}{a_{ji}}(w_j\tau_{ji}+2c_{\overset{\leftrightarrow}{ij}}-T_{ij}) \\
\left(\frac{1}{a_{ij}+a_{ji}}\right)T_{ij} &= \frac{1}{a_{ji}}\left(2c_{\overset{\leftrightarrow}{ij}}\right)-\frac{1}{a_{ij}}(w_i\tau_{ij})+\frac{1}{a_{ji}}(w_j\tau_{ji}) \\
(a_{ij}+a_{ji})\,T_{ij} &= a_{ij}\left(2c_{\overset{\leftrightarrow}{ij}}\right)-a_{ji}(w_i\tau_{ij})+a_{ij}(w_j\tau_{ji}) \\
T^*_{ij} &= \frac{1}{1+\frac{a_{ji}}{a_{ij}}}(2c_{\overset{\leftrightarrow}{ij}})-\frac{1}{1+\frac{a_{ij}}{a_{ji}}}(w_i\tau_{ij})+\frac{1}{1+\frac{a_{ji}}{a_{ij}}}(w_j\tau_{ji})
\end{aligned} \tag{5.1}$$

With freight rates expressed in terms of exogenous variables, solving for p^*_{ij} is relatively straightforward and simplifies solving for l^*_{ij}.

$$
\begin{aligned}
p_{ij}^{*} &= w_i\tau_{ij} + T_{ij}^{*} \\
&= w_i\tau_{ij} + \frac{1}{1+\frac{a_{ji}}{a_{ij}}}(2c_{ij}^{\leftrightarrow}) - \frac{1}{1+\frac{a_{ij}}{a_{ji}}}(w_i\tau_{ij}) + \frac{1}{1+\frac{a_{ji}}{a_{ij}}}(w_j\tau_{ji}) \\
&= \frac{1}{1+\frac{a_{ji}}{a_{ij}}}(2c_{ij}^{\leftrightarrow}) + \frac{1+\frac{a_{ij}}{a_{ji}}-1}{1+\frac{a_{ij}}{a_{ji}}}(w_i\tau_{ij}) + \frac{1}{1+\frac{a_{ji}}{a_{ij}}}(w_j\tau_{ji}) \\
p_{ij}^{*} &= \frac{1}{1+\frac{a_{ji}}{a_{ij}}}\left(2c_{ij}^{\leftrightarrow} + w_i\tau_{ij} + w_j\tau_{ji}\right) \qquad (5.2)
\end{aligned}
$$

To solve for l_{ij}^{*}, plug T_{ij}^{*} into equation (4).

$$
\begin{aligned}
l_{ij}^{*} &= \left(\frac{\epsilon}{\epsilon-1}\frac{1}{a_{ij}}\right)^{-\epsilon}\left(w_i\tau_{ij} + T_{ij}^{*}\right)^{-\epsilon} \\
&= \left(\frac{\epsilon}{\epsilon-1}\frac{1}{a_{ij}}\right)^{-\epsilon}\left(w_i\tau_{ij} + \frac{1}{1+\frac{a_{ji}}{a_{ij}}}(2c_{ij}^{\leftrightarrow}) - \frac{1}{1+\frac{a_{ij}}{a_{ji}}}(w_i\tau_{ij}) + \frac{1}{1+\frac{a_{ji}}{a_{ij}}}(w_j\tau_{ji})\right)^{-\epsilon} \\
&= \left(\frac{\epsilon}{\epsilon-1}\frac{1}{a_{ij}}\right)^{-\epsilon}\left(\frac{1}{1+\frac{a_{ji}}{a_{ij}}}\left(2c_{ij}^{\leftrightarrow} + w_i\tau_{ij} + w_j\tau_{ji}\right)\right)^{-\epsilon} \qquad (5.3)
\end{aligned}
$$

The equilibrium value of trade is simply price times quantity:

$$
X_{ij}^{*} = \left(\frac{\epsilon}{\epsilon-1}\frac{1}{a_{ij}}\right)^{-\epsilon}\left(\frac{1}{1+\frac{a_{ji}}{a_{ij}}}\left(2c_{ij}^{\leftrightarrow} + w_i\tau_{ij} + w_j\tau_{ji}\right)\right)^{1-\epsilon} \qquad (5.4)
$$

A1 (III.) Container Traffic Sample

In Table 5.1, each row reports a given year's number of contributing ports, the total number of loaded and empty container units handled by the set of contributing ports, the total number of loaded and empty container units handled at the national level, and the sample's share of national throughput.

Table 5.1: Sample Representation - US Total Container Throughput

Year	Number of Ports	Sample TEU	National TEU	% of National
2003	8	21,150,609	32,689,484	64.70
2004	8	23,357,414	34,901,628	66.92
2005	8	25,826,230	38,497,839	67.08
2006	8	27,661,831	40,896,742	67.64
2007	8	27,797,684	44,839,390	61.99
2008	9	26,652,498	42,411,770	62.84
2009	10	23,169,814	37,353,575	62.03
2010	10	27,122,000	42,031,000	64.53
2011	11	29,181,883	42,550,784	68.58
2012	12	35,350,843	43,538,254	81.19
2013	12	35,937,976	44,340,866	81.05
2014	12	37,548,916	46,233,010	81.22
2015	13	40,501,360	47,886,446	84.58
2016	13	41,021,434	48,436,472	84.69
2017	13	44,209,298	52,132,844	84.80
2018	13	46,619,407	54,776,341	85.11
2019	13	47,064,791	55,518,878	84.77
2020	13	46,555,563	54,963,689	84.70
2021	13	53,748,362	62,044,503	86.63

Source: National thruflows use 'Container port throughput, annual' from UNCTAD.

A1 (IV.) Unilateral and Port-Specific Results

In this section of the Appendix, I address alternative specifications which mirror those proposed in the main body of this study. Figure 5.2 depicts the co-movement between empty container units and trade flows travelling in the same direction for a given year-month, between the US and RoW. I find no distinct relationship, suggesting that only opposite leg variation in trade flows stimulate systematic adjustments to empty container repositioning. This opposite-leg relationship between trade flows and corresponding empty container unit adjustments is reflected in Table 3.2.

Tables 5.3 & 5.4 and Figure 5.1 mirror national regressions featured in the main

Table 5.2: Empty Container Elasticity with Respect to Trade Flows (kg)

Dependent Variable: Empty Container Flows (TEU)				
	ln(Outbound)		ln(Inbound)	
Model:	(1)	(2)	(3)	(4)
ln(Inbound Trade)	1.582***		-0.0881	
	(0.1152)		(0.2576)	
ln(Outbound Trade)		0.0033		0.6352***
		(0.1292)		(0.1770)
n-obs	120	120	120	120
Within R^2	0.65	2.89×10^{-6}	0.002	0.13

Clustered (month) standard-errors in parentheses. Codes: ***: 0.01, **: 0.05, *: 0.1. US empty container flows are regressed on US containerized trade flows, expressed in terms of kilograms. For example, a one percent increase in the weight of 'Inbound Trade' is associated with a 1.58% rise in outbound empty container flows. I use month and year fixed effects to control for influences of the US business cycle and seasonality.

body of the paper. Generally these findings are weaker, which is partly due to ports not individually maintaining balanced container flows. Only in conjunction with other ports does the US maintain nationally balanced container flows and response relationships between prevailing trade flows and opposite-end empty container movements.

Table 5.3: (Ports) Trade Flow Ratio & Empty Shares

Dependent Variable: Empty Container Share of Total Flows				
	Outbound		Inbound	
Model:	(1)	(2)	(3)	(4)
Export/Import (USD)	-0.0847*			
	(0.0412)			
Export/Import (kg)		-0.0582*		
		(0.0278)		
Import/Export (USD)			-0.0063*	
			(0.0033)	
Import/Export (kg)				-0.0124***
				(0.0027)
Mean Dep. Var	34.6%		15.27%	
Mean Regressor	0.496	0.901	2.865	1.499
n-obs	1,440	1,440	1,440	1,440
Within R^2	0.03	0.06	0.01	0.02

Clustered (port) standard-errors in parentheses. Codes: ***: 0.01, **: 0.05, *: 0.1. Examines variation empty containers as a share of total container outflows, given variation in the skewedness of the trade balance. I use month and year fixed effects to control for influences of the US business cycle and seasonality.

Table 5.4: (Ports) Empty Container Elasticity w.r.t. Opposite-Direction Trade Flows

Dependent Variable: Empty Container Flows (TEU)				
	Outbound		Inbound	
Model:	(1)	(2)	(3)	(4)
ln(Imports, USD)	0.6218***			
	(0.1256)			
ln(Imports, kg)		0.3348**		
		(0.1339)		
ln(Exports, USD)			0.4949*	
			(0.2278)	
ln(Exports, kg)				0.3210*
				(0.1464)
n-obs	1,440	1,440	1,440	1,440
Within R^2	0.064	0.044	0.01	0.005

Clustered (port) standard-errors in parentheses. Codes: ***: 0.01, **: 0.05, *: 0.1. Each variable is log-transformed. The regression results portray the elasticity of total US empty container flows with respect to opposite-direction US containerized trade flows expressed in terms of deflated USD (value) and by total weight (kilograms). All models include port-year, port-month and year-month fixed effects.

Figure 5.1: Balanced Port Container Flows

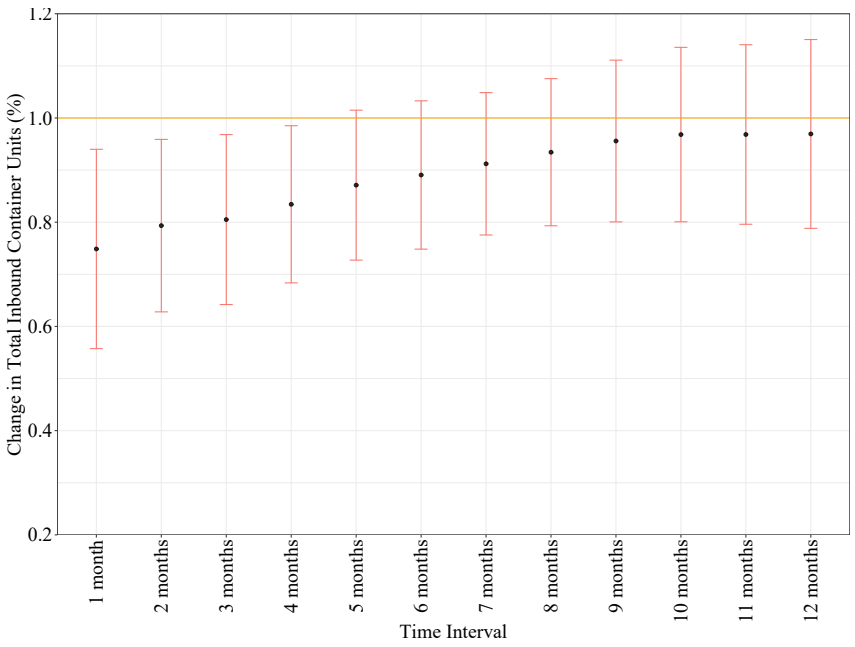

Clustered (port) standard-errors in parentheses. Both the dependent variable and regressor are log-transformed. Total inbound containers are reported across a balanced panel of 12 US ports and represent both loaded and empty containers, is regressed on total outbound containers for these same set of ports. Sums are taken across windows of varying lengths of time, ranging from bilateral exchanges within a single month to exchanges across 12 month backward sums. All models include port-year, port-month and year-month fixed effects.

A1 (V.) US-RoW Model Results

Solution Method and Model Calibration

To establish a baseline set of exogenous parameters, I first calibrate a select subset of exogenous parameters and then estimate the remaining set of unknown model primitives. For a given ij round trip containerized shipping route, the set of unknown exogenous parameters ρ is equal to $\left(a_{ij}, a_{ji}, w_i, w_j, \tau_{ij}, \tau_{ji}, c_{\underset{ij}{\leftrightarrow}}, r_{\underset{ij}{\leftrightarrow}}\right)$ and the elasticity of substitution measure is represented by ϵ.

The wage-tariff product $w_i\tau_{ij}$ is a component of tradeable good prices featured in Section 3. I use an OECD index of monthly manufacturing income growth rates, the International Labor Organization (ILO) annual measure of monthly manufacturing income levels, and UNCTAD Trade Analysis Information System (TRAINS) database on effective manufacturing goods' tariff rates, all of which are reported across a subset of key US trade partners. [1] I deflate these measures using the Bureau of Labor Statistics Consumer Price Index for all urban consumers, which considers all final good items less food and energy, averaged across major US cities.[2] I focus primarily on statistics associated with manufacturing due to its high share of overall containerized goods flows. For more of an elaboration on the calibration of $w_i\tau_{ij}$, see Appendix IV. Lastly, I use an estimate of price elasticity of demand provided by Wong (2022) and specific to containerized trade, where $\hat{\epsilon} = 20.95$ is assumed to be common across individual trade routes.

Given calibrated estimates of real wage levels, tariff rates and the price elasticity of demand, the remaining four unknown parameters, $\tilde{\rho} = \left(a_{ij}, a_{ji}, c_{\underset{ij}{\leftrightarrow}}, r_{\underset{ij}{\leftrightarrow}}\right)$ can be identified via a Generalized Method of Moments (GMM) approach. I minimize

[1] Upon establishing a login for http://wits.worldbank.org/, select 'Advanced Query' and then the 'Tariff and Trade Analysis' subsection. I use the SITC 4 product group labelled 'manufactures' and the

[2] U.S. Bureau of Labor Statistics, Consumer Price Index for All Urban Consumers: All Items Less Food and Energy in U.S. City Average [CPILFESL], retrieved from FRED, Federal Reserve Bank of St. Louis; https://fred.stlouisfed.org/series/CPILFESL, November 1, 2022.

the object function,

$$R = \text{dist}' \times \bar{W} \times \text{dist}, \tag{5.5}$$

where dist represents the log difference in vectors of observed and model-guess trade outcomes, $\log(Y^{\text{data}}) - \log(Y^{G})$ and $\bar{W}$ is a weight matrix that assists in speeding the identification of $\tilde{\rho}$.[3] I use observables from 2017 to estimate these parameters of underlying long-run primitives of containerized trade. This decision allows me to avoid any complications or concerns that the use of data from the proceeding China-US trade war, COVID-19 pandemic and port congestion saga could introduce.

Table 5.5: Key Parameters, 2017

a_{ij}	a_{ji}	$c^{\leftrightarrow}_{ij}$	$r^{\leftrightarrow}_{ij}$
65,972	32,978	20,770	8,929

I provide four means of assessing model fit for this baseline scenario of the counterfactual exercise; (1) referring to Table 5.5, the difference in preference parameters attributes greater demand towards US imports relative to US exports, which is reflective of the existing import-export ratio for 2017; (2) using marginal costs of handling loaded, ($c^{\leftrightarrow}_{ij}$), and empty container flows, $r^{\leftrightarrow}_{ij}$, the implied freight rates suggested these costs are greater for the portion of US round trips that feature a full set of loaded containers, which is reflective of freight rate asymmetries under imbalanced trade (Hummels et al., 2009); (3) the empty container redistribution share of container fleet managing costs is 11%, which places it relatively close to 15% reported by Notteboom et al. (2022); (4) baseline scenario empty container

[3]For each US trade partner, a vector of four observables are used $Y^{\text{data}} = (l_{ij}, l_{ji}, X_{ij}, X_{ji})$. From left to right, these variables represent loaded container inflows, loaded container outflows, containerized imports, and containerized exports between the US and that respective trade partner.

outflows each year of 2012 to 2021 are 99% correlated with untargeted observed empty outflows.

Counterfactual Scenarios

I consider two cases of restrictions to transport equipment use by the US policymaker, where the expressed goal is to discourage empty container redistribution in favor of stimulating US exports. In each case, restrictions are implemented through a per-unit tax on empty outflows from the US, which increases marginal costs to $(1+\gamma)\, r^{\leftrightarrow}_{ij}$. The tax rate, γ, is configured to target a specific ECO quota, represented by $\bar{E}_{ji}$, the maximum share of empties as a percentage of total container outflows. I establish two scenarios which demonstrate how sensitive trade outcomes are to variation in the availability of empty container equipment.

1. In the case of a moderate policy response, the US policymaker set a tax on empty input costs of γ^{mod}, which targets the historical average of empty container share of container net outflows, $\bar{E}_{ji} = 0.3$. This scenario represents a case in which policymakers are content with the former status quo of the empty container redistribution problem.

2. In this second scenario, I consider a case in which policymakers set a sufficiently high tax of γ^{ext}, which eliminates empty container outflows from the US by establishing an extreme quota of $\bar{E}_{ji} = 0$. This second case allows me to quantify the contribution the empty container redistribution problem to variety of US trade outcome variables.

In the next section I outline how this unconventional form of trade policy backfires in each of these exercises, relative to the baseline scenario of $\gamma = 0$, via the round trip effect.

Results

The targeting of ECO quotas, achieved through per-unit taxes on empty container unit outflows, reduces the scale of the empty redistribution problem and lowers overall round trip service capacity. Reduced transport capacity yields debilitating effects on the opposite leg of a given $\overset{\leftrightarrow}{ij}$ trade route.

As displayed in column 2 of Table 5.6, a moderate ECO quota contributes to a one-third decline in the volume empty container redistribution problem. If focusing only on this outbound leg of US round trip transport, the changes appear positive from the policymaker perspective. Relative to the baseline scenario, US containerized exports increase by 12.5% in real value as transport operators substitute away from relocating empties and towards servicing additional loaded container units. The US containerized trade deficit, represented by the import-export ratio, also declines by 21.5%. While the combination of these two findings would likely signal a positive outlook for similar policies of transport equipment restrictions, this outflow perspective alone would ignore malaise effects observed on the opposite leg of a given round trip.

On the opposite leg, US trade partners now face a freight rate which includes a higher cost of redistributing empties back for round trip transport service provisions. The equilibrium quantity of container units declines, which represents a reduction in the transport capacity for containerized transport services for the US. As a result of government intervention on export routes, the opposite leg of trade exhibits the round trip effect where available capacity declines by 6.1% and import prices rise by 0.3%. When combined, this contributes to a 5.8% reduction in the real value of US imports. The gross values of total imports and exports combined declines by 2% relative to the baseline scenario, suggesting an overall reduction in trade activity.

In the extreme quota case $\left(\bar{E}_{ji} = 0\right)$, the backfiring of this policy has far more dramatic effects on bilateral trade flows. The value of imports fall by 16% while

Table 5.6: National Counterfactual Outcomes

US Measures (2017)	$\%\Delta Y_{\bar{E_{ji}}=0.3}$	$\%\Delta Y_{\bar{E_{ji}}=0}$
Import Value with RoW	-5.82%	-15.96%
Export Value with RoW	12.46%	40.96%
Loaded Container Inflows from RoW	-6.11%	-16.68%
Loaded Container Outflows to RoW	13.13%	43.41%
Import-Export Ratio	-21.48%	-40.38%
Empty Share of US container outflows	-16.26%	-100.00%
Empty Container Outflows from US	-32.78%	-100.00%

export activity grows by 41%. The US trade deficit narrows, reflected by a 40 per cent drop in the import-export ratio. Despite empty containers no longer featuring on round trip routes, the US still maintains net importer status with imports being 2 fold that of exports (see Figure 5.3). The gross value of trade flows declines by 3% under these circumstances and the ocean-borne capacity of round trip trade servicing the US declines by 16.7%.

Figure 5.2: Counterfactual Outcomes by Empty Outflow Tax, 2017

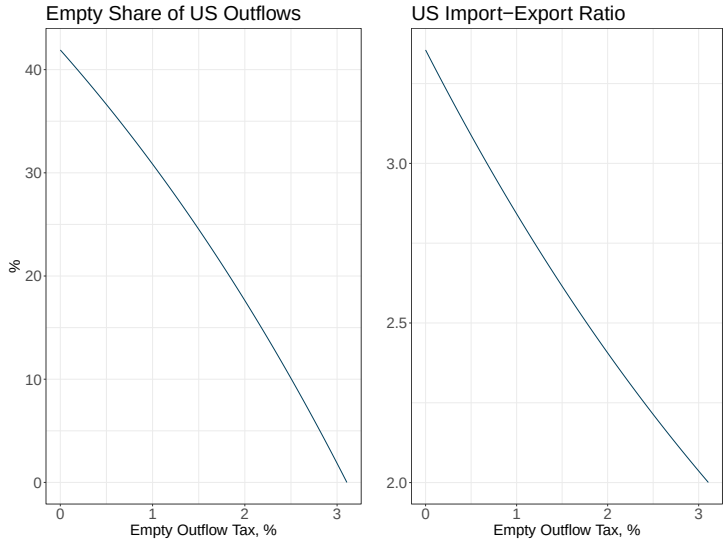

Note: The required rates of tax for moderate and extreme quota outcomes are 1.1 and 3.1 percent rates, respectively. The empty share of US container outflows declines concavely with respect to an empties tax. The Import-Export ratio, although more than 3.5 in the baseline scenario, declines in moderate and extreme counterfactual cases to ratios of 2.8 and 2, respectively.

These results highlight that if policymakers focus only on the immediate goal of stimulating exports, without acknowledging the market response this would have on round trip trade patterns, they may underestimate the costs these policies are likely to have for the general public. Specifically, lower levels of imports at more expensive rates would need to also be taken into account. The combination of the exports increases and import declines, due to the round trip effect, worsens a country's overall level of trade participation, which limits the gains to trade.

A1 (VI.) Loading Factor Estimates & Container Flow Diagnostics

While allowing commodity-specific loading factors to vary by directional flow is one decision worth considering, I have also included aggregations of particularly low volume commodity types to observe how costly a lowering of regressors is to the accuracy of my methodology. As displayed in Table 5.10, I compare the national container predicted by these varying specifications relative to a time series of observed loadedc container flows, both items being aggregated to total container inflows (In) and outflows (Out), respectively. I find that estimating loading factors for specific commodities by direction (separately) across panel data sets of export and import activity yields the most accurate set of results. Additionally, the 'Full' and 'Union' sets of regressors perform best, of which more details are provided for in the notes section of the table. For the purposes of this paper, I use the 'Full – Separately' approach to generate country-specific container flows.

Alternative specifications for regressors have been evaluated with respect to loading factors that vary across spatial– and income–based groupings. Although neither of these specifications are used for the main results of this paper, their associated results are available upon request. In the following section, I detail the

Table 5.7: Jointly Estimated Loading Factors

Weighted	Weighted (M)	Negative LFs	% Trade	% Trade (M)	% Neg Coeff	Fixed Effects
0.145	0.199	19	62.361	85.625	26.39	none
0.078	0.108	21	62.208	85.414	29.17	port
0.125	0.171	21	61.769	84.812	29.17	year
0.126	0.172	22	60.240	82.712	30.56	mon
0.077	0.106	22	60.553	83.142	30.56	port+year
0.077	0.105	23	59.150	81.216	31.94	port+mon
0.126	0.173	21	61.769	84.812	29.17	year+mon
0.071	0.098	18	63.910	87.751	25.00	port-year
0.127	0.174	22	59.969	82.340	30.56	year-mon
0.078	0.107	23	60.485	83.049	31.94	port-mon
0.067	0.091	20	61.062	83.842	27.78	port-year + mon
0.074	0.102	21	60.600	83.207	29.17	year-mon + port
0.076	0.105	23	58.985	80.989	31.94	port-mon + year
0.057	0.078	16	64.163	88.099	22.22	portˆyearˆmon
0.075	0.103	23	60.330	82.836	31.94	port+year+mon

Note: Column (1) reports trade value weighted average of loading factor coefficients. Column (2) reports the same measure limited to manufactured goods. Column (3) reports the number of negative manufacture coefficients estimated. Column (4) reports the non-negative manufacture coefficients' share of total trade flows. Column (5) reports the non-negative manufacture coefficients' share of manufacture trade flows. Column (6) reports the negative coefficient count as a percentage of manufacture coefficient count. Column (7) lists the associated fixed effects used.

performance of these measures, which generally appear to under–perform relative to the directional loading factors used.

Geographic Loading Factors: Loading factors are estimated both jointly – pooling import and export data together – and separately, where commodity-specific loading factors vary based on whether they are an import or export. Groups include Asia, Australia & Oceania, Europe, the Middle East & Africa, and Southern & Central America.

Income Loading Factors: Loading factors are estimated both jointly – pooling import and export data together – and separately, where commodity-specific loading factors vary based on whether they are an import or export. Groups include quartiles of countries, divided by World Bank measures of GDP per capita.

Table 5.8: Import-Specific Loading Factors

Weighted	Weighted (M)	Negative LFs	% Trade	% Trade (M)	% Neg Coeff	Fixed Effects
0.199	0.229	18	71.492	82.449	25.00	none
0.119	0.137	3	86.318	99.546	4.17	port
0.152	0.175	19	70.990	81.869	26.39	year
0.150	0.173	19	71.276	82.199	26.39	mon
0.114	0.132	2	86.410	99.653	2.78	port+year
0.120	0.139	3	86.318	99.546	4.17	port+mon
0.152	0.175	19	70.990	81.869	26.39	year+mon
0.114	0.131	2	86.139	99.340	2.78	port-year
0.153	0.176	20	70.976	81.854	27.78	year-mon
0.119	0.137	4	83.897	96.754	5.56	port-mon
0.113	0.131	2	86.477	99.730	2.78	port-year + mon
0.115	0.132	2	86.410	99.653	2.78	year-mon + port
0.114	0.131	4	82.490	95.132	5.56	port-mon + year
0.115	0.133	2	86.410	99.653	2.78	port+year+mon

Note: Column (1) reports trade value weighted average of loading factor coefficients. Column (2) reports the same measure limited to manufactured goods. Column (3) reports the number of negative manufacture coefficients estimated. Column (4) reports the non-negative manufacture coefficients' share of total trade flows. Column (5) reports the non-negative manufacture coefficients' share of manufacture trade flows. Column (6) reports the negative coefficient count as a percentage of manufacture coefficient count. Column (7) lists the associated fixed effects used.

Table 5.9: Export-Specific Loading Factors

Weighted	Weighted (M)	Negative LFs	% Trade	% Trade (M)	% Neg Coeff	Fixed Effects
0.080	0.150	18	45.637	85.852	25.00	none
0.071	0.133	4	48.449	91.142	5.56	port
0.064	0.121	13	48.464	91.169	18.06	year
0.064	0.121	13	48.464	91.169	18.06	mon
0.072	0.136	4	48.449	91.142	5.56	port+year
0.069	0.129	4	48.449	91.142	5.56	port+mon
0.064	0.121	13	48.464	91.169	18.06	year+mon
0.062	0.117	0	53.158	100.000	0.00	port-year
0.065	0.123	10	48.685	91.584	13.89	year-mon
0.068	0.129	4	48.449	91.142	5.56	port-mon
0.059	0.111	0	53.158	100.000	0.00	port-year + mon
0.070	0.133	5	48.442	91.127	6.94	year-mon + port
0.071	0.134	5	48.423	91.093	6.94	port-mon + year
0.071	0.133	4	48.449	91.142	5.56	port+year+mon

Note: Column (1) reports trade value weighted average of loading factor coefficients. Column (2) reports the same measure limited to manufactured goods. Column (3) reports the number of negative manufacture coefficients estimated. Column (4) reports the non-negative manufacture coefficients' share of total trade flows. Column (5) reports the non-negative manufacture coefficients' share of manufacture trade flows. Column (6) reports the negative coefficient count as a percentage of manufacture coefficient count. Column (7) lists the associated fixed effects used.

Container Flow Diagnostics

Table 5.10: Performance Diagnostics by Methodology

Method	In-RMSE	In-Corr	Out-RMSE	Out-Corr
Full — Jointly	56,638.14	0.980	39,092.72	0.775
Full — Separately	31,520.21	0.993	17,796.20	0.958
Intersect — Jointly	76,182.46	0.973	66,964.02	0.397
Intersect — Separately	34,837.47	0.992	19,368.11	0.951
Union — Jointly	60,875.81	0.979	48,363.68	0.658
Union — Separately	30,748.43	0.994	17,887.69	0.957

Note: The method list indicates which set of commodities were used as regressors in the estimation of commodity-specific loading factors. 'Full' uses the entire set of HS2 product types. 'Intersect' uses a subset of HS2 products that represent the top 50 highest commodity-specific shares of total export weight and total import weight. The resulting commodity set is the intersection of common commodities between these two shortlists. 'Union' uses the full set of top 50 commodities, rather than their intersection. RMSE columns denote root mean square error and Corr columns list the correlation of each measure, relative to observed total container inflows and outflows.

Table 5.11: Jointly Estimated Geographic Loading Factors

Weighted	Weighted (M)	Negative LFs	% Trade	% Trade (M)	% Neg Coeff	Fixed Effects
0.139	0.192	31	65.051	89.550	11.31	none
0.090	0.124	31	65.818	90.606	11.31	port
0.111	0.153	36	61.362	84.472	13.14	year
0.112	0.154	36	62.023	85.382	13.14	mon
0.088	0.122	30	66.755	91.896	10.95	port+year
0.088	0.121	32	64.542	88.850	11.68	port+mon
0.110	0.152	36	62.137	85.538	13.14	year+mon
0.082	0.113	29	67.714	93.216	10.58	port-year
0.110	0.151	38	62.013	85.368	13.87	year-mon
0.091	0.126	31	66.112	91.010	11.31	port-mon
0.078	0.108	26	68.834	94.757	9.49	port-year + mon
0.085	0.117	28	67.002	92.236	10.22	year-mon + port
0.090	0.123	30	65.002	89.482	10.95	port-mon + year
0.065	0.090	29	65.783	90.558	10.58	portˆyearˆmon
0.086	0.118	28	65.829	90.620	10.22	port+year+mon

Note: Column (1) reports trade value weighted average of loading factor coefficients. Column (2) reports the same measure limited to manufactured goods. Column (3) reports the number of negative manufacture coefficients estimated. Column (4) reports the non-negative manufacture coefficients' share of total trade flows. Column (5) reports the non-negative manufacture coefficients' share of manufacture trade flows. Column (6) reports the negative coefficient count as a percentage of manufacture coefficient count. Column (7) lists the associated fixed effects used.

As highlighted in Tables 5.17 and 5.18, models which include port and year fixed effects yield the lowest root-mean-square error (RMSE) scores. These scores compare predicted and observed US – East Asian and US – European container flows, where the measure of interest is the ratio of bilateral loaded container unit

Table 5.12: Import-Specific Geographic Loading Factors

Weighted	Weighted (M)	Negative LFs	% Trade	% Trade (M)	% Neg Coeff	Fixed Effects
0.175	0.203	21	75.554	87.264	8.4	none
0.119	0.137	7	86.090	99.433	2.8	port
0.123	0.142	21	74.528	86.079	8.4	year
0.120	0.138	22	77.493	89.503	8.8	mon
0.115	0.133	7	86.251	99.619	2.8	port+year
0.120	0.139	7	86.004	99.334	2.8	port+mon
0.120	0.138	24	77.213	89.180	9.6	year+mon
0.111	0.129	6	84.942	98.107	2.4	port-year
0.124	0.143	28	75.290	86.959	11.2	year-mon
0.119	0.137	9	86.131	99.480	3.6	port-mon
0.111	0.129	7	84.820	97.966	2.8	port-year + mon
0.117	0.135	5	86.157	99.510	2.0	year-mon + port
0.116	0.133	8	86.162	99.516	3.2	port-mon + year
0.116	0.134	6	86.177	99.533	2.4	port+year+mon

Note: Column (1) reports trade value weighted average of loading factor coefficients. Column (2) reports the same measure limited to manufactured goods. Column (3) reports the number of negative manufacture coefficients estimated. Column (4) reports the non-negative manufacture coefficients' share of total trade flows. Column (5) reports the non-negative manufacture coefficients' share of manufacture trade flows. Column (6) reports the negative coefficient count as a percentage of manufacture coefficient count. Column (7) lists the associated fixed effects used.

Table 5.13: Export-Specific Geographic Loading Factors

Weighted	Weighted (M)	Negative LFs	% Trade	% Trade (M)	% Neg Coeff	Fixed Effects
0.083	0.157	11	52.322	98.630	4.10	none
0.072	0.136	11	52.446	98.864	4.10	port
0.071	0.133	19	51.811	97.666	7.09	year
0.073	0.137	19	51.135	96.393	7.09	mon
0.071	0.134	9	52.723	99.385	3.36	port+year
0.072	0.135	9	52.572	99.101	3.36	port+mon
0.072	0.136	19	51.811	97.666	7.09	year+mon
0.060	0.114	7	53.004	99.914	2.61	port-year
0.072	0.136	17	51.966	97.958	6.34	year-mon
0.076	0.143	9	52.711	99.362	3.36	port-mon
0.058	0.110	7	53.004	99.914	2.61	port-year + mon
0.069	0.130	9	51.818	97.680	3.36	year-mon + port
0.075	0.142	10	52.699	99.341	3.73	port-mon + year
0.071	0.134	8	52.726	99.391	2.99	port+year+mon

Note: Column (1) reports trade value weighted average of loading factor coefficients. Column (2) reports the same measure limited to manufactured goods. Column (3) reports the number of negative manufacture coefficients estimated. Column (4) reports the non-negative manufacture coefficients' share of total trade flows. Column (5) reports the non-negative manufacture coefficients' share of manufacture trade flows. Column (6) reports the negative coefficient count as a percentage of manufacture coefficient count. Column (7) lists the associated fixed effects used.

flows. For East Asian, geographic country groupings perform similarly to loading factors which vary only by commodity. For Europe, the standard approach of commodity-specific loading factors with no interference in the loading factor

Table 5.14: Jointly Estimated Income-based Loading Factors

Weighted	Weighted (M)	Negative LFs	% Trade	% Trade (M)	% Neg Coeff	Fixed Effects
0.131	0.180	45	61.401	84.459	20.55	none
0.083	0.115	38	63.967	87.988	17.35	port
0.111	0.153	47	57.436	79.004	21.46	year
0.111	0.153	45	59.264	81.518	20.55	mon
0.083	0.114	36	64.128	88.209	16.44	port+year
0.080	0.110	39	62.921	86.549	17.81	port+mon
0.111	0.153	47	58.716	80.765	21.46	year+mon
0.078	0.108	31	65.610	90.247	14.16	port-year
0.111	0.152	44	59.028	81.195	20.09	year-mon
0.080	0.110	39	61.791	84.995	17.81	port-mon
0.072	0.100	33	63.906	87.903	15.07	port-year + mon
0.076	0.105	36	64.100	88.170	16.44	year-mon + port
0.080	0.109	39	61.957	85.223	17.81	port-mon + year
0.057	0.079	27	62.860	86.465	12.33	portˆyearˆmon
0.079	0.109	36	63.977	88.001	16.44	port+year+mon

Note: Column (1) reports trade value weighted average of loading factor coefficients. Column (2) reports the same measure limited to manufactured goods. Column (3) reports the number of negative manufacture coefficients estimated. Column (4) reports the non-negative manufacture coefficients' share of total trade flows. Column (5) reports the non-negative manufacture coefficients' share of manufacture trade flows. Column (6) reports the negative coefficient count as a percentage of manufacture coefficient count. Column (7) lists the associated fixed effects used.

Table 5.15: Import-Specific Income-based Loading Factors

Weighted	Weighted (M)	Negative LFs	% Trade	% Trade (M)	% Neg Coeff	Fixed Effects
0.170	0.196	29	78.826	90.925	13.12	none
0.123	0.142	9	86.246	99.484	4.07	port
0.133	0.153	25	79.163	91.314	11.31	year
0.130	0.150	26	79.066	91.202	11.76	mon
0.123	0.142	6	86.528	99.810	2.71	port+year
0.123	0.142	10	86.235	99.471	4.52	port+mon
0.131	0.151	26	79.066	91.202	11.76	year+mon
0.127	0.146	8	85.387	98.493	3.62	port-year
0.133	0.153	25	81.085	93.531	11.31	year-mon
0.120	0.138	6	86.615	99.910	2.71	port-mon
0.125	0.144	7	85.512	98.637	3.17	port-year + mon
0.122	0.141	6	86.521	99.801	2.71	year-mon + port
0.120	0.138	6	86.615	99.910	2.71	port-mon + year
0.123	0.142	7	86.520	99.800	3.17	port+year+mon

Note: Column (1) reports trade value weighted average of loading factor coefficients. Column (2) reports the same measure limited to manufactured goods. Column (3) reports the number of negative manufacture coefficients estimated. Column (4) reports the non-negative manufacture coefficients' share of total trade flows. Column (5) reports the non-negative manufacture coefficients' share of manufacture trade flows. Column (6) reports the negative coefficient count as a percentage of manufacture coefficient count. Column (7) lists the associated fixed effects used.

estimations delivers the most accurate results. Considering both regions jointly, I proceed with using no arbitrary country groupings for estimated loading factors.

Table 5.16: Export-Specific Income-based Loading Factors

Weighted	Weighted (M)	Negative LFs	% Trade	% Trade (M)	% Neg Coeff	Fixed Effects
0.085	0.160	8	52.334	98.629	3.86	none
0.073	0.137	7	52.573	99.078	3.38	port
0.075	0.141	9	52.691	99.301	4.35	year
0.074	0.139	13	52.492	98.927	6.28	mon
0.074	0.140	6	52.614	99.157	2.90	port+year
0.071	0.135	8	52.572	99.076	3.86	port+mon
0.076	0.143	11	52.682	99.284	5.31	year+mon
0.062	0.117	5	52.959	99.806	2.42	port-year
0.077	0.144	11	52.612	99.152	5.31	year-mon
0.075	0.142	11	52.567	99.067	5.31	port-mon
0.058	0.110	5	53.033	99.945	2.42	port-year + mon
0.071	0.133	7	52.573	99.078	3.38	year-mon + port
0.077	0.145	11	52.566	99.065	5.31	port-mon + year
0.073	0.138	8	52.368	98.692	3.86	port+year+mon

Note: Column (1) reports trade value weighted average of loading factor coefficients. Column (2) reports the same measure limited to manufactured goods. Column (3) reports the number of negative manufacture coefficients estimated. Column (4) reports the non-negative manufacture coefficients' share of total trade flows. Column (5) reports the non-negative manufacture coefficients' share of manufacture trade flows. Column (6) reports the negative coefficient count as a percentage of manufacture coefficient count. Column (7) lists the associated fixed effects used.

Table 5.17: RMSE of US - E. Asian Container Flow Ratios

Country Grouping	Coef Filter	Products	none	p	p+y	p+m	py	pm	py+m	ym+p	pm+y	p+y+m
Geographic	None	Agri+Manu	0.388	0.346	0.200	0.528	0.204	0.707	0.291	0.366	0.511	0.342
No Groups	None	Agri+Manu	0.058	0.408	0.224	0.574	0.180	0.908	0.240	0.314	0.695	0.359
Geographic	Directional	Agri+Manu	4.740	0.303	0.271	0.346	2.582	0.342	2.512	0.527	0.674	0.315
Income-based	None	Agri+Manu	0.240	0.423	0.335	0.584	0.231	0.777	0.361	0.505	0.724	0.487
No Groups	Directional	Agri+Manu	2.353	1.154	1.022	1.138	1.773	0.324	1.868	0.833	0.301	0.978
No Groups	None	Manufacturing	3.073	1.812	1.550	1.999	2.469	2.183	2.753	1.551	1.807	1.675
Geographic	None	Manufacturing	4.523	1.845	1.704	1.954	2.788	1.929	3.033	1.794	1.768	1.793
Income-based	None	Manufacturing	2.415	2.063	1.905	2.215	2.706	1.994	3.021	2.094	1.842	2.037
Income-based	Directional	Agri+Manu	3.952	2.718	2.642	2.307	2.598	0.870	3.042	1.808	0.976	2.224
Geographic	Directional	Manufacturing	8.346	2.877	2.735	2.860	6.314	2.616	6.019	3.231	3.496	2.723
No Groups	Directional	Manufacturing	5.422	4.087	3.693	4.038	5.552	2.327	5.207	3.083	2.110	3.579
Income-based	Directional	Manufacturing	8.192	6.129	5.537	6.377	7.118	6.067	8.141	6.212	6.208	5.876

Country Groupings includes (i) No grouping, (ii) Geographic (Asia/Oceania, Europe, South America and Africa/Middle East, and (iii) Income-based (four quartiles based on each country's average GDP per capita between 2012 and 2021). Coef Filter includes (i) None – no corrections to estimated loading factors, and (ii) Directional – replaces negative loading factors with their opposite-direction counterpart for the same country-group, iff the opposite-direction coefficient is of a a lower value. Products represents measures generated using either (i) Agri+Manu – the entire set of commodity weight flows listed in the data set, or (ii) Manufacuturing – the 72 manufactures featured at the HS2 level, as defined on the TRAINS product grouping 'manufactures' set.

A1 (VII.) The European Customs Union and Container Flows

Many of the countries featured in the multi-country baseline scenario of this paper are European. Of those countries, Austria, the Czech Republic, Hungary and

Table 5.18: RMSE of US-European Container Flow Ratios

Country Grouping	Coef Filter	Products	none	p	p+y	p+m	py	pm	py+m	ym+p	pm+y	p+y+m
No Groups	None	Manufacturing	2.130	0.056	0.064	0.045	0.110	0.126	0.216	0.070	0.166	0.055
No Groups	None	Agri+Manu	0.932	0.083	0.071	0.122	0.151	0.070	0.217	0.081	0.046	0.080
No Groups	Directional	Manufacturing	1.640	0.064	0.111	0.170	0.236	0.089	0.321	0.055	0.090	0.091
No Groups	Directional	Agri+Manu	1.636	0.208	0.262	0.292	0.447	0.125	0.495	0.191	0.106	0.221
Income-based	None	Agri+Manu	1.593	0.337	0.401	0.207	0.625	0.183	0.507	0.244	0.218	0.218
Income-based	None	Manufacturing	2.632	0.268	0.420	0.097	1.063	0.070	0.939	0.219	0.111	0.207
Geographic	None	Manufacturing	1.605	0.454	0.545	0.355	1.850	0.320	1.787	0.197	0.335	0.432
Geographic	Directional	Manufacturing	2.236	0.866	0.866	1.021	0.853	0.594	0.427	1.563	0.058	0.309
Geographic	Directional	Agri+Manu	2.337	0.938	0.911	1.045	0.907	0.818	0.564	1.445	0.237	0.373
Geographic	None	Agri+Manu	4.920	1.131	0.965	1.024	1.591	1.381	1.491	0.652	1.111	0.831
Income-based	Directional	Manufacturing	1.984	0.824	0.996	0.772	0.657	0.577	0.623	0.697	0.685	0.875
Income-based	Directional	Agri+Manu	2.288	1.033	1.168	0.874	0.740	0.397	0.685	0.757	0.498	0.932

Country Groupings includes (i) No grouping, (ii) Geographic (Asia/Oceania, Europe, South America and Africa/Middle East, and (iii) Income-based (four quartiles based on each country's average GDP per capita between 2012 and 2021). Coef Filter includes (i) None – no corrections to estimated loading factors, and (ii) Directional – replaces negative loading factors with their opposite-direction counterpart for the same country-group, iff the opposite-direction coefficient is of a a lower value. Products represents measures generated using either (i) Agri+Manu – the entire set of commodity weight flows listed in the data set, or (ii) Manufacuturing – the 72 manufactures featured at the HS2 level, as defined on the TRAINS product grouping 'manufactures' set.

Switzerland represent inland regions which could only be accessed by US containerized trade via third party coastal channels such as the ports of the Rotterdam or Antwerp. Each of these countries is also part of the European Customs Union. Due to the frictionless nature of trade and apparent interdependence of countries with respect to port access, I treat the EU Single Market as a single trade partner entity. Eurostat container flow data suggests that only upon cross-country aggregation does the European Customs Union region function as a balanced container redistribution system. In contrast, individual European countries which form this union maintain imbalanced container flow systems at the national level (Figure 5.3). This pattern of local imbalances is strikingly similar to the heterogeneous roles played by individual US ports which, only when combined, maintain a balanced redistribution system of bilateral container flows.

Figure 5.3: European Specialization by Net Flow Status (2017)

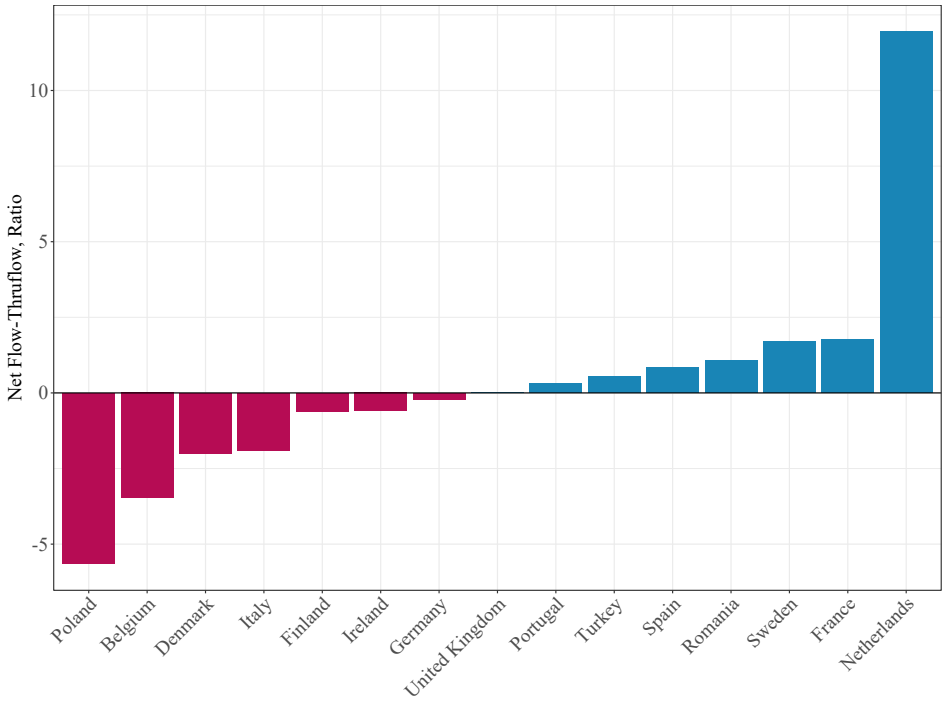

Note: The net flow to thruflow ratio uses inflows less outflows of loaded and empty container units divided by the total flow of loaded & empty container unit traffic. This 2017 data is sourced from "Volume of containers transported to/from main ports by direction, partner entity, container size and loading status", extraction ID: MAR_GO_QM.

A1 (VIII.) Container Monopsony

This section is motivated by a particular quirk of the cost minimization problem that firms would face in a round trip setting and the one-for-one transformation of inputs (inbound loaded and empty containers) into transport services (outbound loaded containers). Suppose trade is imbalanced and the net importer country generates a positive amount of outbound empties ($e_{ji} > 0$). In this case the output of transport services is a function of these two inputs.

$$l_{ij} = f(l_{ji}, e_{ji})$$

Since container flows are assumed to be balanced between countries, this would imply that transport services from i to j are equal to total container inflows at

port i, or, $l_{ij} = f(l_{ji}, e_{ji}) = l_{ji} + e_{ji}$, our usual profit function constraint in a trade imbalance setting. Taking the ratio of marginal products with respect to these two inputs:

$$\text{MRTS} = \frac{MP_{l_{ji}}}{MP_{e_{ji}}} = \frac{\partial f(l_{ji}, e_{ji})/\partial l_{ji}}{\partial f(l_{ji}, e_{ji})/\partial e_{ji}} = 1 = \frac{c_{ji}}{r^{\leftrightarrow}_{ij}} = \text{ Input Price Ratio}$$

Consider a conventional MRTS in a transport setting, where capital K and labour L inputs generate a transport service Y. Normally the MRTS varies along a given isoquant, given different bundles of inputs z_j. For example, should the capital-labor ratio be particularly high, a relatively more capital-intense input bundle that generates the same of output, $\bar{Y}$, requires significantly more units of capital compared to labor-intense input bundle. The input price ratio between capital and labor is fixed across all possible consumption bundles. A cost minimizing firm selects an input bundle where MRTS is tangent to a constant price ratio.

In the container redistribution case, the MRTS is instead fixed to a value of 1 across all consumption bundles, which under constant input price ratios implies corner solutions where a firm will only utilize the cheapest input. To introduce a unique solution on the net importer side which features positive container outflows in both empty and loaded units, I use a loaded container input price that increases in the level loaded container inputs.[4] This yields variation in the input price ratio rather than the MRTS, given variation in input bundles. Tangency occurs at the level of loaded containers l_{ji} necessary to set $c_{ji}(l_{ji}) = r^{\leftrightarrow}_{ij}$, where $c'_{ji}(l_{ji}) > 0$.

[4]Intuition: Additional loaded containers on a net importer route would imply a longer duration with respect to unloading and cleaning at the net exporter port before the containers are ready to be utilized as inputs. Each loaded container takes more time relative to an empty. The shipping service cannot commence until the last arriving loaded unit is processed and emptied. Since the first "processed" loaded container input is not usable until the last loaded container input is prepared, I represent this accumulating time challenge with a rising input price per loaded container input.

The resulting profit maximization problem can be expressed as follows.

$$\pi^{\leftrightarrow}_{ij} = T_{ij}l_{ij} + T_{ji}l_{ji} - c_{ij}(l_{ij})l_{ij} - c_{ji}(l_{ji})l_{ji} - r^{\leftrightarrow}_{ij}(e_{ij} + e_{ji}) \tag{5.6}$$
$$\text{s.t. } l_{ij} + e_{ij} = l_{ji} + e_{ji},$$

There are a number of ways of introducing this increasing input cost parameter. I resort to using the simplest possible expressions, where loaded container input prices increase linearly with respective quantities.

As displayed in Figure 1, the inclusion of rising input prices for one particular input eliminates the possibility of corner solutions, as arbitrage opportunities across input prices are eliminated by a perfectly competitive market. The higher slope of $c_{ji}(l_{ji})$ implies there is a greater cost or more rapid elevating trade-off associated with loading containers at the net importer country compared to the net exporter country. Upon intersection with the input price of empty containers, the loaded container quantity is identified.

The relative differences in slopes establish the capacity $\max\{l_{ji}, l_{ij}\}$, empty container load $|l_{ij} - l_{ji}|$ and associated input prices of providing a shipping service. These differences should be representative of exogenous supply and demand factors. For example, should relative demand for l_{ij} increase due to an exogenous preference shock, the slope of $c_{ji}(l_{ji})$ should increase and the slope of $c_{ij}(l_{ij})$ should decrease, causing the trade imbalance displayed above to widen, shipping capacity to increase and empty, $e_{ji} = l_{ij} - l_{ji}$ container flows to rise.

I display two variations and solve for both balanced and imbalanced trade.

1. This first form of input price rises as loaded container inputs rise on route ji. The producer will continue to stack loaded containers onto the 'backhaul' route until the input price is equal to the constant input price of an empty

Figure 5.4: Input Price by Loaded Container

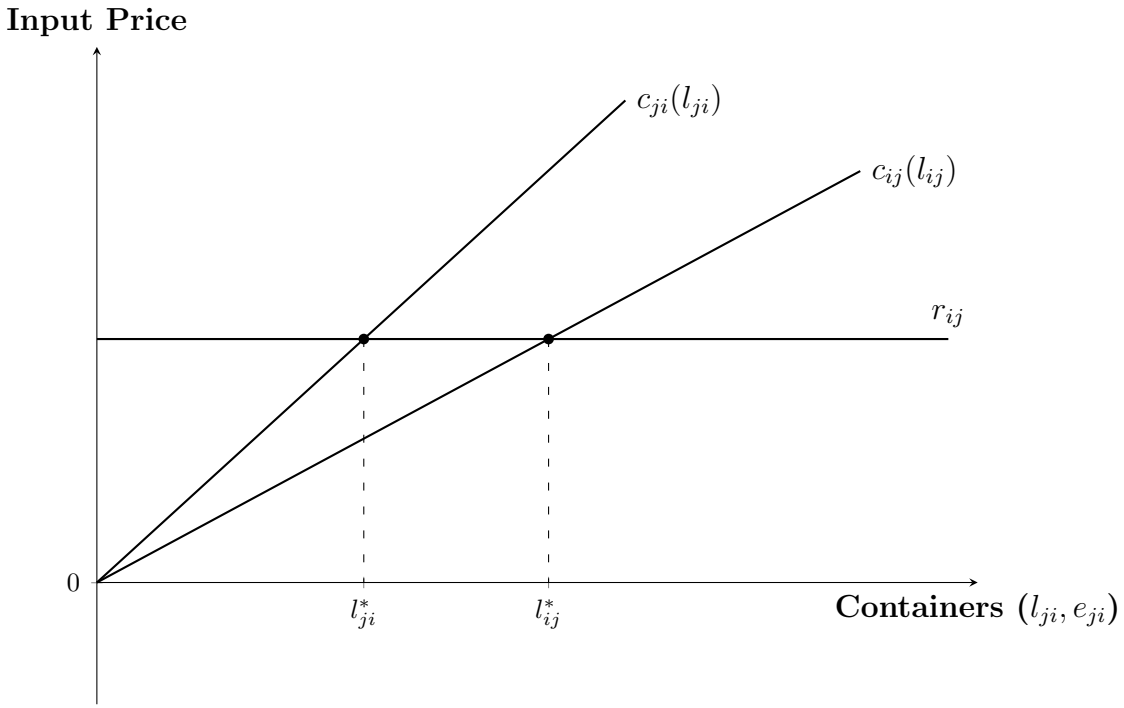

container, e_{ji}. Form: $c_{ji}(l_{ji}) = \theta_{ij} l_{ji}$

2. The inclusion of an added loaded container input, l_{ji}, yields the corresponding freight rate, T_{ji} but comes at the cost of a percentage θ_{ij} of a completed 'full' haul trip's from i to j, T_{ij}. The percentage scales as the loaded input rises. This adjustment captures hows the increased velocity that round trips can complete laps at in cases where the 'backhaul' features a relatively greater level of empties per container input. Form: $c_{ji}(l_{ji}) = \theta_{ij} T_{ij} l_{ji}$

Case I: Balanced Trade

The production function for transport services appears as $l_{ij} = f(l_{ji})$, where the marginal product of the input (MP^L_{ij}) is equal to 1 since $l_{ij} = l_{ji}$. Plugging this updated production constraint into the profit maximization problem of equation (11), the problem becomes analogous with Section 1.2.1 and Wong (2022). Using

the first increasing input price function, the transport operator problem becomes:

$$\begin{aligned}
\max_{\{l_{ij}\}} \ & \pi^{\leftrightarrow}_{ij} = T_{ij}l_{ij} + T_{ji}l_{ij} - (\theta_{ij}l_{ij})l_{ij} - (\theta_{ji}l_{ij})l_{ij} \\
\text{FOC: } & \frac{\partial \pi}{\partial l_{ij}} = 0 \implies T_{ij} + T_{ji} = 2\theta_{ij}l_{ij} + 2\theta_{ji}l_{ij} \\
& l_{ij} = l_{ji} = \frac{T_{ij} + T_{ji}}{2(\theta_{ij} + \theta_{ji})}
\end{aligned} \tag{5.7}$$

Consider the inverse demand function implied by equation (4).

$$T_{ij} = \frac{\epsilon - 1}{\epsilon} a_{ij} l_{ij}^{-\frac{1}{\epsilon}} - w_i \tau_{ij}$$

Substituting out freight rates in equation (12),

$$l_{ij} = l_{ji} = \frac{\frac{\epsilon-1}{\epsilon} a_{ij} l_{ij}^{-\frac{1}{\epsilon}} - w_i\tau_{ij} + \frac{\epsilon-1}{\epsilon} a_{ji} l_{ji}^{-\frac{1}{\epsilon}} - w_j\tau_{ji}}{2(\theta_{ij} + \theta_{ji})} = \frac{\frac{\epsilon-1}{\epsilon}(a_{ij} + a_{ji}) l_{ij}^{-\frac{1}{\epsilon}} - w_i\tau_{ij} - w_j\tau_{ji}}{2(\theta_{ij} + \theta_{ji})}$$

Appears to be a non-linear solution. Below I detail a case in which the $w_i\tau_{ij}$ terms do not feature. In this scenario, I divide by $(l_{ij})^{-\frac{1}{\epsilon}}$ to solve for l^*_{ij},

$$(l^*_{ij})^{1+\frac{1}{\varepsilon}} = \frac{\epsilon - 1}{\epsilon} \frac{a_{ij} + a_{ji}}{2(\theta_{ij} + \theta_{ji})} \implies l^*_{ij} = \left(\frac{\epsilon - 1}{\epsilon} \frac{a_{ij} + a_{ji}}{2(\theta_{ij} + \theta_{ji})} \right)^{\frac{\epsilon}{1+\epsilon}}$$

Substituting this expression into the inverse demand function, the equilibrium

freight rates are;

$$\begin{aligned}
T_{ij}^{*} =& \frac{\epsilon-1}{\epsilon} a_{ij} \left(\left(\frac{\epsilon-1}{\epsilon} \frac{a_{ij}+a_{ji}}{2(\theta_{ij}+\theta_{ji})} \right)^{\frac{\epsilon}{1+\epsilon}} \right)^{-\frac{1}{\epsilon}} \\
=& \frac{\epsilon-1}{\epsilon} a_{ij} \left(\frac{\epsilon-1}{\epsilon} \frac{a_{ij}+a_{ji}}{2(\theta_{ij}+\theta_{ji})} \right)^{-\frac{1}{1+\epsilon}} \\
=& \left(\frac{\epsilon-1}{\epsilon} \right)^{1-\frac{1}{1+\epsilon}} a_{ij} \left(\frac{2(\theta_{ij}+\theta_{ji})}{a_{ij}+a_{ji}} \right)^{\frac{1}{1+\epsilon}} \\
=& \left(\frac{\epsilon-1}{\epsilon} \right)^{\frac{\epsilon}{1+\epsilon}} a_{ij} \left(\frac{2(\theta_{ij}+\theta_{ji})}{a_{ij}+a_{ji}} \right)^{\frac{1}{1+\epsilon}}
\end{aligned}$$

Shifting to the increasing input price function based on opportunity cost and round trip velocity, solving the model involves the following steps.

$$\begin{aligned}
\max_{\{l_{ij}\}} \ & \pi_{ij}^{\leftrightarrow} = T_{ij} l_{ij} + T_{ji} l_{ij} - (\theta_{ji} l_{ij} T_{ji}) l_{ij} - (\theta_{ji} l_{ij} T_{ij}) l_{ij} \\
\text{FOC:} \ & \frac{\partial \pi}{\partial l_{ij}} = 0 \implies T_{ij} + T_{ji} = 2\theta_{ij} T_{ij} l_{ij} + 2\theta_{ji} T_{ji} l_{ij} \\
& l_{ij}^{*} = l_{ji}^{*} = \frac{T_{ij} + T_{ji}}{2(\theta_{ij} T_{ij} + \theta_{ji} T_{ji})}
\end{aligned} \tag{5.8}$$

A similar non-linear solution case is arrived upon.

Case II: Imbalanced Trade

The production function for transport services on the net exporter route is $l_{ij} = f(l_{ji}, e_{ji})$, where the marginal product of a loaded input (MP_{ij}^{L}) is equal to the marginal product of an additional empty input (MP_{ij}^{E}), since $l_{ij} = l_{ji} + e_{ji}$. In this case the marginal rate of technical substitution, $\frac{MP_{ij}^{L}}{MP_{ij}^{E}}$, is equal to 1. Using the first form of the increasing input cost function, the profit maximization problem can be expressed as:

$$\max_{\{l_{ij},l_{ji},e_{ji}\}} \pi^{\leftrightarrow}_{ij} = T_{ij}l_{ij} + T_{ji}l_{ji} - (\theta_{ij}l_{ji})l_{ji} - (\theta_{ji}l_{ij})l_{ij} - r^{\leftrightarrow}_{ij}(0 + e_{ji}) \text{ s.t. } e_{ji} = l_{ij} - l_{ji}$$

$$\max_{\{l_{ij},l_{ji}\}} \pi^{\leftrightarrow}_{ij} = T_{ij}l_{ij} + T_{ji}l_{ji} - (\theta_{ij}l_{ji})l_{ji} - (\theta_{ji}l_{ij})l_{ij} - r^{\leftrightarrow}_{ij}(l_{ij} - l_{ji})$$

FOC:

$$\frac{\partial \pi}{\partial l_{ij}} = 0 \implies T_{ij} - 2\theta_{ji}l_{ij} - r^{\leftrightarrow}_{ij} = 0$$
$$\frac{\partial \pi}{\partial l_{ji}} = 0 \implies T_{ji} - 2\theta_{ij}l_{ji} + r^{\leftrightarrow}_{ij} = 0$$

Supply and inverse supply of transport services can be expressed as follows, implying an upward sloping supply curve.

$$l^S_{ij} = \frac{T_{ij} + r^{\leftrightarrow}_{ij}}{2\theta_{ji}} \quad , \quad l^S_{ji} = \frac{T_{ji} - r^{\leftrightarrow}_{ij}}{2\theta_{ij}} \quad , \quad T^S_{ij} = 2\theta_{ji}l_{ij} + r^{\leftrightarrow}_{ij} \quad , \quad T^S_{ji} = 2\theta_{ij}l_{ji} - r^{\leftrightarrow}_{ij}$$

Using equation (4), the demand for these goods are downward sloping in freight rates, points of intersection can be identified.

$$l^D_{ij} = \left(\frac{\epsilon}{1-\epsilon}\frac{1}{a_{ij}}\right)^{-\epsilon}\left(w_i\tau_{ij} + T^*_{ij}\right)^{-\epsilon} = \frac{T^*_{ij} + r^{\leftrightarrow}_{ij}}{2\theta_{ji}} = l^S_{ij}$$
$$T^D_{ij} = \frac{\epsilon - 1}{\epsilon}a_{ij}l^{*-\frac{1}{\epsilon}}_{ij} - w_i\tau_{ij} = 2\theta_{ji}l^*_{ij} + r^{\leftrightarrow}_{ij} = T^S_{ij}$$

In this case, the round trip effect does not present itself. Ships are not setting maximum capacity due to circumstances pertaining to both i and j. Need an expression in which these equilibrium outcomes of price and quantity reflect use of $\{a_{ij}, a_{ji}, \tau_{ij}, \tau_{ji}\}$.

Using instead the increasing function based on opportunity cost of a slower com-

pletion rate of round trips:

$$\max_{\{l_{ij},l_{ji},e_{ji}\}} \pi^{\leftrightarrow}_{ij} = T_{ij}l_{ij} + T_{ji}l_{ji} - (\theta_{ij}l_{ji}T_{ij})l_{ji} - (\theta_{ji}l_{ij}T_{ji})l_{ij} - r^{\leftrightarrow}_{ij}(0 + e_{ji}) \text{ s.t. } e_{ji} = l_{ij} - l_{ji}$$

$$\max_{\{l_{ij},l_{ji}\}} \pi^{\leftrightarrow}_{ij} = T_{ij}l_{ij} + T_{ji}l_{ji} - (\theta_{ij}l_{ji}T_{ij})l_{ji} - (\theta_{ji}l_{ij}T_{ji})l_{ij} - r^{\leftrightarrow}_{ij}(l_{ij} - l_{ji})$$

FOC:

$$\frac{\partial \pi}{\partial l_{ij}} = 0 \implies T_{ij} - 2\theta_{ji}T_{ji}l_{ij} - r^{\leftrightarrow}_{ij} = 0$$
$$\frac{\partial \pi}{\partial l_{ji}} = 0 \implies T_{ji} - 2\theta_{ij}T_{ij}l_{ji} + r^{\leftrightarrow}_{ij} = 0$$

$$l^S_{ij} = \frac{T_{ij} - r^{\leftrightarrow}_{ij}}{2\theta_{ij}T_{ji}} \quad , \quad l^S_{ji} = \frac{T_{ji} + r^{\leftrightarrow}_{ij}}{2\theta_{ji}T_{ij}}$$

Using the inverse demand function implied in equation (4), the solutions for quantities become:

$$l^*_{ij} = \frac{\frac{\epsilon-1}{\epsilon}a_{ij}l^{*-\frac{1}{\epsilon}}_{ij} - w_i\tau_{ij} - r^{\leftrightarrow}_{ij}}{2\theta_{ij}\left(\frac{\epsilon-1}{\epsilon}a_{ji}l^{*-\frac{1}{\epsilon}}_{ji} - w_j\tau_{ji}\right)} \quad , \quad l^*_{ji} = \frac{\frac{\epsilon-1}{\epsilon}a_{ji}l^{*-\frac{1}{\epsilon}}_{ji} - w_j\tau_{ji} + r^{\leftrightarrow}_{ij}}{2\theta_{ji}\left(\frac{\epsilon-1}{\epsilon}a_{ij}l^{*-\frac{1}{\epsilon}}_{ij} - w_i\tau_{ij}\right)}$$

Rearranging l_{ij}^*

$$2\theta_{ij}(\frac{\epsilon-1}{\epsilon}a_{ji}l_{ji}^{*-\frac{1}{\epsilon}} - w_j\tau_{ji})l_{ij}^* = \frac{\epsilon-1}{\epsilon}a_{ij}l_{ij}^{*-\frac{1}{\epsilon}} - w_i\tau_{ij} - r_{ij}^{\leftrightarrow}$$

$$2\theta_{ij}(\frac{\epsilon-1}{\epsilon}a_{ji}l_{ji}^{*-\frac{1}{\epsilon}})l_{ij}^* = \frac{\epsilon-1}{\epsilon}a_{ij}l_{ij}^{*-\frac{1}{\epsilon}} - w_i\tau_{ij} - r_{ij}^{\leftrightarrow} + (w_j\tau_{ji})l_{ij}^*$$

$$2\theta_{ij}\frac{\epsilon-1}{\epsilon}a_{ji}l_{ji}^{*-\frac{1}{\epsilon}} = \frac{\epsilon-1}{\epsilon}a_{ij}l_{ij}^{*-\frac{1}{\epsilon}-1} - (w_i\tau_{ij} - r_{ij}^{\leftrightarrow})l_{ij}^{-1} + w_j\tau_{ji}$$

$$l_{ji}^{*-\frac{1}{\epsilon}} = \frac{1}{2\theta_{ij}}\frac{a_{ij}}{a_{ji}}l_{ij}^{*-\frac{\epsilon+1}{\epsilon}} - \frac{1}{2\theta_{ij}}\frac{\epsilon}{\epsilon-1}\frac{1}{a_{ji}}(w_i\tau_{ij} - r_{ij}^{\leftrightarrow})l_{ij}^{-1} + \frac{1}{2\theta_{ij}}\frac{\epsilon}{\epsilon-1}\frac{1}{a_{ji}}(w_j\tau_{ji})$$

$$l_{ji}^* = \left(\frac{1}{2\theta_{ij}}\frac{a_{ij}}{a_{ji}}l_{ij}^{*-\frac{\epsilon+1}{\epsilon}} - \frac{1}{2\theta_{ij}}\frac{\epsilon}{\epsilon-1}\frac{1}{a_{ji}}\left(w_i\tau_{ij} - r_{ij}^{\leftrightarrow}\right)l_{ij}^{-1} + \frac{1}{2\theta_{ij}}\frac{\epsilon}{\epsilon-1}\frac{1}{a_{ji}}\left(w_j\tau_{ji}\right)\right)^{-\epsilon}$$

$$l_{ij}^* = \left(\frac{1}{2\theta_{ji}}\frac{a_{ji}}{a_{ij}}l_{ji}^{*-\frac{\epsilon+1}{\epsilon}} - \frac{1}{2\theta_{ji}}\frac{\epsilon}{\epsilon-1}\frac{1}{a_{ij}}\left(w_j\tau_{ji} - r_{ij}^{\leftrightarrow}\right)l_{ji}^{-1} + \frac{1}{2\theta_{ji}}\frac{\epsilon}{\epsilon-1}\frac{1}{a_{ij}}\left(w_i\tau_{ij}\right)\right)^{-\epsilon}$$

In this case I have two equations and two unknowns, but the explicit solutions for $\{l_{ij}, l_{ji}\}$ are not clear nor would the associated comparative statics be. Likely need to reconsider another method of going about solving this model, or else go down a computational route where the comparative statics can only be assessed through simulation. The benefit of this approach would be incorporating round trip effects in an unbalanced trade setting.

Appendix II

A2 (I.) Data Appendix

Our dataset of vessel movements and characteristics extends from 1977 to 2023 and requires the use of multiple data sources. We first detail two daily records of containership visits at US ports. Lastly, we describe our automatic identification system (AIS) data of individual vessels' geo-locations within US waters, which varies at a minute level. This description includes our means of converting position records into port call data, which yields a precise minute-level measure of containership dwell times at port. Lastly, we elaborate on VesselTracker data which complements all three data sets by allowing us to update each vessels build year and maximum container capacity.

Port Statistical Areas (USACE)

We identify the top ports of containerized shipping based on Panjiva records of twenty-foot equivalent unit (TEU) container traffic.[5] We then access public records of port statistical areas, provided by the USACE. There are some ports missing from this list. We construct polygon areas manually for these ports, taking guidance from each ports provided facility maps. In cases where facility maps are not provided, we research to satellite imagery provided by Google Earth. These port polygons are used to track the entry and exit of individual vessels, using their geolocations which are updated in minute intervals.

US port callings (Lloyd's List Intelligence)

Lloyd's List Intelligence (LLI) maintains a network of agents on the ground at ports worldwide to validate information and address customized information requests. Ultimately, the Lloyd's Agency Network, which is exclusively operated

[5]See https://www.logisticsmgmt.com/article/top_30_u.s._ports_big_ports_got_bigger_in_2020

by Lloyd's List Intelligence, is the signature capability that distinguishes the company's data collection and validation process from any other company within the maritime trade data industry. We have partnered with Lloyd's to secure ports callings data for 1977–2002. This data is the product of hands-on effort maintaining presences across US ports and frequently referring to on-site paper records of visits. Given that AIS (vessel tracking) technology not coming into the market until 2009, our source offers a unique edge over our competitors that do not have access to this historical data. As a result, LLI is the sole source of reliable human intelligence capable of providing port callings data from 1977 – 2002. We must also highlight that while we focused our attention on US data, there are global historical records of port callings available through LLI.

This data reports the International Maritime Organization code of each containership offloading or onloading goods at ports across the US. Additionally, we observe the arrival and departure times of vessel visits and the vessel name of each ship. For post-2002 data, we refer to public data made available through the US Army Corps of Engineers (USACE).

Port Entrances and Clearances (USACE)

The publication of data from the CBP form 1300 is done so via the CBP form 1400 (Entrance) and 1401 (Clearance). The CBP publishes the latest 1400 and 1401 from the previous week. The USACE has established a feed for the data from CBP and compiles records of port entrances and clearance, releases these statistics via the Waterborne Commerce Statistics Center. The CBP form 1300 dates back to 1965 where an international convention successfully unified the forms necessary for processing vessels arriving into countries. The agreement was adopted in London, England on 9 April 1965 and entered into force on 5 March 1967.[6] The US used to have the CBP form 1300 and the CBP form 1301. Both forms were consolidated

[6]See IMO documentation on the Convention on Facilitation of International Maritime Traffic (FAL).

into the CBP form 1300.

Upon the late 90s and early 2000s, it was a big time for CBP as far as electronic records and digitizing information. The CBP form 1400 and 1401 used to be "published" on paper at each Customhouse around the country for the local records of that particular port, where any individual could walk up and browse through the records. Now they are published via PDF on CBP.gov, updated weekly each Friday morning. According to speculation from our contacts with the CBP, the 'late 90s and early 2000s' CBP was in the process of automating this data collection and publication and it simply took time for all ports to get onboard. Upon a national security disaster on September 11th 2001, these processes were accelerated by the then Customs Service. We note sparseness in records of port calls from 1997–2001, which underreport vessel activity at US ports relative to LLI data. Based on our understanding of the CBP's transition into digitalized records, we assume records are representative of US containerized transport services from 2002 onward.

These records list individual vessel IMO codes, along with each visiting vessel's name, the date at which they enter, the port of entrance, the date at which a vessel leaves and fixed characteristics such as the gross and net tonnage of each vessel. Gross Tonnage (GT) is the volume of all enclosed spaces on a vessel. This includes the Engine Room and other non-cargo spaces. Most Maritime Regulations (SOLAS, MARPOL, etc.) apply to vessels based on their Gross Tonnage. Net Tonnage (NT), on the other hand, is the volume of only the cargo-carrying spaces on the vessel. This is the tonnage that determines the earning capability of the vessel. Most port/anchorage dues apply to vessels based on their Net Tonnage. Crucially, each record of a visit also yields a vessel's ICST code, which details the 'International Classification of Ships'. This allows us to identify which cargo ships in the AIS data set are containerships (ICST code 310).

Upon combining 2002–2021 records, we correct a subset of IMO codes that

appear to have been incorrectly entered by those filing 1400 and 1401 forms. In cases of non-reported gross tonnages of vessels, we refer to each vessel's IMO code and draw upon the single reported measure of gross tonnage. In cases where multiple tonnages are reported, we use the most recent reported gross tonnage of a uniquely identified vessel for each one of its port dwell events. This is due to records, on average, exhibitiing more accuracy in data entry we advance further in the reported years of the dataset.

Vessel Position, AIS data (MarineCadastre)

For minute-level vessel activity between January 1st 2010 and December 31st 2014, available data is provided in a .zip format, where each issued file represents vessel movements within a specific Coordinated Universal Time (UTC) section of the US. These files each feature an entire month's worth of vessel position data, in some cases reaching half a GB in size before unzipping. Upon unzipping each file, the resulting .gdb file contains separate broadcast, vessel and voyage data. We merge these items together into a single data object and save specific year–month–zone files across the timezones belonging to ports in our 30 Port Statistical Areas of interest. Vessels are identifiable only through reported MMSI codes, which have been scrambled in order to mask vessel identities. We have been provided with a descrambler by the National Oceanic and Atmospheric Administration (NOAA) which allows us to revert MMSI codes back to their original state. Upon consultation with the U.S. Coast Guard, we can been provided with the associated IMO code of each one of these unscrambled MMSI code identifiers for vessels, which is crucial in pairing fixed characteristics from the Port Entrance and Clearances (USACE) data.

Upon a series of cross validation checks on raw monthly and daily data of vessel positions with overlapping USACE records, a narrowing sparseness in AIS-imputed dwell events up to 2016 was identified. After March 2016, USACE containership

visit records mirror the scale of activity reflected by AIS movements. We attribute the prior pattern of under reported vessel movements to the fact that AIS transport use only became a requirement as of the issuing of a federal mandate on January 30 2015, entitled "Vessel Requirements for Notices of Arrival and Departure, and Automatic Identification System".[7] This filing required the fitting of AIS transponders for all commercial vessels and their persistent use in US waters by March 2016. We settle on relying on vessel position data from March 2016 to December 2023 to ensure we are studying port call activity in an environment in which transponder use is mandatory.

For minute-level vessel activity between January 1st 2015 and December 31st 2023, available data is provided in a .csv format, where each issued file represents all vessel movements within US waters for a single calendar date. Vessel identities were not scrambled and each file not only reports MMSI codes, but also each vessels IMO code and name. The download and processing of AIS data is automated and takes the following steps.

1. Download raw data daily (March 2016- December 2023) vessel positions.

2. IMO codes for positions between 2016 and 2022 allow us to identify cargo vessels, which includes – containerships, vehicle carriers, bulk carriers, roll-on roll-off (ro-ro) cargo ships, reefers, livestock carriers, and general cargo multi-deck carriers.

3. Filter out any vessels that neither report a cargo-related ICST code or do not maintain a cargo/vessel type code of 79.

4. Filter out any vessels that do not operate within our port polygon areas of interest.

[7]For more details, see 80 FR 5282 Docket No. USCG-2005-21869. Last visited on April 17 2024 at https://www.federalregister.gov/documents/2015/01/30/2015-01331/vessel-requirements-for-notices-of-arrival-and-departure-and-automatic-identification-system

5. For each month of observations: Apply algorithm to remaining set of vessel positions which identifies key timestamps in which vessels (i) enter a port region, (ii) come to a full stop, (iii) begin moving, and (iv) exit the same port. While we originally paired items (ii) and (iii) with AIS status signals of "mooring" and "underway", respectively, subsequent analysis revealed that vessel operators are not always diligent or prompt in indicating their vessel's current status. Each of these four states represents a specific stage of a port dwell event.

6. The time elapsed between when mooring starts and ends is recorded as the duration of a dwell period between states (ii) and (iii). This allows us to capture any dwell events that occur within a month or across the last 20 days of a given month (monthly) and subsequent 20 days of the following month (month–gap). Dwell experiences that exceed 40 days in length are not captured.

7. We combine the monthly and month–gap dwell events and retain the subset of distinct visits to avoid any duplications of containership activity.

8. We apply post-processing filtration to these dwell events, in adherence with the guidelines detailed by the Bureau of Transport Statistics (BTS). This includes combining multiple dwell events at a single port together, if the time elapsed between each dwell event is less than two hours. Furthermore, any dwell events that take place in two separate ports and imply an average travel speed of over 25 knots are discarded as such as travel speed is infeasible for cargo vessels. Lastly, we discard short dwell events of less than 2 hours to avoid any over–counting of dwell events which can instead be attributed to crew changes and refueling.

Vessel Characteristics Registry Data (VesselTracking)

Through use of the 'xml2' R package, we have scraped 233,581 vessels' fixed characteristics (name, IMO code, build year, container capacity and length) from records published on www.vesseltracking.net/ships (VT). This data applies across the global fleet of existing and decommissioned vessels and offers a near 100% match rate across the vessels listed in our LLI, USACE and AIS data sets. We combine the three datasets and further enhance the granularity of the data by merging in these fixed characteristics.

Any cleaning attributed to the data is very minimal, due to the high quality of the source material. In the case of ten distinct IMOs, the VT data yields container capacities of zero. We utilize third-party vessel–spotting & –tracking portals, which offers details pertaining to relatively old vessels and newly built containerships. Below we detail our matches for each distinct vessel:

Table 5.19: Manually Entered IMO–TEU Capacity Pairs

Vessel IMO	9849643	9719068	9809904	9809916	9819947	9819959	9869667	9757228	9757230	9757216
TEU Capacity	1268	3600	1148	1148	1148	1148	1268	14220	14220	14000

A2 (II.) Coastal Stylized Facts

We also examine these shifts towards new technology by coastal region in Figure 5.5. The West Coast exhibits a far more smooth adoption of technology, relative to the East Coast. This is likely driven by many shipbuilding sites and large manufacturing centers being based in East Asia. Upon the expansion of the Panama Canal, Post Panamax vessels – designed for the greater width of the Canal – rapidly gained market share on the East Coast. In contrast, the Gulf Coast appears to utilize such technology far more sparsely. This is potentially attributable to factors such as older port infrastructure and lower population density.

Figure 5.5: Vessel Category Shares of Coastal Containership Activity

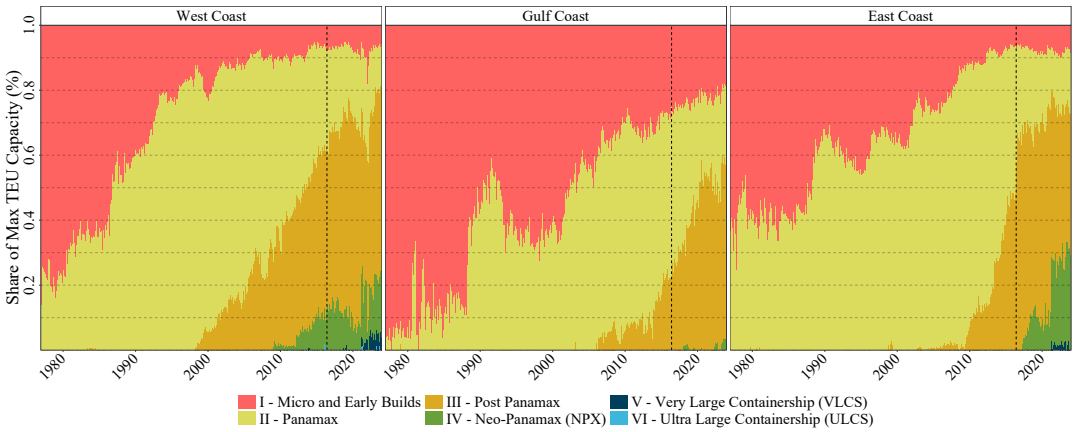

Note: The long dashed vertical line indicates the point at which the Panama canal was expanded, June 26 2016.

As displayed in Figure 5.6, growth in the total mass of vessel transit to the US West Coast has stagnated since 2002 and begun declining from 2018. Limited port resources are becoming increasingly depended upon along the US East Coast. While the West Coast was the main host for some of the largest vessels servicing the US between 1995–2016, the gap has largely narrowed since the expansion of the Panama canal.

Figure 5.6: Container Capacity of Vessel Visits by Region

(a) Total TEU Capacity

(b) Average TEU Capacity

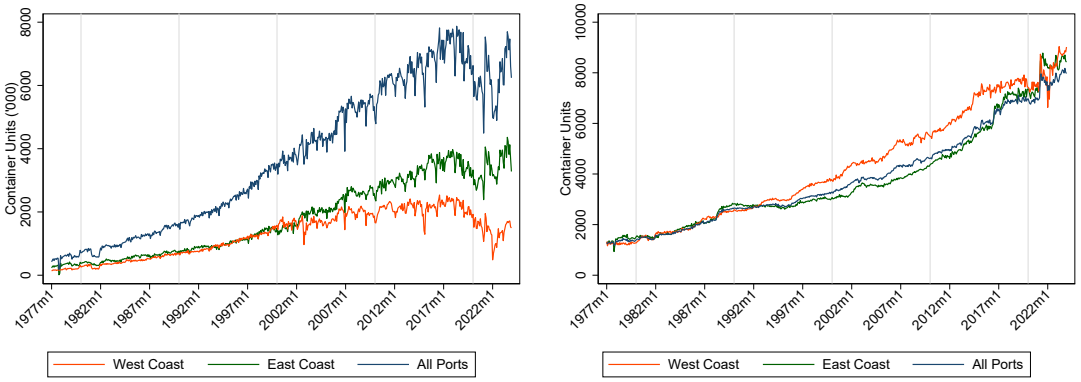

A2 (III.) Panjiva Records

Given the supportive nature of the port of laden records we rely upon for validation exercises, we encapsulate all data discussion, cleaning methodology and associated empirical exercises in the following Appendix section. We acquired Panjiva Inc. data – a division of Standard and Poor's – which details bill of lading information for all seaborne US imports from January 2007 to September 2023. Panjiva cleans this data to standardize the names of the ports, ships, companies, and associated unloaded container volumes. We subset this data to only consider goods that arrive on seaborne container ships. To do so, we use the vessels' IMO codes, which uniquely identify ships across time. Paired with our knowledge of the population of IMO's associated with containership voyages at key US ports, this allows us to focus on containerized shipping specifically.

The bill of lading data Panjiva offers is an industry-standardized system, which act as receipts of shipment, recording all information on the shipment and all the parties involved in the shipping process. The US Customs and Border Patrol (CBP) agency collects these bills in addition to customs information at all ports of entry into the US. We apply the following steps in order to further clean and wrangle the provided data;

1. All IMO entries that do not contain 7 digits are dropped from the sample – 3% sample attrition,

2. Observations with missing IMO codes are isolated and vessel names are matched to VesselTracking records. In cases where one unique IMO code is associated with these records, we assign the IMO code to the vessel – 6.5% of IMOs remain missing,

3. We repeat Step 2 but focus on unique IMO codes associated with distinct vessel name and port combinations.

4. Subset the remaining set of vessel names with missing IMOs and postive TEU offloadings. Using the set of unique vessel names from VesselTracker, apply a Jaro Winkler algorithm which yields a numeric value of $[0, 1]$ regarding the similarity of two string variables (Winkler, 1990) – we use matches of 0.93789 similarity or higher and repeat Steps 3 & 4 – 4.4% of IMO entries are missing.

5. For multiple observations of a distinct Arrival Date, Port Name, IMO, Vessel Name offloading event, we sum the number of offloaded containers into one single entry

6. We subset our combined sample of vessel dwell events to 2007–2023. For each row of our port call data, we filter the Panjiva sample for an identical IMO–port match. Among these matches, we calculate the difference in arrival time by days and isolate the minimium difference. Any port dwell events that are within a 9 day window of time – 4 days before or after a Panjiva arrival – are labelled a match.[8]

We attribute differences in arrival times to administrative differences in the submission of paperwork and the differing natures of these two items. Dates in which a portion of containerized goods imports are processed do not always reflect with the date a given vessel carrying those goods arrives. In scenarios where individual vessel dwell times elongate abnormally and cause the timing between a vessel arrival and completion of the offloading process to increase in length, such as in the COVID-19 period, our matching process weakens. Nevertheless, only very thin windows of time are necessary to achieve match rates of over 90% across our sample.

Additionally, Panjiva imputes TEU (twenty-foot equivalent) container volumes

[8]Match rates are displayed across 0 to 9 day windows of time in Figure 5.7

based on container information and other shipment characteristics (Flaaen et al., 2023). In appraising the accuracy of these estimates, we find that Panjiva systematically under-reports the number of offloaded container units associated with imports, when compared aggregated data of port–level container inflows via two sources. Roughly half of TEU imports are represented by Panjiva data.

These extensive and intensive margins of missingness should be considered when evaluating our findings, relative to those from Section 4. In Table 5.20, we revisit differences in efficiency across containership classes of increasing capacity, length and volume. Our measure of efficiency, dwell time per unloaded TEU container, tends to exhibit higher performance rates across vessels of larger size categories. However, evidence suggests that the largest containerships in this subsample are handled handled any better than our reference group of micro-build and Panamax containership classes. Referring to Figure 5.5, this may be due to US ports not yet being well-optimized for the latest generation of supersized containerships. Upon incremental adjustments to port infrastructure and market shares of these vessels elevating beyond 1%, we anticipate that the efficiency of port service interactions with these vessels may become highly rewarding.

Figure 5.7: Match Rate, Panjiva Vessel Offloading to Port Call Records

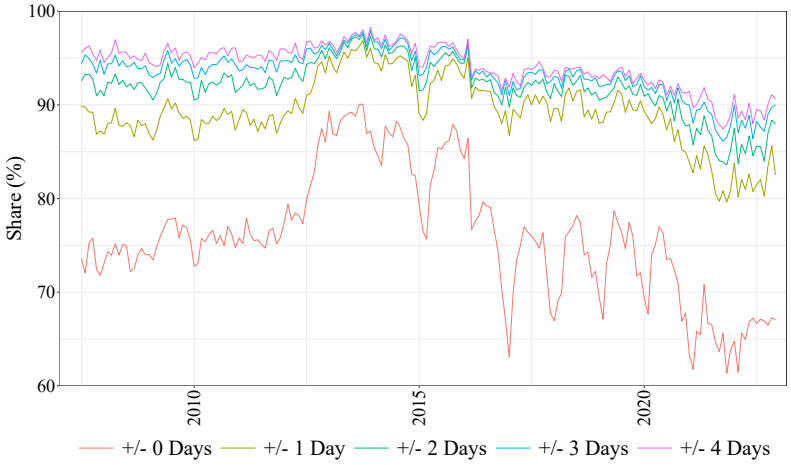

Note: Day windows range across port call records and are in reference to individual arrival dates of Panjiva data.

Table 5.20: OLS Vessel Efficiency by Ship Category – Panjiva

Dependent Variable:	Efficiency			
	(1)	(2)	(3)	(4)
Post Panamax	-0.3528***	-0.3633***	-0.3635***	-0.3518***
	(0.0604)	(0.0585)	(0.0584)	(0.0609)
Neo-Panamax (NPX)	-0.4483***	-0.4046***	-0.4049***	-0.4439***
	(0.0518)	(0.0590)	(0.0589)	(0.0529)
Very & Ultra Large Containerships	-0.3485	-0.2710	-0.2729	-0.3647*
	(0.2107)	(0.2106)	(0.2101)	(0.2082)
Vessel Age	0.1028***	0.0999***	0.1000***	0.1039***
	(0.0283)	(0.0277)	(0.0278)	(0.0282)
Day-Month-Year	Yes	Yes	Yes	Yes
Port-Year	Yes			
Port		Yes		
Port-Month			Yes	
Port-Year-Month				Yes
Region				Yes
Observations	226,078	226,078	226,078	226,078
R^2	0.12	0.10	0.10	0.13

Notes: Clustered port standard-errors in parentheses. Codes: ***: 0.01, **: 0.05, *: 0.1. Examines variation container handling efficiency of individual vessels relative to our reference group of early-build/micro vessels and Panamax category containerships.

Table 5.21: IV Elasticity of Vessel Efficiency with respect to Port Traffic – Panjiva

Dependent Variables:	Efficiency OLS	Port Vessel Count First Stage	Efficiency 2SLS			
	(1)	(2)	(3)	(4)	(5)	(6)
Port Vessel Count	0.2351***		0.2390	-2.782	0.0834	-1.676
	(0.0652)		(0.3004)	(225,593.7)	(0.3062)	(62,994.3)
HHI	-0.0433**	-0.1612***	-0.0427	-0.6765	-0.1130*	-0.1737
	(0.0160)	(0.0208)	(0.0573)	(45,013.1)	(0.0636)	(5,656.3)
Vessel Age	-0.0280	-0.0016	-0.0280	-0.0259	-0.0141	-0.0263
	(0.0447)	(0.0021)	(0.0449)	(988.3)	(0.0459)	(47.72)
Large Share (%)	0.0663	0.1113***	0.0659	-0.0063	0.0910	0.3023
	(0.0479)	(0.0306)	(0.0609)	(7,782.0)	(0.0590)	(7,349.9)
Port Trade Exposure		0.1740***				
		(0.0467)				
Ship FE	✓	✓	✓	✓	✓	✓
Port–Year FE	✓	✓	✓			
Port FE				✓		
Port–Month FE					✓	
Port–Year–Month FE						✓
Coastline FE						✓
Observations	226,078	226,078	226,078	226,078	226,078	226,078
R^2	0.23	0.96	0.23	0.11	0.22	0.23

Notes: Clustered port standard-errors in parentheses. Codes: ***: 0.01, **: 0.05, *: 0.1. All variables are in logs excluding 'large vessel share' which reports the percentage of visiting vessels in the 4th and 5th quintiles of vessel size across ports and time. 'Efficiency' is dwell time per offloaded TEU. 'Port Traffic' reports the weekly tonnage of containership vessels present at port p, excluding ship i's contribution. 'Port Vessel Count' reports the number of containership vessels present at port for a given week. 'HHI' reports a Herfindahl–Hirschman index of vessel tonnage concentration. The higher the value, the more densely concentrated total weekly mass is across visiting containerships at a given port p. 'Vessel Age' reports the difference in year and build year of ship i. New entrant vessels are those built in the same year they are actively servicing US ports. We apply an age of 0.5 to new entrants to preserve them in the sample. These vessels are potentially key drivers of spillover variation in surrounding vessel dwell times.

Appendix III

A3 (I.) Data Appendix

The construction of voyage data yields each individual vessel's associated emissions in lieu of arriving at a given port. These measures are constructed through many stages of cleaning with respect to vessel position data provided by MarineCadastre.

Port Statistical Areas (USACE)

I identify the top ports of containerized shipping based on Panjiva records of twenty-foot equivalent unit (TEU) container traffic.[9] i then access public records of port statistical areas, provided by the United States Army Corps of Engineers (USACE). I construct polygon areas manually for any missing ports, taking guidance from each ports provided facility maps. In cases where facility maps are not provided, I refer to satellite imagery provided by Google Earth. These port polygons are used to track the entry and exit of individual vessels, using their geolocations which are updated in minute intervals.

Matching MarineTraffic and MarineCadastre

MT provides records of port departure timestamps across vessels bound for the US west coast. MC provides the individual micro-movements of uniquely identified vessels for the same time period in US waters. Using unique identifiers, the MMSI and IMO codes of each vessel, and range of calendar dates between a prior departure and US west coast arrival, I capture the initial moment each vessel enters US waters. For the subset of uniquely identified vessels that are not detected in US waters between these key dates, I label these vessels as "missing". The rate of missingness is relatively low, averaging less than 1 percent of the MT sample. However, I do detect a notable spike in missingness in 2020 for the months

[9] See https://www.logisticsmgmt.com/article/top_30_u.s._ports_big_ports_got_bigger_in_2020

of July, August and September. This appears to be largely concentrated among the ports of California (Figure 5.8).

Figure 5.8: Matching AIS positions to Port Call Records

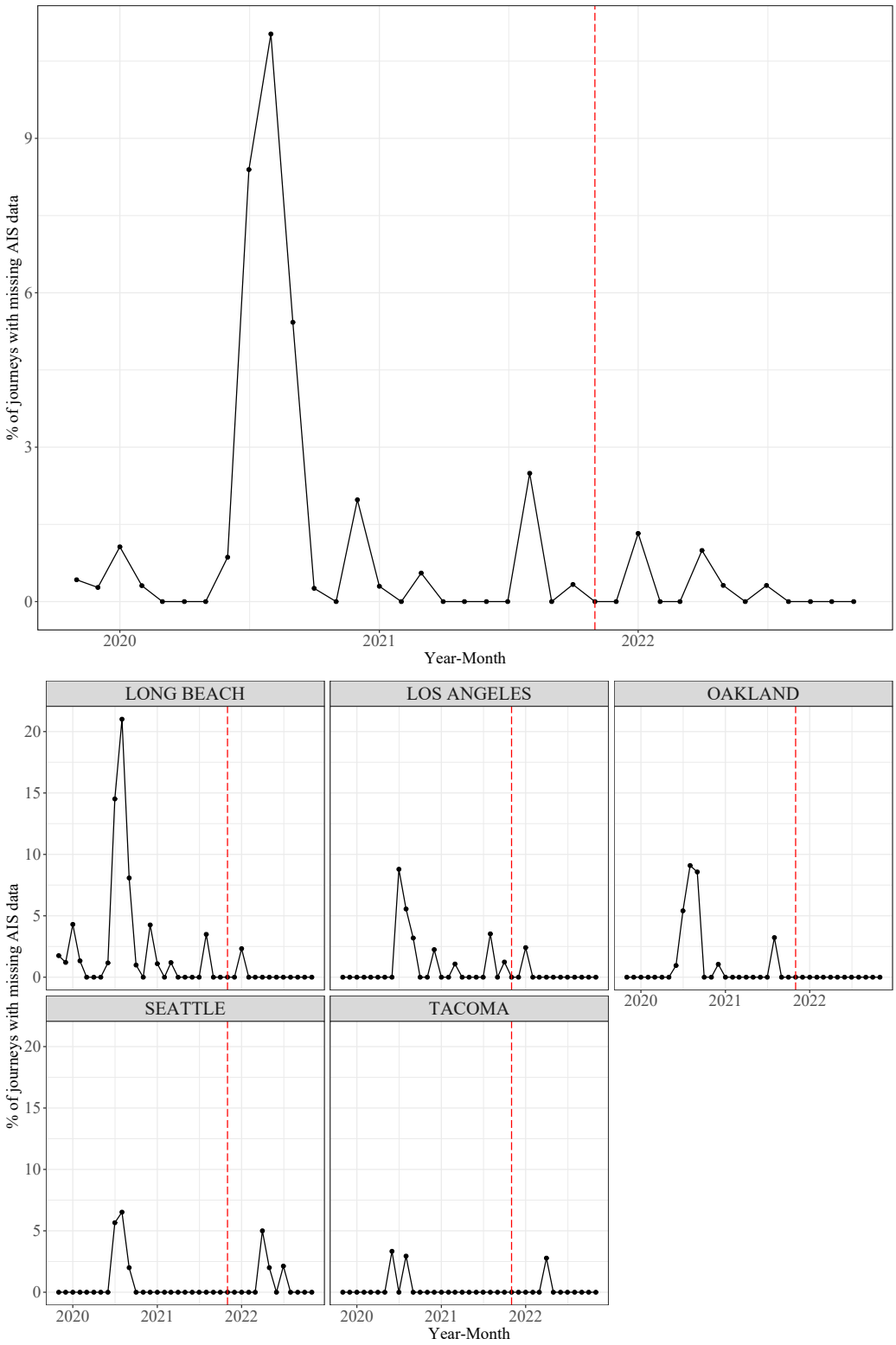

A3 (II.) Fuel Consumption Function

Using Figure 4.5 from Rodrigue (2020), I digitalize each function into a set of coordinates, paired with the midpoint of ship size value based on the ranges displayed. I then generate an approximated function to represent each of these five functions, excluding "10,000+" for representing an undefined midpoint. Taking 1,000 equidistant grid points of speed (knots) between 0 and 25, I feed this range into each function and generate a dataframe of speeds (X), fuel consumption levels (Y), and container capacities (Z).

I regress the following specification of interacted and polynominal terms to estimate fuel consumption (Y), given a combination of speed (X) and TEU capacity values (Z).

$$Y_i = \alpha + \beta_1 X + \beta_2 Z_i + \beta_3 X_i^2 + \beta_4 Z_i^2 + \beta_5 X_i \times Z_i + \beta_6 X_i^2 \times Z_i + \varepsilon_i \tag{5.9}$$

Taking the set of estimated parameters $\{\hat{\alpha}, \hat{\beta}_1, \ldots, \hat{\beta}_6\}$, I use the resulting bivariate polynomial function to convert a given vessel's speed and container capacity into estimated fuel consumption. The resulting function is convex in speed and appears to rise non-linearly with increased to vessel mass. In Figure 5.9 below, I plot these estimates against the defined functions featured in 4.5 for select capacity ranges to better represent the appropriate fit this specification delivers. It should be highlighted that the function performs poorly at levels of speed less frequently observed in practice. In these extreme cases of slow speed, I refer to maritime transport estimates detailed in the next appendix subsection.

Figure 5.9: Fuel Consumption Function

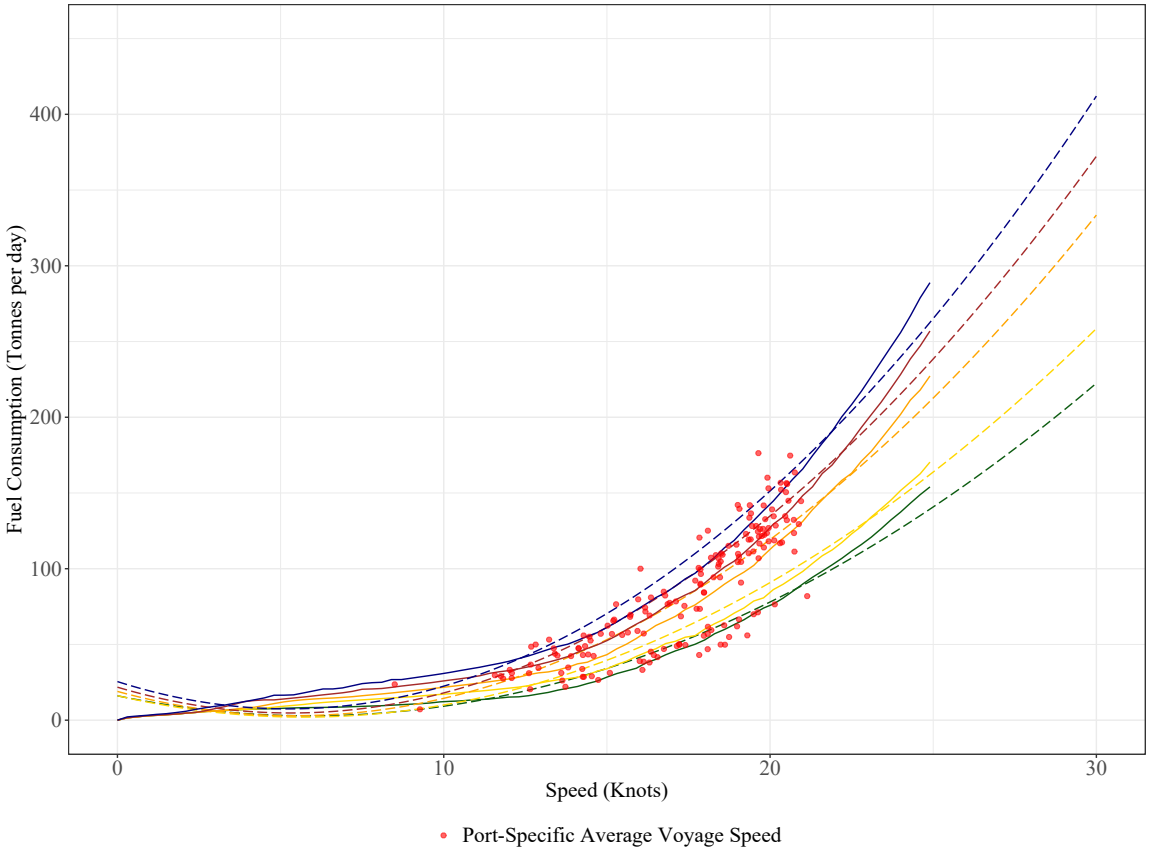

Note: Dashed lines represent imputed functions with TEU fixed at the midpoint of ranges associated with solid line. These solid line functions are mapped using cartesian-based graph readers, which were applied to figures featured in Rodrigue (2020).

A3 (III.) Queuing Emissions & Additional Findings

In this section, I provide further insight into how queuing emissions are summarised for individual vessel–voyages. Additionally, I provide supportive evidence of my main findings in which I broaden the sample of relevant vessels.

Local Queuing Emissions Calculations

I refer to Bai et al. (2020) to estimate fuel consumption associated with queuing activity – a combination of stationary and active movements, which includes cruising, maneuvering, and anchored stauses. This study decomposes time and speed across these various stages of local presence, and identifies associated emissions as momentum of large vessels slowly accumulates from a stationary position. Figure 5.11 demonstrates how speed adjusts across difference stages of vessel transit. Figure 5.11 provides a depiction of the corresponding adjustments in emission types based on these stages and speeds within each stage.

Figure 5.10: Speed by Stage

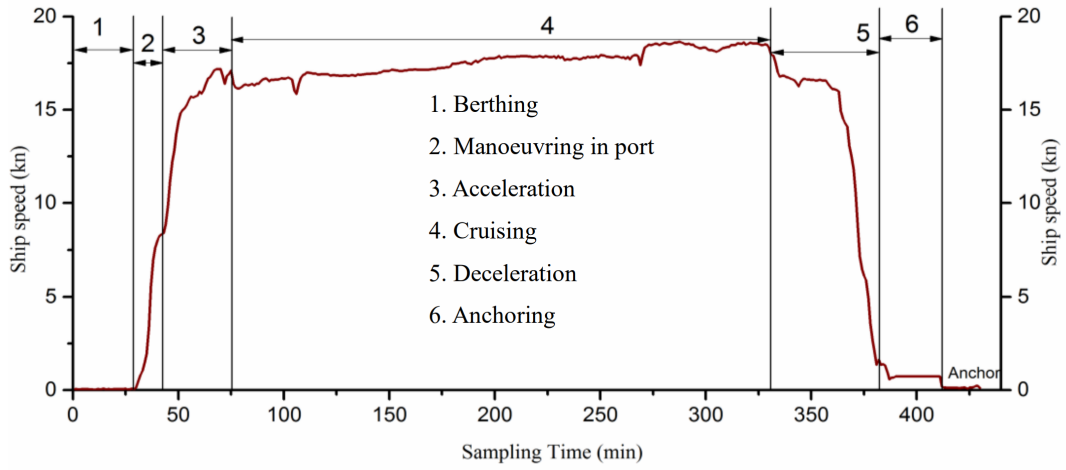

Source: Bai et al. (2020), Gaseous Emissions from a Seagoing Ship under Different Operating Conditions in the Coastal Region of China, Atmosphere, Vol. 11(3), pp 305.

For a given series of local movements, I observe the travel speed S and container capacity C of each vessel within US waters at timestamp t. Timestamps are updated at a minute-level resolution and the previous observation's timestamp for vessel i corresponds to the earlier point of t'. The set of emissivity indices are represented by $(3206, 10.50, 50.50, 2.30)$, which assumes compliance with the IMO 2020 sulfur content mandate. For each reported position p of vessel i, I take the following steps.

Figure 5.11: Emissions by Speed-Stage

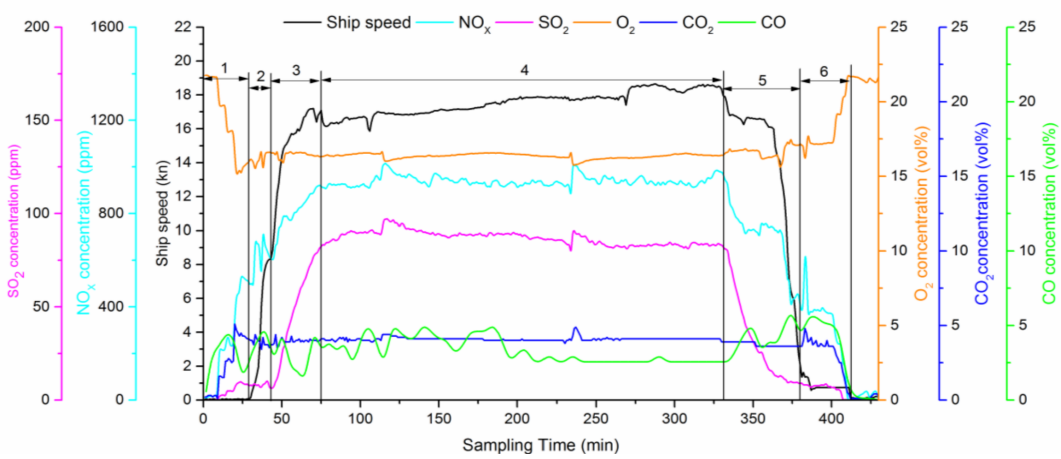

Source: Bai et al. (2020), Gaseous Emissions from a Seagoing Ship under Different Operating Conditions in the Coastal Region of China, Atmosphere, Vol. 11(3), pp 305.

If $S_{ipt} > 10$:

- Generate $\Phi_{ipt}\left(S_{ipt}, C_i\right)$ for fuel consumption in tonnes per day
- Measure $\Phi_{ipt}\left(S_{ipt}, C_i\right) *$ (Emissivity Indices) as the kilograms rate of associated emissions per day
- Take timestamps t and $t-1$ to calculate $\gamma_{ipt}\left(t, t'\right) = \frac{t-t'}{24}$ to scale for the percentage of a day that has elapsed between two consecutive vessel coordinate pings
- Calculate $\delta_{ipt}(S_{ipt}, C_i, t, t') = \gamma_{ipt}\left(t, t'\right) \Phi_{ipt}\left(S_{ipt}, C_i\right)$ (Emissivity Indices) to indicate the total kilogram emissions of vessel i between time t and t', for CO_2, SO_X, NO_X and $PM_{2.5}$, respectively

If $S_{ipt} \leq 10$, repeat the above steps with speed held fixed at 10 for fuel consumption, $\Phi_{ipt}\left(10, C_i\right)$. Upon multiplying by the appropriate emissivity index value, the total kilogram emissions contribution between t' and t is reduced by an emissions scaling factor, based on slow travel speed pollutant levels mapped in Figure 5.11.[10]

[10] At a speed of zero, NO_X during the maneuvering stage is measured at a concentration of 450ppm (64.29% of 10 knot speed emissions). Plotting each knots per hour measure relative to their emission concentrate deviations from 700 (the 10 knot maximum) allows for the mapping of an increasing, concave emission scaling factor function of speed. This approach assumes that each emission type accumulates at the same diminishing marginal rate at maneuvering speeds between 0–10 knots per hour. The exact formula I estimate is $ESF = 64.28571 + 7.539686x - 0.3968257x^2$.

DiD – All International Voyages

Rather than keeping vessel voyages on fixed lanes, I relax the sample to allow for vessels to adjust which origins they stem from following the introduction of the new queuing system. As displayed in Figure 5.22, I find strikingly similar results to those featured in Figure 4.10 across each of my indicators of local vessel activity and emissivity.

Table 5.22: Difference-in-Difference Estimates – Queuing Emissions

	Total Emissions (1)	Duration (2)	Speed (3)	Em. per Knot (4)	Distance (5)	Em. per Hour (6)
Post–Period	-0.4646**	-0.5030**	0.0733	0.1206	-0.5852**	0.0384
	(0.1969)	(0.2179)	(0.1507)	(0.1542)	(0.2306)	(0.0920)
Treatment	0.7243***	0.8548***	-0.4183***	-0.3460***	1.070***	-0.1305**
	(0.0970)	(0.1082)	(0.0746)	(0.0776)	(0.1296)	(0.0539)
DiD	-0.2125***	-0.2865***	0.3617***	-0.3787***	0.1662*	0.0741
	(0.0754)	(0.1000)	(0.0801)	(0.0755)	(0.0946)	(0.0563)
Vessel–Voyage FE	✓	✓	✓	✓	✓	✓
Year–Month FE	✓	✓	✓	✓	✓	✓
Observations	5,090	5,090	5,089	5,090	5,090	5,090
R^2	0.70	0.70	0.72	0.66	0.63	0.78

Note: ***: 0.01, **: 0.05, *: 0.1. Standard-errors are robust to clustering within vessel–voyage lanes of transport service. Each observation is a distinct queuing experience of a vessel arriving on the US west coast between Nov 2019 and Nov 2022. I filter only for vessel voyages that maintained international trade routes pre- and post-policy and drop any observations that lack matching vessel movement data. To limit extreme outlier distortions, I exclude any voyages with emissions less than the 25th percentile minus three times the interquartile range (75th percentile - 25th percentile) or higher than the 75th percentile plus three times the interquartile range (Davies and Jeppesen, 2015).

Appendix References

Bai, C., Y. Li, B. Liu, Z. Zhang, and P. Wu (2020). Gaseous emissions from a seagoing ship under different operating conditions in the coastal region of china. *Atmosphere 11*(3).

Behrens, K. and P. Picard (2011). Transportation, freight rates, and economic geography. *Journal of International Economics 85*(2), 280–291.

Davies, R. and T. Jeppesen (2015). Export mode, firm heterogeneity, and source country characteristics. *Review of World Economics (Weltwirtschaftliches Archiv) 151*(2), 169–195.

Flaaen, A., F. Haberkorn, L. Lewis, A. Monken, J. Pierce, R. Rhodes, and M. Yi (2023). Bill of lading data in international trade research with an application to the COVID-19 pandemic. *Review of International Economics 31*(3), 1146–1172.

Hummels, D., V. Lugovskyy, and A. Skiba (2009). The Trade Reducing Effects of Market Power in International Shipping. *Journal of Development Economics 89*(1), 84–97.

Notteboom, T., A. Pallis, and J.-P. Rodrigue (2022, January). *Port Economics, Management and Policy*. Routledge.

Rodrigue, J.-P. (2020, May). *The Geography of Transport Systems*. Fifth edition. — Abingdon, Oxon ; New York, NY : Routledge, 2020.: Routledge.

Winkler, W. E. (1990). String Comparator Metrics and Enhanced Decision Rules in the Fellegi-Sunter Model of Record Linkage. In *Proceedings of the Section on Survey Research*, pp. 354–359.

Wong, W. F. (2022). The Round Trip Effect: Endogenous Transport Costs and International Trade. *American Economic Journal: Applied Economics 14*(4), 127–66.